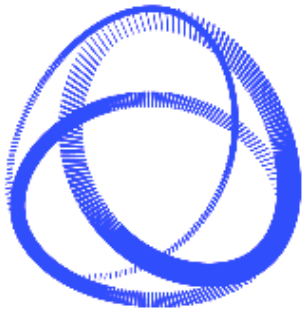

Canterbury Christ Church University

Evaluation of a bicarbonate-based algal carbon capture system for mushroom farms with concomitant generation of value-added products

By

Kusi Philip Asare

Canterbury Christ Church University

Thesis submitted for

The Degree of Doctor of Philosophy

October 2023

Declaration

No part of this thesis has been submitted in support of an application for any degree or qualification of Canterbury Christ Church University or any other University or institute of learning.

Kusi Philip Asare

October 2023

Acknowledgement

First and foremost, all praise is due to God Almighty for providing me with this wonderful opportunity throughout my academic journey. I would like to extend my gratitude to Dr Asma Ahmed and Dr Joe Burman for proposing this scientific research work. Dr Asma Ahmed has been an exceptional supervisor over the past three years. Throughout my PhD, she guided me by improving my scientific progress and skills in the lab, where she provided valuable inputs for data analysis, polishing write-ups, and teaching me essential skills that have made me a more proficient scientist. I am also grateful for her understanding and support outside the laboratory. I would also like to extend my gratitude to the industrial partners at AlgaeCytes Ltd and Margate Mushrooms. The microalgal strains used throughout this research project was provided by AlgaeCytes Ltd. I am grateful to Dr Donal McGee for the knowledge transfer on microalgae and the countless conversations and expertise that helped me shape my experiments and interpretation results. I would also like to thank the entire AlgaeCytes Ltd staff for their roles in helping me with my PhD analysis and the frequent visits to their laboratory. AlgaeCytes Ltd also provided me with photobioreactors for scale-up experiments from bench-top. Access to AlgaeCytes Ltd laboratory gave me the opportunity to enjoy collaborative input on the industrial side of things, which has helped me broaden my perspective beyond academia towards potential scale-up, implications, and difficulties of implementing my bench-top research into larger-scale and gain insight into an algal business.

I would like to extend my sincere gratitude to the entire Life Sciences department and the technicians at Canterbury Christ Church University, who played a crucial role in my research by providing me with the necessary assistance requested, as well as Dr Shamas Tabriaz, Dave Belson, Krupa Bhatt, Naomi Stead, Csenga, and the entire technical team, who have been instrumental in helping me over the past years, whether it be with equipment-related issues, experiment design, or simply providing a much-needed discussions. To express my heartfelt appreciation to my family; Mr. Charles Osei Agyemang and Mrs. Dorothy Osei Agyemang for their unwavering support throughout my career, as well as a special thank you to Mrs. Afua Boatemaa (mother), my father Mr. Douglas Asare, and my siblings, Lubbica Asare Mensah, Linda Yeboah, Augustine Attah Gozar, Evans Owusu-Ansah, Benjamin Appiah-Kubi, The Owusu-Ansah family (United Kingdom), the entire family in Bekwai-Ashanti, and all my friends. Your efforts are greatly appreciated and may God bless you all.

Table of content

List of Figures

List of Tables

List of Abbreviations

AA	Ascorbic acid
ABTS	2,2-azinobis (3-ethylbenzothiazoline-6-sulfonic acid)
ARA	Arachidonic acid
BHA	Butylated hydroxyanisole
BICCAPS	Bicarbonate-based carbon capture and algae production systems
CA	Carbonic anhydrase
CCM	Carbon dioxide concentration mechanism
CCS	Carbon Capture and Storage
CCU	Carbon Capture and utilisation
Ci	Inorganic carbon transport
CO_2	Carbon dioxide
DEA	Diethanolamine
DPPH	2,2-diphenyl-1-picryl-hydrazyl-hydrate
DW	Dry weight
EPA	Eicosapentaenoic acid
FAME	Fatty acid methyl esters
FTIR	Fourier transform infrared spectroscopy
GA	Gallic acid
GC-FID	Gas chromatography flame ionisation detector
HPLC	High-performance liquid chromatography
IC	Inorganic carbon
MEA	Monoethanolamine
$NaHCO_3$	Sodium bicarbonate
OD	Optical density
PBP	Phycobiliprotein
PBS	Phosphate buffer solution
PUFAs	Polyunsaturated fatty acids
RuBisCO	Ribulose biphosphate carboxylase oxygenase
SPF	Sunscreen protective factor
TAC	Total antioxidant capacity
TDA	Tridecanoic acid
TPC	Total phenolic content

Abstract

The rise in anthropogenic carbon dioxide emissions has led to a need for efficient and scalable carbon capture systems. Microalgae offer a promising approach to carbon capture from a variety of sources, including industrial gases and dissolved inorganic carbon. The resulting algal biomass can serve as feedstock for biofuels and high-value products such as polyunsaturated fatty acids, carotenoids, and proteins, with applications in the personal care, healthcare, and nutraceutical markets. The aim of this thesis was to develop a bicarbonate-based microalgal system for carbon capture from mushroom production and the concomitant generation of value-added products from the spent algal biomass and mushroom waste. Firstly, three freshwater microalgal species *Parachlorella kessleri, Scenedesmus quadricauda,* and *Vischeria* sp.*,* and two marine microalgal species *Phaeodactylum tricornutum,* and *Porphyridium purpureum* were evaluated at varying inorganic carbon concentrations to identify the most tolerant and suitable species. *Vischeria* sp. and *Porphyridium purpureum* were selected for further studies based on their growth profiles, carbon removal efficiencies, and concentrations of value-added products including fatty acids and pigments. Using these two species, a bicarbonate based integrated carbon capture and algal production system was developed for mushroom cultivation at small scale. This involved the capture of carbon dioxide generated from a mushroom growth chamber in a modified microalgal growth medium, followed by the cultivation of the selected microalgal species in this medium. The effects of pH on cell growth, carbon capture efficiencies, and biochemical profiles of both species were studied in (1) 'mushroom-bicarbonate media', containing dissolved inorganic carbon generated from the carbon dioxide captured during mushroom cultivation and (2) 'synthetic media' containing commercial sodium bicarbonate. *Vischeria* sp. performed better in the synthetic media whereas *Porphyridium purpureum* performed significantly better in the mushroom-bicarbonate media. The inorganic carbon removal efficiency by *Vischeria* sp. from the synthetic media (94.9%) was higher compared to mushroom-bicarbonate media (30.6%). Similarly, the estimated removal of inorganic carbon was 85.4% in mushroom-bicarbonate media, which was 2.1 times higher than in synthetic media (40.7%) by *Porphyridium purpureum*. These results suggest that *Porphyridium purpureum* exhibited higher adaptability and tolerance to high sodium concentrations in mushroom-bicarbonate media, while carbon utilisation was lower in synthetic media due to lower sodium content. Furthermore, the study highlighted the importance of culture pH in improving inorganic carbon utilisation. Finally, based on the results of the small-scale studies, an integrated process was evaluated in

photobioreactors to demonstrate the scalability of the process. A small-scale study on *Porphyridium purpureum* performed significantly better in the mushroom-bicarbonate media with 87.3% inorganic carbon removal at pH 7 compared to *Vischeria* sp. (67.3%) at pH 9. The biochemical profiles of *Vischeria* sp. revealed that the carbohydrate content was similar, with 47.6% in synthetic media and 48.9% in mushroom-bicarbonate media. In *Porphyridium purpureum*, the lipid content in mushroom-bicarbonate media was similar compared to synthetic media, at 17.2% and 3.1%, respectively. The carbohydrate content was 47.7% in synthetic media and 51.7% in mushroom-bicarbonate media. *Vischeria* sp. in the synthetic media showed higher antioxidant properties compared to *Porphyridium purpureum*. Additionally, this study evaluated the antioxidant and photoprotective properties of extracts from spent algal biomass and mushroom exudate for potential applications in bio-based cosmetics. This suggests that the system could not only function as an effective model for evaluating the carbon dioxide sequestration capacities of microalgae, but also be integrated into a working mushroom farm to capture the carbon dioxide as well as generated value-added products from the spent algal biomass and mushroom waste.

CHAPTER 1

Introduction

1.1 Research background

Growing industrialisation and urbanisation have led to a significant increase in the concentration of greenhouse gas especially carbon dioxide in the atmosphere. This has resulted in a series of problems that the world currently faces, including global warming and ocean acidification. For a balanced ecosystem, biological and geological sources for carbon capture must be in equilibrium through carbon deposition in soils and oceans and carbon utilisation by photosynthetic organisms (Sayre, 2010). Since the commencement of the industrial age, there has been a shift in the carbon balance from 280 to 400 ppm in the atmosphere due to increased emissions from fossil fuel combustion, reduction in carbon sequestration by deforestation, increase in domestic energy consumption (heating and cooling), and agricultural activities (Maryshamya *et al*., 2019). Approximately 80% of the total energy consumed in the industrial sectors generates about 24 giga tons of carbon dioxide produced annually through the combustion of fossil fuels, which has caused an increase in the atmospheric carbon dioxide concentration (Beigbeder *et al*., 2021; IPCC, 2022). According to the International Energy Agency, approximately 45 million tons of carbon dioxide are captured by carbon capture, utilisation, and storage (CCUS) facilities globally. These facilities are still lagging expectations and require substantial development to achieve this goal from industrial sectors such as power plants, cement, fertiliser industries, and chemicals (IEA, 2021).

The agricultural sector accounts for about 10% of carbon dioxide emissions through activities such as crop production, burning of biomass, decay, and usage of agrochemicals (Waheed *et al.,* 2018). Mushroom farming is the process of cultivating fungi for food, medicinal use, and other purposes. It involves the use of agricultural waste as a growing medium, which not only provides a sustainable method of farming but also contributes to waste management. There has been a notable increase in consumer demand for mushrooms, particularly specialty varieties like *Pleurotus* spp., over the recent years (Barh *et al*., 2019). Among agarics, the genus *Pleurotus* has a higher number of reported cultivated species than any other genera. The genus *Pleurotus* recognised as oyster mushroom belongs to the class Basidiomycota and the family Pleurotaceae (Singh and Kamal, 2017). Globally, *Pleurotus* spp. is the second most widely cultivated mushroom after shiitake mushroom, (Royse *et al*., 2017).

The economic importance of edible mushrooms has been valued at over US$30 billion globally amounting to approximately 7 million tons of production per year (Pavlík *et al*., 2020). Mushroom cultivation has become a commercial farming technique in both developed and developing countries such as the USA, Great Britain, China, and some African countries such as Ghana and South Africa, with China being the largest producer of approximately 4 million tons per year. *Pleurotus ostreatus* (oyster mushroom) comprises nutritional sources such as iron, carbohydrates, vitamins, protein, and dietary fibre, and contains high proportions of polyunsaturated fatty acids (PUFAs) with low fat content for human consumption (Muswati *et al*., 2021). Mushrooms are not only cultivated for their nutritional benefits but also for optimal industrial fermentation processes on lignin and cellulose substrates, nitrogen and carbon sources, temperature, light, and growth media. However, mushrooms generate significant levels of carbon dioxide during respiration, in which fungi consume oxygen and organic material to produce carbon dioxide and water. Mushroom farming is estimated to produce 2.1 – 4.4kg of carbon dioxide equivalent for each kilogram produced (Rogers, 2015; Širić *et al*., 2023). For example, a mushroom farm with a capacity of 460 m^3, which is estimated to produce about 7 kg of mushrooms can replace 13,000L of air several times per hour, and is projected to produce about 9.1kg CO_2 per day (Walker and White, 2017). If not removed from the mushroom growth environment, these high levels of CO_2 results in significant effects such as poor respiration, slow pinning, fruiting bodies, disconnection of the mycelial network, and short life cycles of the fungi (Ahlawat, 2011). There is therefore a need for a carbon capture process that can be integrated into mushroom farms, to effectively remove the excess CO_2 to maintain optimal mushroom yield and quality, whilst avoiding the release of CO_2 to the atmosphere.

1.2 Overview of carbon capture technologies

Global energy comes from one-third of industrial activities which account for 40% of carbon dioxide emissions, with approximately 30% released into the atmosphere by power plant activities (Kuramochi *et al.,* 2012). Carbon dioxide capture is a complex challenge that requires diverse context-specific solutions worldwide. By investing heavily in carbon dioxide capture, we can reduce emissions from power plants and other major sources more effectively. Various strategies have been proposed to mitigate carbon dioxide levels including the development of processes that emit lower levels of carbon and carbon capture, utilisation, and storage (CCUS) technologies (Singh, J. & Dhar, 2019a). Carbon capture and storage (CCS) is

a promising technology for reducing greenhouse-gas emissions (Gerard & Wilson, 2009). To tackle the carbon dioxide challenge, various carbon capture and conversion techniques have been suggested, including separation of carbon dioxide from flue gas mixtures using solvents, adsorbents, membranes, and cryogenic methods (Singh, J. & Dhar, 2019b). The captured carbon dioxide is then stored in various reservoirs, such as geological forms, by underground deposition or through the oceanic system by injecting carbon dioxide into the deep sea, or as saline (Lackner, 2003). A safer and more sustainable solution would be to store carbon dioxide in solid or liquid form, which would not damage the natural environment. These techniques include mineral carbonisation (carbonates) and chemical absorption of carbon dioxide conversion using amine-based solvents, such as monoethanolamine (MEA), sodium hydroxide (NaOH), and diethanolamine (DEA) which is a commercialised process (Nguyen *et al.,* 2010). The use of amines still has some gaps owing to solvent loss in the process and requires a high amount of energy to regenerate the solvent (Nouha *et al.,* 2015). However, physicochemical carbon capture storage methodologies have limitations in capturing carbon dioxide from point sources that produce high concentrations of carbon dioxide. They are not effective in capturing diffused, nonpoint emissions, and low concentrations of carbon dioxide (Nouha *et al.,* 2015). The feasibility of these carbon capture, utilisation, and storage processes depends on their cost, carbon storage capacity, and environmental impact.

1.3 The use of absorbents for capture carbon dioxide from flue gases

Several techniques and processes have been proposed for carbon dioxide removal from flue gases before feeding microalgae cultures. (Kim *et al*., 2011) reported the use of amines and potassium carbonate for carbon dioxide capture (Chi *et al.,* 2013). The efficiency of various carbon capture systems, such as biological systems like microalgae and chemical systems like carbon capture and storage (CCS), can be significantly influenced by parameters like pH. In chemical absorption-based carbon capture, the pH of the solvent (such as an amine solution) affects the rate and efficiency of carbon dioxide absorption, with higher pH levels (alkaline conditions) generally enhancing absorption. The composition of the solvent used in chemical absorption processes also impacts its capacity for carbon dioxide absorption, with different solvents having different pH levels and affinities for carbon dioxide, which can affect efficiency. However, it is important to note that microalgae have an optimal pH range for photosynthesis, typically between 7 and 9, within which they are most efficient at capturing carbon dioxide and converting it into biomass. Deviations from this range can decrease

photosynthetic efficiency and, consequently, carbon capture efficiency. Another proposed method for capturing carbon dioxide from power plants through electrolysis involves the use of monoethanolamine (MEA) to produce chemical products such as hydrochloric acid, sodium hypochlorite (NaOCl), and bicarbonate (Kim, G. *et al.,* 2019). MEA reacts with carbon dioxide through the gas-liquid phase to produce different ions, such as carbonate ions, carbonic acid, bicarbonate ions, and carbamate intermediates. Amine-based solvents can be used to remediate carbon dioxide from flue gas (Thomas *et al.,* 2016). The process of using MEA also has disadvantages which can result in high energy consumption and equipment corrosion. The use of mixed amines requires less energy than that of amines alone (Idem *et al.,* 2006).

The application of microalgae-based biological carbon-capture technology can reduce the carbon footprint and production of bioenergy, making it a carbon dioxide-neutral replacement for fossil fuels. The use of microalgae to biologically capture and store carbon is one of the most promising methods of carbon sequestration worldwide (Moreira & Pires, 2016). About 30-40% of atmospheric CO_2 can be captured by many eukaryotic algae which contains pyrenoids, a proteinaceous sub-cellular structure due to the presence of ribulose-1,5-biphosphate carboxylase/oxygenase enzyme (RuBisCO). The simple cell structure and energy-saving structure of microalgae's photosynthetic efficiency is 10 folds higher than terrestrial plants (Farooq, 2022).

1.4 Gas-liquid conversion from flue gases for microalgal cultivation

Algae have the potential to decrease direct carbon dioxide emission by absorbing carbon dioxide from flue gases on large-scale has shown a promising system for converting carbon dioxide into high value biomass with the potential of releasing oxygen. The injection of carbon dioxide from flue gas into microalgae cultivation controls culture pH and contributes to mixing of the culture. Microalgae cells can utilise both carbon forms such as bicarbonates and carbonates which can permeate the cell walls. Bicarbonate and carbonate forms are provided to microalgae culture as inorganic carbon feedstock to reduce desorption costs. To tackle the urgent problem of carbon dioxide emissions, we need a comprehensive strategy that involves shifting to low-carbon technologies and conducting research on carbon capture and storage (CCS) methods (Singh and Dhar, 2019). The process typically applied on carbon capture from concentrated carbon sources generated by industries such as power plants, cements, and metals involve chemical absorption, physical adsorption, or membrane separation. The complexity of the entire carbon capture and storage technology arises from the

process where the captured carbon is compressed prior to being transported to an underground storage site. This can introduce geological challenges that complicate risk and monitoring of the storage sites (Cao *et al*., 2020). There has been significant interest in the cultivation system of microalgae with enriched carbon dioxide such as flue gases. There are several factors that affects gas-liquid transfer rate including the solubility of the gas in the liquid, the surface area of the interface between the gas and the liquid, temperature, and the partial pressure of the gas (Moorberg and Crouse, 2021). The physical and chemical properties of the liquid (or solvent) in which the gas is being dissolved can also influence the rate of transfer. A study found that the higher the liquid temperature, the higher the air flow rate above the liquid surface, and the higher the gas-liquid mass transfer rate (Liu *et al*., 2020). According to Boyle's law, the pressure of a gas is inversely proportional to its volume at a constant temperature. This implies that a decrease in the volume of the gas (as might occur when a gas is dissolved in a liquid) leads to an increase in its pressure, thereby influencing the rate of gas-liquid transfer (Ham *et al*., 2021). Furthermore, the residence time, which refers to the average time a molecule of gas spends in a liquid before being released back into the gas phase, also significantly impacts the rate of gas-liquid transfer (Cheng *et al*., 2019). A longer residence time can lead to a higher rate of transfer, as it provides more opportunity for the gas molecules to dissolve in the liquid. Therefore, both Boyle's law and residence time are key factors in understanding and predicting gas-liquid transfer rates in various scientific and industrial applications (Reichmann *et al*., 2021).

Alkaline absorbers such as sodium hydroxide (NaOH), monoethanolamine (MEA), and diethanolamine (DEA) have been identified as an alternative method for gas-liquid transfer with high mass transfer rate. One of the advantages of using absorption-based carbon dioxide capture in bicarbonate and carbonate forms is easy transportation under normal pressure. To prevent carbon loss into the atmosphere, it is crucial to maintain high pH levels during the process of carbon capture from flue gas as an inorganic carbon source (Chi *et al.,* 2014). A study on direct injection of carbon dioxide showed limitations due to lower mass transfer between the gas-liquid conversion rate with solubility efficiency of ≤ 10 % for an agal culture (González-López *et al*., 2012). About 78% carbon dioxide removal with 0.3 mol/L sodium carbonate (Na_2CO_3) ranged from a pH of 11.6 – 9.2 which is suitable for some pH-resistant algae species (Acién Fernández *et al.,* 2012). Algae that thrive in alkaline conditions and have high growth rates between pH levels of 7 to 10 are ideal for this purpose, especially when an alkali scrubber is used to initially capture the carbon dioxide from the flue gas. A study on the use of sodium bicarbonate ($NaHCO_3$) has been reported for microalgae strains such as *C.*

vulgaris, which has extracellular carbonic anhydrase (CA) on their cell surface, which effectively utilise $NaHCO_3$ as a carbon source. These strains could act as transporters of HCO_3^- under conditions of low dissolved CO_2 (dCO_2) (Li *et al*., 2018a), they are more effective at utilising carbon source when $NaHCO_3$ used compared to gaseous CO_2. They are also easier to handle than gaseous CO_2 in terms of storage and transportation making it a cost-efficient alternative carbon source (Lam and Lee, 2013). A study showed that *Cyanothece sp.,* and *Dunaliella salina* were able to tolerate up to 0.60 M sodium bicarbonate ($NaHCO_3$) among six screened microalgal species (Ravelonandro *et al.,* 2011). One of the challenges in cultivating alkaline strains is their tolerance to high ionic condition media. Slow growth has been observed when natural alkaline strains are cultivated in a synthetic alkaline medium (Chi *et al.,* 2014).

1.5 Carbon concentration mechanism in microalgae

Chlamydomonas reinhardtii is a prime candidate for carbon concentrating mechanism (CCM) studies due to its robust genetic foundation. It has a CCM that ensures an adequate supply of inorganic carbon (C_i) for its growth and development (Jungnick *et al*., 2014). This CCM is activated when the CO_2 concentration drops to or below atmospheric levels and consists of a protein assembly that facilitates efficient C_i uptake into the cell and its targeted transport to the location where RuBisCO converts CO_2 into biomolecules (Tirumani *et al*., 2014). However, other species may be preferred for CCM research for several reasons: physiological relevance as some species exhibit similar pharmacological responses, and environmental adaptability based on varying CO_2 levels in different environments. *C. reinhardtii* is an excellent model for CCM studies, the selection of species for research is influenced by a range of factors, including the specific research question, the physiological traits of the species, and practical considerations (Jungnick *et al*., 2014; Tirumani *et al*., 2014). The CCM can help understand the utilisation of carbon by microalgal species. The process of photosynthesis, which plays a crucial role in carbon metabolism, is vital for the survival of most living organisms. Within this process, the conversion of inorganic carbon into organic carbon results in the accumulation of carbohydrate molecules, serving as a source of energy in cellular organisms. This fundamental process contributes significantly to the global carbon cycle and is facilitated by the Calvin-Benson cycle, a series of reactions described by (Benson and Calvin, 2003). Green algae, such as *Chlamydomonas reinhardtii*, have emerged as a significant model organism for research on photosynthesis, life cycles, genetics, accessible genome sequence, and the advancement of molecular tools (Wang *et al*., 2015a). In aquatic

systems, CO_2 serves as a critical substrate, yet its availability often limits biological processes. Predominantly, in conditions where the pH ≥ 7 and the temperature is below 30°C, bicarbonate emerges as the principal form of CO_2 in water. The process of aquatic carbon sequestration requires the bicarbonate form, which subsequently contributes to algal growth and biomass production. The primary function of the carbon concentration mechanism is to fix the CO_2 produced in the thylakoid lumen which diffuses in the pyrenoid matrix of the ribulose-1,5-bisphosphate carboxylase-oxygenase (RuBisCO) enzyme in the photosynthetic carbon assimilation. Photosynthetic organisms such as microalgae are subjected to a spectrum of physicochemical stresses influenced by factors such as the water chemistry, the concentration of dissolved inorganic carbon, and the environmental conditions (Singh *et al*., 2014). Hence, these organisms have evolved CCMs as an adaptive strategy to optimise photosynthetic efficiency under conditions of low CO_2 or inorganic carbon availability. Several environmental parameters, including but not limited to temperature, pH, and alkalinity, exert a direct impact on the rate at which inorganic carbon is supplied to phytoplankton. These aquatic environment experiences a deficiency in CO_2 in water due to its slower diffusion rate, which leads to a relative decrease in HCO_3^-. The implementation of various CCM strategies across a range of algal strains has been reported in several research (Tabita *et al*., 2007).

There are three primary types of CCMs which vary across different organism, and they include the C4 pathways, inorganic carbon transportation, and the conversion mechanism which elevate the CO_2 concentration around the enzyme. The algal CCM occurs mostly in prokaryotic and eukaryotic algae where CO_2 fixation takes place within the microcompartment of the pyrenoid and carboxysome (Badger *et al*., 2002). This CCM operates on the principles of C_4 and crassulacean acid metabolism (CAM) pathways, where CO_2 is incorporated by phosphoenolpyruvate to form oxaloacetic acid (OAA), which subsequently undergoes decarboxylation to regenerate CO_2. This mechanism also recaptures the CO_2 produced from the oxygenation of the RuBisCO through photorespiration, thereby optimising CO_2 assimilation (Sayre, 2010). Meanwhile, the C_4 pathway is extensively studied in higher plants, its presence has been identified in the marine diatom *Thalassiosira weissflogii*, meanwhile C_3 photosynthesis remains the dominant process in algae (Prasad *et al*., 2021a). The inorganic carbon (Ci) transportation and conversion mechanism is a critical component of the CCMs in prokaryotes. The carboxysome, a bacterial microcompartment, plays a pivotal role in CO_2 fixation in all cyanobacteria and other chemoautotrophs (Badger *et al*., 2002; Klein *et al*., 2009). The CCMs in prokaryotes encompass (i) bicarbonate pumps/transporters and membrane-bound hydration enzymes that amplify bicarbonate concentrations in the cytosol;

and (ii) the carboxysome, a selectively permeable protein shell encapsulating RuBisCO and carbonic anhydrase (CA). This shell facilitates the feeding and conversion of enhanced bicarbonate levels to CO_2, initiating the first step of the C_3 cycle (Sun *et al*., 2019). Elevation of CO_2 concentration surrounding the enzyme represents the third category of CCMs, as depicted in Figure 1.1. This mechanism is regulated by the arrangement of the pH gradient across the chloroplast and thylakoid membrane upon exposure to light. In light conditions, the chloroplast stroma reaches a pH of approximately 8.0, while the thylakoid lumen attains a pH ranging between 4.0 and 5.0. The pH gradient plays a crucial role, particularly at a pKa of 6.3, where the conversion of bicarbonate to CO_2 occurs. However, the CO_2 component of Ci is also present in substantial quantities within the thylakoid lumen. Any bicarbonate that moves into the thylakoid lumen undergoes transformation into CO_2, consequently elevating the CO_2 concentration beyond its range. It has been stated that this form of CCM necessitates the presence of CA within the acidic environment of the thylakoid lumen to promptly convert the infiltrating bicarbonate (HCO_3^-) into CO_2 (Pronina and Semenenko, 1990). Several computational analyses have indicated that algae equipped with pyrenoids potentially exhibit superior efficacy in sustaining elevated CO_2 concentrations surrounding RuBisCO, compared to their counterparts devoid of pyrenoids (Atkinson *et al*., 2017).

Although *Chlamydomonas reinhardtii* has been studied as a model organism particularly for the study of photosynthesis, the focus of this research was on evaluating microalgae with the potential to produce high-value compounds for various industrial applications and was based on the recommendations of the industry partner, AlgaeCytes Ltd. For example, *Vischeria* sp: This microalga can accumulate high content of lipids rich in nutraceutical fatty acids and has excellent biomass yield in nitrogen-limiting culture (Gao *et al*., 2023). *Phaeodactylum tricornutum* is known for its ability to produce several industrially relevant molecules such as biofuels, pharmaceuticals and nutraceuticals, and beta-glucans. It also has a high photosynthetic efficiency of carbon fixation (Quelhas *et al*., 2019). *Porphyridium purpureum*, a red microalga has the ability to synthesise a number of high-value bioactive substances, such as polysaccharides, long-chain polyunsaturated fatty acids (LC-PUFAs), and phycobiliproteins. These substances have potential applications in food, nutraceuticals, pharmaceuticals, and bioremediation industries (Yi *et al*., 2024). *Parachlorella kessleri* is known for its high carbohydrate content, making it a strong candidate for biofuel production. It also has a high capacity for CO_2 capture, which can help mitigate the effects of climate change (Ciempiel *et al*., 2022). Lastly, *Scenedesmus quadricauda* is recognised for its

high growth rate and biomass productivity, making it suitable for biofuel production. It also has a significant ability to absorb and remove pollutants from water, making it an excellent candidate for bioremediation. The choice of microalga species (table 2.1) for was dependent on the specific requirements of the industry suitable for certain applications.

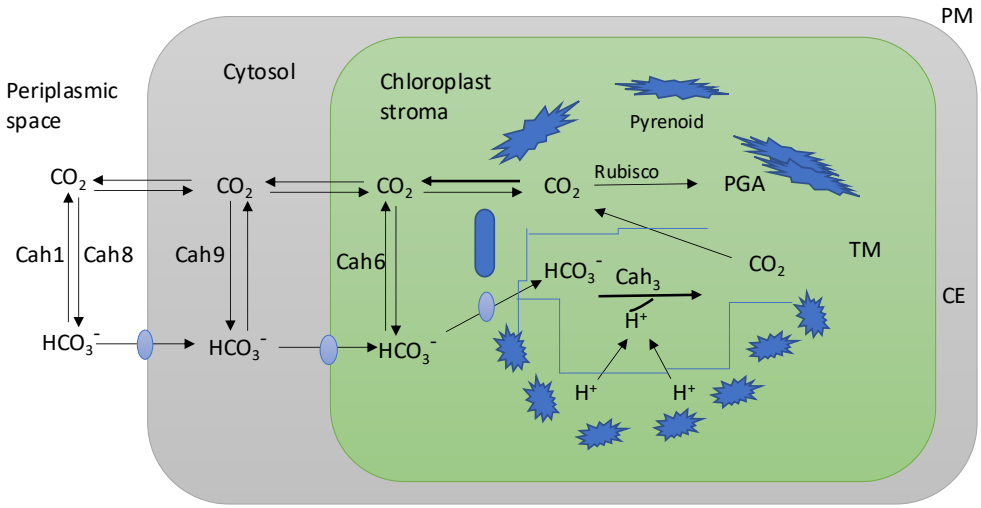

Figure 1.1 Carbon concentration mechanism (CCM) of *Chlamydomonas reinhardtii* of a single chloroplast cell containing with a single pyrenoid. This presents elevated carbon dioxide and bicarbonate levels within the chloroplast than the external cell environment. The isoforms of carbonic anhydrase of CAH1, CAH3, CAH6, CAH8, and CAH9. The PM represents plasma membrane, chloroplast envelop (CE), thylakoid membrane (TM), 3-phosphoglyceric acid (PGA). The bicarbonates or Ci transporter represents the filled circle and photosynthetic electron from the hydrogen ion (H^+) adapted from (Prasad *et al*., 2021a).

1.6 Overview of microalgal cultivation parameters

1.6.1 Light intensity

The intensity of light plays a crucial role in the photosynthetic activity of microalgae and other photosynthetic organisms. Two processes that are significantly influenced by light intensity are photorespiration and photoinhibition. Photorespiration, which mainly occurs in C_3 plants, is an enzymatic process that fixes oxygen instead of carbon dioxide, reducing the photosynthetic efficiency. High rates of photorespiration can lower the net carbon fixation rate of microalgae. Photoinhibition in algal cultivation reduces the photosynthetic efficiency due to exposure to high light intensities (Amini Khoeyi *et al*., 2012). Elevated temperatures can harm photosystem II (PSII), the oxygen-evolving complex (OEC), and the electron transport on both the donor and acceptor sides of PSII in the photosynthetic machinery. PSII's stability is compromised at high temperatures, leading to a decrease in its activity. Heat stress could result in the separation of the OEC, thereby disrupting the balance of electron flow from the OEC to

the acceptor side of PSII. (Krzemińska *et al.,* 2014). Prolonged exposure to high light intensities without appropriate protective mechanisms can lead to significant losses in carbon capture efficiency. Many microalgae possess adaptive mechanisms to cope with varying synthesis of light-harvesting pigments such as chlorophyll-*a* and phycobiliproteins under low light conditions and protective pigments like carotenoids under high light conditions (Wahidin *et al.,* 2013). Besides chlorophyll-*a*, other types include chlorophyll-*b*, *c*, *d*, and *f*, are the second additional pigment while other light-harvesting pigments include phycobiliprotein (Airs *et al*., 2014; M. Chen *et al*., 2010).

1.6.2 Temperature

Biological processes and growth of microalgae cultivation are affected by temperature, which varies among microalgal species. Temperature is a key factor that can be used for process optimisation for enhanced biomass productivity and composition (Gonçalves *et al*., 2016). Culture temperature affects the solubility of gases and the carbon equilibrium in the cultivation media. The primary impact of temperature on photosynthesis is attributed to a decrease in the activity of the enzyme ribulose-1,5-bisphosphate (RuBisCO). This enzyme has two roles; it can function as an oxygenase or a carboxylase, contingent on the relative concentrations of O_2 and CO_2 in the chloroplasts. The CO_2 fixation activity of the RuBisCO enzyme escalates with an increase in temperature up to a specific threshold, beyond which it starts to diminish (Salvucci and Crafts-Brandner, 2004). When the solubility of carbon dioxide decreases with increase in temperature, it results in the reduction of carbon source for microalgae, which could negatively affect their growth and carbon capture efficiency. Additionally, changes in temperature causes shift in pH which affect distribution of carbon species in the culture medium, causing higher pH values in the equilibrium towards bicarbonate (HCO_3^-) and carbonate (CO_3^{2-}) ions, which are less available to microalgae for carbon utilisation. (Chovancek et al., 2019) reported that photosynthetic functions in algal cells can be affected at high temperatures up to 38^{o}C, which affects metabolism of cells in the photosystems and the electron transport chain which leads to cell mortality (Ras *et al*., 2013). Photosynthesis is impacted by low temperatures due to a decrease in carbon assimilation activity, while excessively high temperatures can diminish photosynthesis by deactivating photosynthetic proteins and disrupting the cell's energy balance. Additionally, an increase in temperature can lead to a reduction in cell size and respiration (Salvucci and Crafts-Brandner, 2004). The optimum growth temperature for most microalgae ranges from 20 to 30 °C (Suthar and Verma,

2018). However, a few species such as *Dunaliella salina* and *Chaetoceros* sp. can thrive in higher temperatures up to 40^{o}C whiles species such as *Chlamydomonas nivalis* and *Chloromonas pichinchae* which can also thrive at a temperature range between 0^{o}C to 1^{o}C (Hüner *et al*., 2013).

1.6.3 Nutrients

The nutritional requirements may vary among different algal species, the fundamental needs are consistent across all species. Nitrogen, phosphorus, and carbon constitute the essential elements for microalgae, serving as macronutrients for their growth (Juneja *et al*., 2013a). The levels of macronutrients, including nitrogen and phosphorus, can vary among different algae species. Studies have indicated that the growth of *Chlorella* sp. decreased as the concentrations of nitrogen and phosphorus were reduced from 31.5 and 10.5 mg L^{-1}, respectively (Aslan and Kapdan, 2006). Micronutrients such as molybdenum, potassium, cobalt, iron, magnesium, manganese, boron, and zinc are essential in trace amounts with a significant impact on microalgae growth by influencing many enzymatic activities within algal cells (Gardner-Dale *et al*., 2017). The growth rate of microalgae is substantially impacted by nutrient deficiency, leading to reduced biomass. Moreover, the availability of nutrients plays a crucial role in influencing the synthesis and accumulation of carbohydrates and lipids in microalgae (Khan *et al*., 2018a). In autotrophic cultures, the only carbon sources are sodium bicarbonate and carbon dioxide through environmental exposure during cultivation which provides a low cost of production and utilisation efficiency (Wang *et al*., 2019). Other related carbon sources, such as glucose, acetate, and sucrose, are mostly used for heterotrophic cultures and in combination with mixotrophic cultures (Khoo *et al*., 2020). In addition, specific bacteria can boost the growth speed of microalgae by providing essential nutrients. These bacteria break down nutrients into forms that microalgae can easily absorb, like ammonia or nitrate (Zhu *et al*., 2011).

1.7 Overview of microalgae cultivation techniques

There are two main types of microalgal cultivation techniques: open ponds and closed photobioreactors. Several systems have been designed for the cultivation of microalgae which are dependent on the type of microalgae and their applications. Microalgae have been cultivated in natural systems such as ponds, lagoons, and lakes for a long time. However, the cultivation of microalgae has been practiced by humans for many years, even beyond the 100-year timeframe mentioned. For instance, the Aztecs harvested *Arthrospira* sp., in Lake Texcoco

in the 14th century (Thorat *et al*., 2023). In the mid-nineteenth century, work on artificial culture of microalgae started in Europe (Qin *et al*., 2023). The specific techniques and systems used in microalgae cultivation have evolved significantly over the years (Moheimani *et al*., 2015; Sarker and Kaparaju, 2023). Today, microalgae are cultivated using various techniques, including autotrophic, heterotrophic, and mixotrophic cultivation, and can be done in open ponds or closed photobioreactors (PBRs) (Sarker and Kaparaju, 2023).

1.7.1 Open ponds

Raceway ponds are shallow concrete trenches lined with thick plastics using a simple design that allows high biomass production with low maintenance and operation costs. Open raceway ponds are oval-shaped channels with a depth of 0.2 to 0.5 m and mechanical devices for mixing with a velocity range of 0.15 to 0.25 m/s (Doucha & Livansky, 2006). The advantages of raceway ponds include a simple design for high biomass production, low maintenance costs, and relatively simple operation. However, they also have some drawbacks such as contamination by microbes, low carbon dioxide diffusion, high evaporation of media, and large surface area (Ugwu *et al.,* 2008). The key parameters of an open pond for microalgal cultivation are sunlight, nutrition, carbon dioxide, and hydrodynamics (Hadiyanto *et al.,* 2013). Open systems require mechanical methods such as proper mixing and environmental properties which make it more difficult to manage on a large scale owing to pollution and contaminants which are related to mass transfers. Studies have investigated the adaptation of algal species to environmental conditions in open cultivation, as well as their tolerance to flue gas mitigation (Hamasaki *et al.,* 1994).

Figure 1.2 Open raceway microalgae production pond adapted from (Kumar and Jain, 2014).

1.7.2 Closed system photobioreactor

Closed systems, also known as photobioreactors (PBRs), are transparent containers specifically designed for the cultivation of microalgae. Different models of photobioreactor cultivation systems have been patented and developed with different geometries and sizes (Singh and Sharma, 2012). Among the patented PBR types are vertical bubble columns and airlift reactors, tubular photobioreactors, helical photobioreactors, combined bubble column and inclined tubular reactors, and flat plate photobioreactors. There are some limitations associated with photobioreactors such as high installation costs and maintenance (Ugwu *et al.,* 2008). Photobioreactors are mostly designed to produce high biomass owing to their optimum environmental conditions. These reactors are designed with exchange ports or vessels connected to the main reactor for the provision of other conditions during cultivation, such as carbon supply, nutrients, and oxygen removal (Jacob-Lopes *et al.,* 2010). Closed photobioreactors are favoured over raceway ponds because they demonstrate high carbon dioxide capture efficiencies, low water loss through evaporation, and high biomass productivity (Wilson *et al.,* 2016), and are therefore less prone to contamination. However, the elevated maintenance costs associated with photobioreactors could be reduced through the utilisation of cost-effective materials, such as wastewater, and by employing energy-efficient pumps to facilitate resource recovery.

1.7.2.1 Flat Panel Photobioreactor

A flat panel photobioreactor is a type of reactor consisting of a series of transparent plates arranged parallel to each other, forming a thin layer of culture medium between them. These reactors are exposed to natural or artificial light to absorb energy for photosynthesis, through which carbon supplements are provided by either sparging or dissolving in the medium (Fuchs *et al*., 2021). The flat panel photobioreactor provides a high and uniform light input for microalgae growth, reduces contamination risk, facilitates gas exchange, and enhances mass transfer. These reactors can be used to improve the quality and quantity of functional biomolecules, such as lipids, carbohydrates, and pigments, by manipulating the carbon dioxide concentration and light intensity (Benner *et al*., 2022). They can be integrated with greenhouses to provide a symbiotic relationship between microalgae and fungi, where microalgae can utilise the carbon dioxide released by fungi (Sukačová *et al*., 2021).

Figure 1.3 Picture of an indoor aerated flat panel photobioreactor adapted from (Carvalho *et al*., 2006).

1.7.2.2 Tubular photobioreactor

Tubular photobioreactors are commonly present in three configurations: airlift and bubble column, characterised by transparent vertical tubing forming a vertical tubular reactor enabling light penetration and carbon dioxide supply through bubbling, the horizontal tubular reactor, composed of horizontal transparent tubing, often equipped with gas transfer systems at the connections; and lastly the helical tubular reactor, constructed from a flexible plastic tube coiled in a circular pattern. The airlift reactor boasts the advantageous characteristic of generating a circular mixing pattern, enabling the continuous passage of liquid culture through both dark and light phases. This results in a flashing light effect for algal cells. The proposal also includes the utilisation of a rectangular airlift photobioreactor, which is noted for improved mixing characteristics and higher photosynthetic efficiency. However, its drawback lies in its complexity and challenges in scaling up the system (Egbo *et al*., 2018).

1.7.2.3 Bubble column photobioreactor

Bubble columns are the predominant type among vertical tubular photobioreactors. These reactors are characterised by their height, which is over twice their diameter, resulting in a high ratio of surface area to volume. They are designed to provide efficient mass transfer and gas-liquid interfacial transfer (Van Tran *et al.,* 2018). The size and rate of bubbles affect mass transfer and distribution and promote algal growth within the reactor. Some of the factors that influence the mechanism of the bubble are gas flow velocity, and carbon dioxide concentration which contribute to adsorption by microalgae cells (Ding *et al*., 2016). A smaller capillary size and larger carbon dioxide concentration can result in a decrease in bubble detachment and increase in velocity which is an advantage for carbon dioxide transportation

and utilisation (Holdt *et al*., 2014). The formation of bubbles created by the force propels the liquid/gas by creating a continuous cycle of fluid circulation within the photobioreactor (Egbo *et al*., 2018; Narala *et al*., 2016). The efficiency of photosynthesis is significantly influenced by the gas flow rate, which, in turn, is dependent on the light and dark cycles. This occurs as the liquid circulates regularly from the central dark zone to the external photic zone at a higher gas flow rate (Janssen *et al*., 2003; Singh and Sharma, 2012).

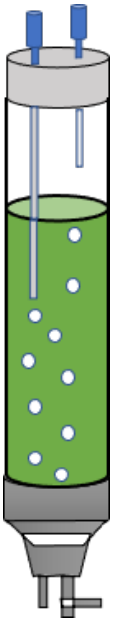

Figure 1.4 A schematic diagram of bubble column photobioreactor

1.8 Biochemical compositions in microalgae

Microalgae biomass are excellent sources of diverse bioactive compounds such as lipids, proteins, carbohydrates, chlorophylls, carotenoids, phycobiliproteins. These high value-added products have been identified as potential sources for food, pharmaceuticals, nutraceuticals, and cosmetics industries (Chew *et al*., 2017). For example, microalga *Dunaliella salina* is known to produce vitamin A and E, as well as pyridoxine, nicotinic acid, thiamine, riboflavin, and biotin (Seyfabadi *et al*., 2010) while *Porphyridium cruentum* produces substantial amounts of vitamins E and C and *Haslea ostrearia* for vitamin E (tocopherols) (Hosseini Tafreshi and Shariati, 2009; Khan *et al*., 2018).

Table 1.1 Biochemical composition of different species of microalgae.

Species	Carbohydrate (%)	Lipid (%)	Protein (%)	Reference
Nannochloropsis oculata	33	11	56	(Wan Mahari *et al*., 2022)
Chlorella vulgaris	12-17	14-22	51-58	(López *et al*., 2010)
Porphyridium cruentum	40-57	9-14	28-39	(Becker, 2007)
Scenedesmus obliquus	10-17	12-14	48-56	(López *et al*., 2010)
Spirulina maxima	13-16	6-7	60-71	(Becker, 2007)
Phaeodactylum tricornutum	16.8	16.1	34.8	(Brown, 1991)
Nannochloropsis granulata	27-36	24-28	18-34	(Tibbetts *et al*., 2015)

1.8.1 Lipids

The lipid content in microalgae can vary between 4-30% depending on the microalgal species, culture medium, and other growth parameters. Under conditions of high salt, intense light, and limited nutrients like nitrogen and phosphorus, microalgae have the ability to produce lipids in excess (Sulochana and Arumugam, 2020). Under nutrient stress, microalgae undergo a metabolic shift in the synthesis and accumulation of triacylglycerols, constituting up to 80% of the total lipid content in the cell (Kwak *et al*., 2016). Major lipid components present in microalgae biomass are triacylglycerides (TAG), other lipids such as phospholipids and glycolipids. Lipids from microalgae are being produced by many industries such as AlgaeCytes Ltd for applications in the pharmaceuticals and food industries (Yen *et al*., 2013). Extraction of lipid from microalgal biomass can be achieved through solvent extraction, ultrasonic extraction, and microwave-assisted extraction, although each technique has its drawbacks, such as high operational temperature, low selectivity, high organic solvent consumption, and high energy consumption. Solvent-free processes, including osmotic pressure, enzyme extraction, and isotonic extraction, are also available for extracting lipids from microalgal biomass. Following the extraction of high-value products such as ß-carotene, astaxanthin, docosahexaenoic acid, phycobilin pigments, flavonoids, and polysaccharides while the spent biomass is being utilised for other industrial purposes such as animal feed and fertilisers (Hernández *et al*., 2014). Other extraction methods, such as ultrasound-assisted extraction, is known to improve lipid yields with shorter reaction times (Cravotto *et al*., 2008).

Another technique, known as supercritical fluid extraction, is suitable for indoor and small-scale experiments. A study on *N. oleoabundans* under normal growth conditions produce 10-30% of lipid content but under stress conditions, such as nutrient and light intensity, can influence biomass content beyond ≥ 50% (Schenk *et al*., 2008). Selection of the right solvent

is crucial for the effective extraction of lipids by industries because neutral lipids dissolve well in nonpolar organic solvents, while polar lipids, particularly glycerophospholipids (fatty acid-glycerol-phosphate ester) are soluble in polar solvents (Saini *et al*., 2021). Therefore, a mixture of solvents (chloroform/methanol), including polar ones to break down the lipids from cell membranes and lipoproteins, and nonpolar ones to dissolve the neutral lipids, is ideal for efficient lipid extraction from biological tissue (Saini *et al*., 2021). These extraction methods are less expensive, less volatile, non-toxic, and highly selective for lipids. These neutral lipids can be converted to fatty acid methyl esters (FAMEs) with the dominant profiles of palmitic acid and stearic acid, which have been demonstrated to be the most effective to produce biofuel (Ge *et al*., 2017).

1.8.2 Proteins

Microalgae are capable of synthesising all essential amino acids within their cells, resulting in a high protein content. Higher quantities of different amino acids and proteins which can be utilised in food and protect the body against diseases are found in many microalgal species which makes them a great alternative to other proteins like fish meals (Ravindran *et al*., 2016). About 2.5-7.5 tons/Ha/year of proteins are being produced by microalgae according to (Bleakley and Hayes, 2017). The composition of amino acids in algae is positively comparable to that of other proteins (Williams and Laurens, 2010a). In addition, proteins have both structural and metabolic functions, with cellular proteins forming a significant part of the photosynthetic pathway, cell growth mechanisms, and CO_2 fixation pathways (Lee *et al*., 2010). Moreover, microalgal species with elevated protein levels can be considered an excellent nutrient source for functional foods, nutraceuticals, and food additives. Microalgal species such as *Spirulina maxima* (60%–71%), *Synechoccus* sp. (63%), *Anabaena cylindrical* (43%–56%), and *Chlorella vulgaris* (41%–58%) have been reported to exhibit exceptionally high protein content (Ahmad *et al*., 2022; Ravindran *et al*., 2016). Microalgae can synthesise all amino acid molecules, amino acids derived from algae are favoured over other sources of protein-rich foods (Guil-Guerrero *et al*., 2004). An additional protein extracted from microalgae is R-phycoerythrin, a type of phycobiliprotein commonly employed as a fluorescent dye in diagnostic and research applications (Sekar and Chandramohan, 2008).

1.8.3 Carbohydrates

Microalgae are rich in carbohydrates, a broad group that includes sugars (monosaccharides) and their polymers (di-, oligo-, and polysaccharides), which perform both

structural and metabolic roles. The carbohydrates that are most prevalent are primarily glucose (21%-87%), galactose (1%-20%), and mannose (2%-46%) (Gorgônio *et al*., 2013). Carbohydrates in algal cells are synthesised within the chloroplast, whereas in prokaryotes, carbohydrate synthesis occurs in the cytosol (Ravindran *et al*., 2016). The percentage of carbohydrates within the cells depends on the microalgal species, cultivation methods, and conditions. Several microalgal species, including *Spirogyra* sp. (33%-64%), *Porphyridium cruentum* (40%-57%), *Chlorella emersonii* (37.9%), and *Chlorogloeopsis fritschii* (37.8%), possess high carbohydrate contents (Biller and Ross, 2014; Ravindran *et al*., 2016). Carbohydrates from microalgae biomass are used as precursors or feedstocks for biofuel production (MARKOU *et al*., 2014). These compounds can be utilised in various industries, such as cosmetics, food products, and natural therapeutic treatments (Karemore & Sen, 2016).

1.8.4 Pigments

Pigments are coloured molecules present in photosynthetic organisms which function in harvesting light and photoprotection. Absorption of light by photosynthetic pigments converts photons into chemical energy to produce biomass, lipids, carbohydrates, and proteins. Photosynthetic pigments found in microalgae are categorised into chlorophylls, carotenoids, and phycobilins. The primary light harvesting pigment in all photosynthetic organisms is chlorophyll which comes in different forms such as chlorophyll-*a*, chlorophyll-*b*, and chlorophyll-*c*. It comprises of a porphyrin ring containing a magnesium ion and phytol ester side chain (Egeland, 2016). For example, chlorophyll-*a* absorbs light at different wavelength within the red (740-590 nm), blue (520-435 nm), and violet (435-380 nm) wavelength while mainly reflecting green (565-520 nm). Carotenes are a class of tetraterpenoid pigments derived from eight isoprene units, terminating in cyclic β-ionone rings (e.g., β-carotene). Xanthophylls are derived from the addition of oxygenated functional groups to carotenes (e.g., violaxanthin, astaxanthin or fucoxanthin). They play a role in light harvesting and photoprotection through the xanthophyll cycle (Egeland, 2016). These pigments are applied for several industrial purposes, such as pharmaceuticals, cosmetics, food additives as colouring agents, and biomaterials (Krupa *et al*., 2010). Photosynthetic pigments such as chlorophyll and carotenoids such as ß-carotene, xanthophylls, fucoxanthin, zeaxanthin are fat-soluble pigments with a chemical formula which provides unique colour identification to some parts of plants (Chen *et al*., 2016).

Pigments are very sensitive to light and temperature and for precise quantification, pigment extraction should be undertaken on freeze dried biomass with ice cold solvents and

under subdued lighting. The organic solvent and Soxhlet method of extracting carotenoids are the major techniques applied to microalgal biomass. This process was used to achieve the maximum degree of affinity for carotenoids. Other methods, such as supercritical fluid extraction (SFE), require low selectivity and less solvents (Nobre *et al*., 2013). Other techniques have been applied to disrupt microalgal cells to extract maximum bioactive compounds such as zeaxanthin which forms types of carotenoid compounds (Singh *et al*., 2013). Phycobiliproteins, found in cyanobacteria, red algae, cryptomonads, and cyanelles, are water-soluble photosynthetic light-harvesting proteins. These water-soluble proteins are characterised by covalent binding through cysteine amino acid chromophores known as phycobilins (Kovaleski *et al*., 2022). The extraction of water soluble phycoerythrin is more efficient due to their accelerated molecular diffusion and solubility of other proteins compared to other pigments which is related to temperature and extraction processes (Castro-Varela *et al*., 2022). One of the factors that positively influences phycobiliproteins production is their chromatic adaptability to specific wavelength like red, green, and blue which plays a specific role in the photosynthetic activity of *Porphyridium purpureum* (H. B. Chen *et al*., 2010). In functional terms, the phycoerythrin-chlorophyll complex in rhodophytes and the peridinin-chlorophyll complex in dinoflagellates capture photons. This process broadens the range of the spectrum that can be utilised for photosynthesis (Williams and Laurens, 2010b). A study on cyanobacterium *Nostoc* sp. showed significant changes in phycobiliprotein levels in response to specific LED wavelengths under red wavelengths results in an elevated phycocyanin production, whereas exposure to green wavelengths induces an increased synthesis of phycoerythrin (Johnson *et al*., 2014a). Phycobilin has been used in various pharmaceutical and food applications owing to its antiviral, anticancer, antioxidant, anti-inflammatory, and anti-allergic effects (Tang *et al*. 2020).

1.9 Project rationale and gaps

Microalgae have generated a lot of interest in carbon capture from various industries, as well as the generation of high-value products including biofuels and food supplements (Sharma *et al*., 2018; Tripathi *et al*., 2023). However, the CO_2 generated from mushroom farms has not yet been explored in this context. Given the growing mushroom industry in several parts of the world, there is a need for a process that can capture and utilise waste CO_2 from mushroom farming to promote high mushroom yields and quality, whilst preventing the environmental issues associated with CO_2 release into the atmosphere. Microalgal cultivation

offers a promising technique for the photosynthetic fixation of CO_2 from gas streams to generate valuable bioproducts. However, gas-liquid mass transfer issues limit the extent of direct conversion of CO_2 by microalgae (González-López *et al*., 2012). Moreover, mushroom farming generates large quantities of spent substrate, which are currently untapped resources for high-value products. This research aims to address these gaps developing a microalgal carbon capture system that can be integrated into mushroom farms. This system involves the conversion of gaseous CO_2 into inorganic carbon in the medium, which can be more readily utilised by microalgae. A second aspect of this research is the evaluation of the potential of spent algal biomass and the spent mushroom substrate for generating high-value products to contribute to a circular process.

1.10 Hypotheses

Based on the rationale discussed above, the following hypotheses were tested in this work:

1. The ability of different algal species to tolerate bicarbonate can influence their growth patterns, biochemical composition, and how efficiently they use carbon when exposed to varying levels of bicarbonate.
2. The waste CO_2 from mushroom farming can be used as a carbon source for microalgal cultivation via conversion into inorganic carbon-based growth media.
3. Value-added compounds can be extracted from the spent algal biomass as well as the spent mushroom substrate to contribute to the sustainability of the integrated microalgal carbon capture process.

1.11 Aims and objectives

The overall aim of this research project is to develop a microalgal carbon capture system that can be integrated into mushroom farm for efficient carbon capture as well as the production of value-added products from the spent algal biomass and mushroom waste.

The objectives designed to accomplish the aim are as follows:

a. To select the most suitable microalgal species in a bicarbonate-based system based on the carbon capture efficiency and biochemical composition.
b. To design a two-step integrated bicarbonate-based system for capturing carbon dioxide generated during mushroom growth and estimate the carbon utilisation efficiency of microalgae species.

c. To demonstrate the scalability of the bicarbonate-based integrated algal production system for carbon capture during mushroom cultivation and assess the properties of valuable products extracted from microalgal biomass and mushroom exudate for potential applications.

CHAPTER 2

2.1 Materials and Methods

2.1.1 Preparation of microalgal growth media

Modified growth media was prepared by following protocol on media recipes from the Culture Collection of algae protozoa (CCAP) (Walter L. Smith, 1975) supplemented with sodium bicarbonate, $NaHCO_3$ as inorganic carbon source for entire experimental process in table 2.1. All culture media were prepared using deionised water (dH_2O) and sterilised by autoclaving at 121 °C for 60 minutes. For marine species, marine salt was added to their media and filtered to remove any precipitates after sterilisation before inoculation. The pH of the stock cultures was consistently monitored to maintain the optimal growth pH. An electronic pH meter (Orion Star A211, Thermo Scientific) was used to adjust the pH between 7.5 and 8.0 using 1.0 M sodium hydroxide (NaOH) and hydrochloric acid (HCl). All the microalgae cultures were incubated at 25 °C with continuous illumination at 50 - 200 µmol m^{-2} s^{-1} light. The listed microalgal strains from table 2.1 were provided by AlgaeCytes Ltd based on their high value-added products and research requirements.

Table 2.1 Represent the list of selected microalgae strains for the inorganic carbon tolerance study.

No	Strain ID	Taxonomic Identification	Growth media (CCAP)	pH study	Carbon Capture
1	ALG04	*Parachlorella kessleri*	BG-11	-	-
2	ALG05	*Scenedesmus quadricauda*	BG-11	-	-
3	ALG06	*Vischeria* sp.	BG-11	BBM	NaOH-BBM
4	ALG15	*Phaeodactylum tricornutum*	*f/2* + marine salt	-	-
5	ALG16	*Porphyridium purpureum*	*f/2* + marine salt	BBM + marine salt	NaOH-BBM + marine salt

Marine salt: Tropic Marin® (The aquatic life science company, Switzerland).

CCAP: https://www.ccap.ac.uk/index.php/media-recipes/

2.1.2 Preservation of microalgae cells on broth agar

Microalgal cultures were preserved by dissolving 2% agar (bacteriological agar) in 20 mL L^{-1} of medium (Bold's Basal medium-BBM or Blue-green medium, BG-11). For 1 L media solution, 20 mL L^{-1} of BBM or BG-11 and 20 g of agar was dissolved into 1 L of deionised

water. The agar media was autoclaved at about 40 minutes and allowed to cool down before transferring into storage plates. After solidification of the agar media, the plates are stored or ready for streaking with microalgae cells. This preparation process was performed using aseptic techniques, about 10 - 15 µL of liquid algae culture inoculum or using inoculum loop for streaking across the surface of the agar plates and stored 24ºC in incubator.

2.1.3 BG11 medium

The BG11 medium was prepared using a modified version (Allen, 1968) with sodium bicarbonate ($NaHCO_3$) concentrations from table 2.2. Gram per litre of the BG11 medium. The culture media solutions were autoclaved at 121 °C for 15 min, and the pH was adjusted to 7.5 with 1 M NaOH or HCl using an electronic pH meter (Orion Star A211, Thermo Scientific).

Table 2.2 Media recipe for Blue-Green algae (BG-11)

Medium	Component	Per 500ml dH_2O
Blue - Green (BG11)	$NaNO_3$	75.00 g
	K_2HPO_4	2.00 g
	$MgSO_4.7H_2O$	3.75 g
	$CaCl_2.2H_2O$	1.80 g
	Citric acid	0.30 g
	Ammonium ferric citrate green	0.30 g
	$EDTANa_2$	0.05 g
	Na_2CO_3	1.00 g
Trace metals solution		Per litre dH_2O
	H_3BO_3	2.860 g
	$MnCl_2.4H_2O$	1.810 g
	$ZnSO_4.7H_2O$	0.220 g
	$Na_2MoO_4.2H_2O$	0.390 g
	$CuSO_4.5H_2O$	0.050 g

2.1.4 Synthetic media and mushroom-bicarbonate culture media

Culture media supplemented with purchased sodium bicarbonate (Sigma-Aldrich) is referred to as ‘synthetic media’ (commercial sodium bicarbonate high purity grade) and mushroom-bicarbonate media generated from the mushroom production as a result of carbon capture is referred to as ‘mushroom-bicarbonate’ media.

2.1.5 Guillard’s *f/2* medium

Modified Guillard’s *f/2* medium was prepared using (Walter L. Smith, 1975) sodium bicarbonate ($NaHCO_3$) and tropic marine salt table 2.3. All chemicals were purchased from Sigma–Aldrich. The culture media solutions were autoclaved at 121 °C for 15 min, and the pH

was adjusted to 7.5 with 1 M NaOH or HCl using an electronic pH meter (Orion Star A211, Thermo Scientific). To prepare *f/2* 'Quad' medium, 4.0 mL of nitrate ($NaNO_3$) and phosphate ($NaH_2PO_4.2H_2O$) stock solutions were used (Lananan et al., 2013).

Table 2.3 Media recipe for *f/2* preparation

Medium	Component	Per 400ml dH_2O
	$NaNO_3$	75.00 g
	$NaH_2PO_4.H_20$	5.65 g
	Trace metals solution	Per litre dH_2O
	Na_2.EDTA	4.160 g
	$FeCl_3.6H_2O$	3.150 g
	$CuSO_4.5H_2O$	0.010 g
	$MnCl_2.4H_2O$	0.180 g
	$Na_2MoO_4.2H_2O$	0.006 g
	Vitamins	Per litre dH_2O
	Cyanocobalamin (Vitamin	0.0005 g
	B_{12})	0.1000g
	Thiamine HCl (Vitamin B_1)	0.0500 g
	Biotin	

2.1.6 Bold's Basal medium for carbon capture (NaOH-BBM)

The Bold's Basal medium composition for carbon capture was prepared using a modified version by adding 3 g L^{-1} NaOH to the media recipe from Table 2.4. To prepare per litre media, 10 mL of each macronutrient and 1 mL each of trace stocks by adjusting pH of 7.5 using 1.0 M NaOH or HCl using an electronic pH meter (Orion Star A211; Thermo Scientific).

Table 2.4 Media recipe for Bold's Basal Medium (BBM)

BBM	Components	Per 400ml dH_2O
	$NaNO_3$	10.00 g
	$MgSO_4.7H_20$	3.00 g
	NaCl	1.00 g
	K_2HPO_4	3.00 g
	KH_2PO_4	7.00 g
	$CaCl_2.H_2O$	1.00 g
Trace metals solution	$ZnSO_4.7H_2O$	Per litre dH_2O
	$MnCl_2.4H_2O$	8.82 g
	MoO_3	1.44 g
	Co $(NO_3)_2.6H_2O$	0.71 g
	$CuSO_4.5H_2O$	0.49 g
		1.57 g
	H_3BO_3	Per litre dH_2O
	Alkaline EDTA solution	11.42 g
	KOH	50.00 g
	$FeSO_4.7H_2O$	31.00 g
	H_2SO_4	4.98 g
		1.00 mL

2.1.7 Preparation of start-up cultures growth

All sample cultures were prepared aseptically within a laminar flow hood system. Microalgae agar plates were observed using microscope with 40x magnification minimum (Leica DM2500, Germany) for possible bacteria or fungi contaminations. An autoclaved media of 50 mL working volume in 150 mL Erlenmeyer flask was inoculated with microalgae cells from streaked agar plates (revive cells). The flasks were labelled and incubated at 25^{o}C temperature with 150 µmol/m^2/s light (BT-881D lux meter). Microalgal growth (optical density) was measured at 680 nm using a Multiskan Go microplate spectrophotometer (1510-04220C Thermo Scientific, UK).

2.1.8 Sub-culturing/transferring liquid cultures

The cultures were observed under a microscope for possible contamination before transferring. For subculturing, a part of stock culture was transferred into a new sterile media of 250 mL in an Erlenmeyer flask. The initial cultures were refilled with fresh media by flaming the flask neck using a Bunsen burner before replacing with foil caps under the laminar flow hood. Stock culture was transferred into a 50 mL centrifuge tube and centrifuged at 1000 *g* to remove dead cells and the supernatant was discarded, the cells were washed with deionised water before resuspended in an autoclaved media.

2.2 Mushroom cultivation processes

2.2.1 Spawn and substrate processing

Commercial Oyster mushroom *Pleurotus ostreatus var. florida* (mycelia spawn) and mushroom grow kit (straw substrate) were purchased from Urban-Farm it, Kent, UK. Straw substrate (800 g) in a polypropylene bag (30.5 cm x 22.9 cm x 15.2 cm) was autoclaved with distilled water and left overnight to cool. The water was drained off and placed under a laminar flow hood to reduce the moisture content about 60 - 70% (Iqbal Muhammad, 2005). Under aseptic conditions, about 150 g of mushroom spawn was well-mixed with the sterilised substrate to ensure uniform distribution of the inoculum and transferred into plastic trays (Figure 2.1). The trays were covered with aluminium foil and placed in an incubator for colonisation by the mycelia before transferring into a growth box (60 cm × 40 cm × 25 cm). After 10 – 14 days of incubation with full colonisation by the mycelia growth, the aluminium foils were removed for pinning phase of mushroom fruiting bodies. The mycelia cakes were transferred into growth box (60 cm × 40 cm × 25 cm) designed using a transparent container.

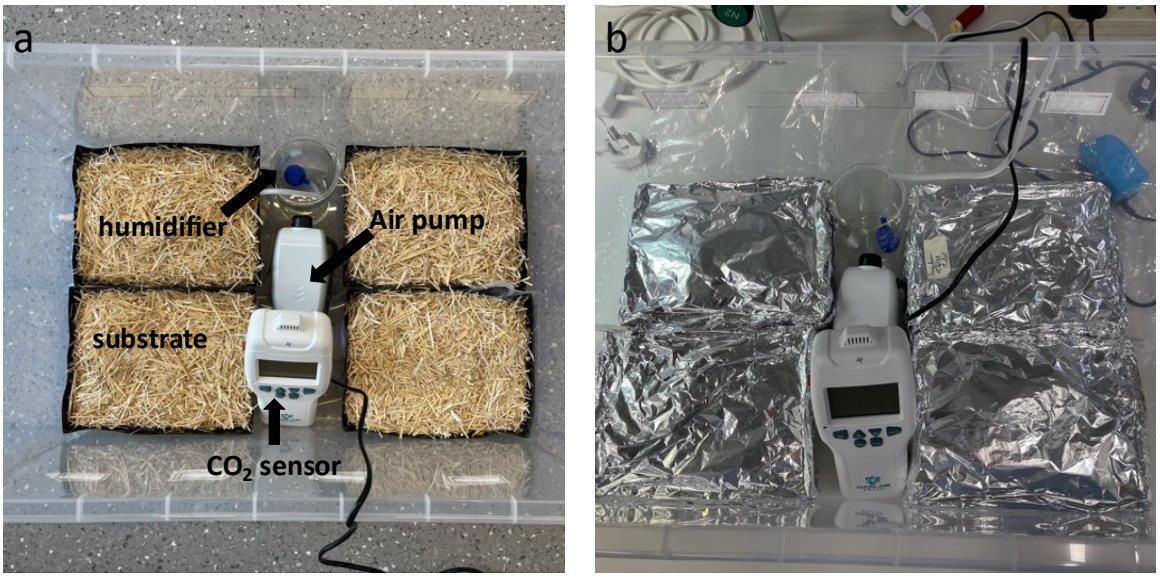

Figure 2.1 Schematic showing (a) preparation of mushroom substrate before inoculation in growth box connected with carbon dioxide monitor, air pump, and humidifier to control cultivation conditions during fruiting stage, (b) inoculated substrate covered in foils before incubation for mycelia colonisation.

2.2.2 Cultivation of *Pleurotus ostreatus* for CO_2 measurement

The construction of the growth box used can be seen in Figure 2.1, using a transparent and light-transmitting ability plastic container with a volume of 60 litres. About 6-8 holes were drilled on each side of the box at 15-20 cm from the top. The holes were covered with sterile filter sheets to create gas exchange for the mushroom during observation of different CO_2 concentrations on the fruiting bodies shown in Figure 4.3. A separate hole was made to connect the air pump (Pawfy MC-3000, UK) inside the box to transfer gas from the box to the absorption media. An air pump hose was connected to a beaker with autoclaved water to create humidity for the mushrooms. A CM-501 GasLab monitor was placed in the box for measuring CO_2, temperature, and humidity in the box. The chamber was connected with light which is needed for pinhead initiation and to set the direction of growth for mushroom bodies. The picture of the system control is shown in Figure 2.2 with the help of the GasLab monitor to determine the growth conditions. The relative humidity was maintained between 80 – 90% with an autoclaved water connected with a sparger from the air pump to keep the temperature between 23 – 25°C. During the pinning phase, the concentration carbon dioxide emitted by the mycelia was measured. From Figure 2.2, 2 L BBM media coupled with sodium hydroxide (3 g L^{-1}) was used as the absorption unit for the carbon capture. A small air pump was placed

inside the growth box connected with the enriched NaOH-BBM with filters. The concentrated carbon dioxide in the growth box was transferred into the media and the pH was continuously monitored. After monitoring the decrease in pH, the inorganic carbon was estimated using titrimetric method to determine the total inorganic carbon absorbed in the media (section 2.4.5).

Figure 2.2 Experimental setup for carbon dioxide harvesting from mushroom production to generate inorganic carbon media for microalgae cultivation.

2.3 Photobioreactor (PBR) scale-up

Glass bubble column photobioreactors (PBR) of 8-10 L capacity with 5 L working volume (length 100 cm, 110 mm OD, 104 mm ID) with an inlet/outlet port for sparging and sampling were used for scale-up cultivation. The bubble column photobioreactors were provided by AlgaeCytes Ltd. For the scale-up processes, an autoclaved bicarbonate media from the carbon capture set up was transferred into the bubble column photobioreactor. The bubble columns were illuminated with an intensity of 150 µmol/m^2/s^2 and an air pump (Pawfy MC-3000) with a flow rate of 5 L/min. To investigate the overall cultivation parameters such as growth, inorganic carbon utilisation, and pH of the media was studied by continuous measurement. The scale–up cultivation parameters were set before inoculation. Experimental measurements were analysed by taking samples for optical density and inorganic carbon removal every two days to establish mass balance.

Figure 2.3 Bubble column photobioreactor scale-up with bicarbonate media generated from mushroom production before inoculation.

2.4 Analytical methods

All experimental procedures were performed within the University laboratory, while the analytical techniques such as High-performance liquid chromatography, Gas chromatography – flame ionisation detector, and Fourier transform infrared spectroscopy were executed at the AlgaeCytes Ltd laboratories.

2.4.1 Microalgae growth measurement

The initially optical density reported in chapter 3 was recorded at 680 nm. However, after further reviews, the optical density was changed to 750 nm because chlorophyll-*a* absorbs light within the red (740-590nm), blue (520-435nm) and violet (435-380nm) wavelengths while mainly reflecting green (565-520nm). The standard growth media used were BG-11, BBM, and *f/2* described in section 2.1. The optical density for the experimental reactors were measured at 750 nm Multiskan Go microplate spectrophotometer (1510-04220C Thermo Scientific, UK) every two days and their specific growth rate (μ, d^{-1}) was calculated using equation (2.1) below:

$$\mu = \frac{\ln (OD_2 / OD_1)}{t_2 - t_1} \quad (2.1)$$

where OD_1 and OD_2 are the beginning and end of the growth phase, respectively, and t_2 and t_1 denote the end and start days of cultivation, respectively.

2.4.2 Determination of biomass concentration

For biomass concentration, an aliquot of 10 mL of culture was sampled and centrifuged at 3000 *g* for 3 min, and the cells were washed twice with deionised water to remove media traces (freshwater species) whiles ammonium formate was used to remove salt traces from the marine species. The biomass pellets were filtered using a 1.5 µm pore size (Whatman Cat No. 1822–070 GF/C), and dried at 50 °C for 24 h. The resulting biomass content (*c*) was calculated according to this formula:

$$\text{Biomass concentration (g L}^{-1}) = \text{m} / 0.01 \text{ L} \quad (2.2)$$

where *m* is the mass of the estimated dry weight after determining the difference between the pre-weighed filter paper and biomass-filtered paper.

2.4.3 Determination of inorganic carbon removal rate

The inorganic carbon removal rate (mg $L^{-1}d^{-1}$) was calculated as the difference between the initial and final concentrations divided by the number of days of cultivation.

$$\text{IC removal rate} = \frac{IC_i - IC_f}{t} \quad (2.3)$$

Where IC_i is the initial and IC_f final concentrations of inorganic carbonate present in the cultivation media and t, days.

2.4.4 Estimation of Phycobiliprotein (PBP) content

The total phycobiliprotein content was estimated using modified freeze-thaw method by adding 5 mg of lyophilised algal biomass to 1.5 mL 0.1 M L^{-1} phosphate buffer (pH 6.8) and freeze at − 20ºC for 24 hrs (Mc Gee *et al*., 2020a). The extracts were thawed at room temperature and vortexed with glass beads for 5 min. The extraction process was repeated in triplicates, and the samples were centrifuged at 3000 *g* for 5 min. The absorbance of the supernatants was measured at 455, 564, 592, 618, and 645 nm using a Multiskan Go microplate spectrophotometer (1510-04220C Thermo Scientific, UK) to determine phycoerythrin (PE) and phycocyanin (PC) content using the equations developed by (Beer and Eshel, 1985).

$$PE = [(OD_{564nm} - OD_{592nm}) - (OD_{455nm} - OD_{592nm}) \times 0.2] \times 0.12 \quad (2.4)$$

$$PC = [(OD_{618nm} - OD_{645nm}) - (OD_{592nm} - OD_{645nm}) \times 0.51] \times 0.15 \quad (2.5)$$

Where PE (mg mL^{-1}) and PC (mg mL^{-1}) represents phycoerythrin and phycocyanin respectively.

2.4.5 Inorganic carbon utilisation efficiency (HCO_3^-)

At pH 8.2 to 8.4, the alkalinity of bicarbonate is found in most natural waters, and carbon dioxide (CO_2) ceases to exist in measurable quantities above this pH. The carbonate and bicarbonate ions mostly exist together at pH above 8.2 to 9.6 and the distribution of these two ions can be determined by measuring the phenolphthalein and methyl-orange alkalinities using the equation below. According to DeMartini (1938), the equations based on the three forms of alkalinity using the hydrogen ion concentration and total alkalinity of water are as follows:

$$HCO_3^- = \frac{50{,}000 \times [\frac{Alk}{50{,}000} + (H^+) - \frac{10^{-14}}{(H+)}}{1 + \frac{11.22 \times 10^{-11}}{(H^+)}} \quad (2.6)$$

$$(CO_2) = 9.70 \times 10^{10}(H^+) \times \frac{[\frac{Alk}{50{,}000} + (H^+) - \frac{10^{-14}}{(H^+)}}{1 + \frac{11.22 \times 10^{-11}}{(H^+)}} \quad (2.7)$$

$$(CO_3^-) = \frac{5.61 \times 10^{-6}}{(H^+)} \times \frac{[\frac{Alk}{50{,}000} + (H^+) - \frac{10^{-14}}{(H^+)}}{1 + \frac{11.22 \times 10^{-11}}{(H^+)}} \quad (2.8)$$

$$(OH^-) = \frac{5 \times 10^{-10}}{(H^+)} \quad (2.9)$$

All the samples were centrifuged, and the supernatants were titrated against 0.02 N of standardised sulfuric acid (H_2SO_4). An aliquot of 10 - 15 mL of the culture media was centrifuge at 3000 *g*, the supernatant was transferred into in a beaker with 2 drops of phenolphthalein indicator titrated against 0.02N sulfuric acid for the first endpoint. The titration was followed by 2 drops of methyl orange indicator with the same sample and titrating against the acid to reach the second endpoint. The final reading was also noted, and these readings were used to determine the dissolved inorganic species (H_2CO_3, HCO_3^-, CO_3^{2-}) to determine the total alkalinity in the culture media.

2.4.6 Pigment analysis on biomass composition

The harvested algal biomass was analysed for pigment content using reverse-phase high-performance liquid chromatography (C18-RP HPLC). For sample preparation,

approximately 4-5 mg of each freeze-dried biomass sample was transferred into a 2 mL tube and two scoops of glass beads (~500mg) were added. The samples were extracted using 1 mL of organic solvent (acetone: methanol, 7:3 v/v) containing an internal standard (α-tocopherol acetate, 100 mg L^{-1}) by homogenizing them in a VelociRuptor V2 Microtube Homo ™ (, SLS1401) at 6.00 m/s for 15 seconds (3x cycles). The extracts were filtered through a 0.2 µm PTFE syringe filter into 2 mL RP-HPLC vials and analysed using a Hewlett Packard instrument with a Nova-Pak C18 4 µm, 3.9x150 mm column with a guard column. The injection volume was 25 µL, the flow rate was 1 mL/min, and the run time was 24 min. The mobile phase A consisted of methanol:0.5 M ammonium acetate (80:20 v/v), the mobile phase B consisted of acetonitrile: deionized water (90:10 v/v), and the mobile phase C consisted of 100% ethyl acetate (Coward *et al*., 2016). Pigments were detected by absorbance of 440 nm and identified by comparison of retention time and spectra from the internal standards within AlgaeCytes laboratory.

2.4.7 Estimation of total lipids

The lipid content of the freeze-dried microalgal biomass was determined by converting cellular fatty acids into fatty acid methyl esters (FAME) and analysing them using a Gas Chromatography-flame ionisation detector (GC-FID) equipped with a variable spit-flow injector and a 52 CB GC column (Agilent 6890A). For each sample, 8-10 mg of biomass was weighed into a 2 mL vial, and 50 µL of standard tridecanoic acid (TDA) was added as an internal standard. The samples were saponified and trans-esterified by adding 225 µL of HCl: methanol and 225 µL of chloroform: methanol (2:1 v/v) and heating them in an oven at 70 °C for 2 h. After cooling, 1 mL of heptane was added to each vial and the samples were vortexed for 30s to allow phase separation. The hexane layer (upper liquid) containing FAME was transferred into new vials with a glass pipette, and an injection volume of 1 µL was loaded onto a capillary column (length 25m, internal diameter 0.25 mm, film thickness 0.2 µm) using helium as the carrier gas. The FAME were identified and quantified based on their retention times and peak areas compared to those of Supelco® 37 Component FAME mix standard solutions (Sigma Aldrich).

$$\text{Fatty acid content } (mgg^{-1}) = \frac{\text{Fatty acid weight (mg)}}{\text{weight of algae biomass (g)}} \quad (2.10)$$

$$\text{Fatty acid yield } (mgL^{-1}) = \text{Fac } (mgg^{-1}) \times \text{Bc } (gL^{-1}) \quad (2.11)$$

Where Fac is the fatty acid content and Bc is the biomass concentration (g L^{-1}).

2.4.8 Estimation of biochemical composition

The lipid, protein, and carbohydrate content of the freeze-dried microalgal biomass was analysed by Fourier Transform Infrared Spectroscopy (FTIR) using a Cary 630 FTIR instrument. For each sample, a small amount of biomass was applied to the diamond sample window and compressed four times. The FTIR knob was turned until there was full contact on the sample press, and this was repeated three to four times to ensure the reproducibility of the analysis. The IR spectra were scanned in the range 4000–450 cm^{-1}, and the characteristic absorbance peaks based on specific chemical groups within the biomass were selected. Lipid (C =O ester stretching at 1760–1715 cm^{-1}), protein (C =O amide II band at 1545 cm^{-1}), and carbohydrate (C-O-C stretching at 1070–020 cm^{-1}) contents were calculated as a percentage of the biomass composition using standard calibration of glyceryl tripalmitate, bovine serum albumin, and glucose, respectively, as described previously (Coward *et al*., 2016; Mayers *et al*., 2013). Scanning the IR spectra in the range of 4000 - 450 cm^{-1} produces a characteristic absorbance spectrum based on specific chemical groups within the biomass (Figure A.2). As the absorption pattern of proteins, lipids and carbohydrates is distinct, this method can identify and quantify the biochemical composition of microalgal biomass. Total biomass composition (% DW) was determined by developing a multi-point calibration curve of standards (D-glucose, bovine serum albumin, glyceryl tripalmitate) prepared in potassium bromide. Peak integration was carried out by ensuring the blue area covers the relevant bandwidth range by moving the grey squares on either side of the peak as detailed in Figure D.2, selecting the peak range detailed below:

- Lipid bandwidth range: 1761 – 1714 cm^{-1}, Peak maxima at 1735 cm^{-1}
- Protein (Amide II) bandwidth range: 1550 – 1500 cm^{-1}, Peak maxima at 1542 cm^{-1}
- Carbohydrate bandwidth range: 1134 – 926 cm^{-1}, Peak maxima at 1029 cm^{-1}

2.4.9 Extraction of polyphenols from microalgae biomass

Lyophilised microalgae biomass of 50 mg was dissolved in 50 mL 99.9% methanol with a stirrer and placed stirring plate for 24 hours extraction. After 24 hours, the sample was centrifuge at 3000 *g* for 5 mins and the supernatant collected through filtration. The algal pellet was resuspended with fresh solvent and the extraction processes was repeated twice (2x). The extracted solvents were pooled together after extraction processes, the solvent was collected using rotary evaporator (Buchi-Rotavapor R-300) at 40^{o}C under reduced pressure. The crude

extract was dried under nitrogen gas and the total crude polyphenol was estimated using equation (2.15) (Jesumani *et al*., 2020).

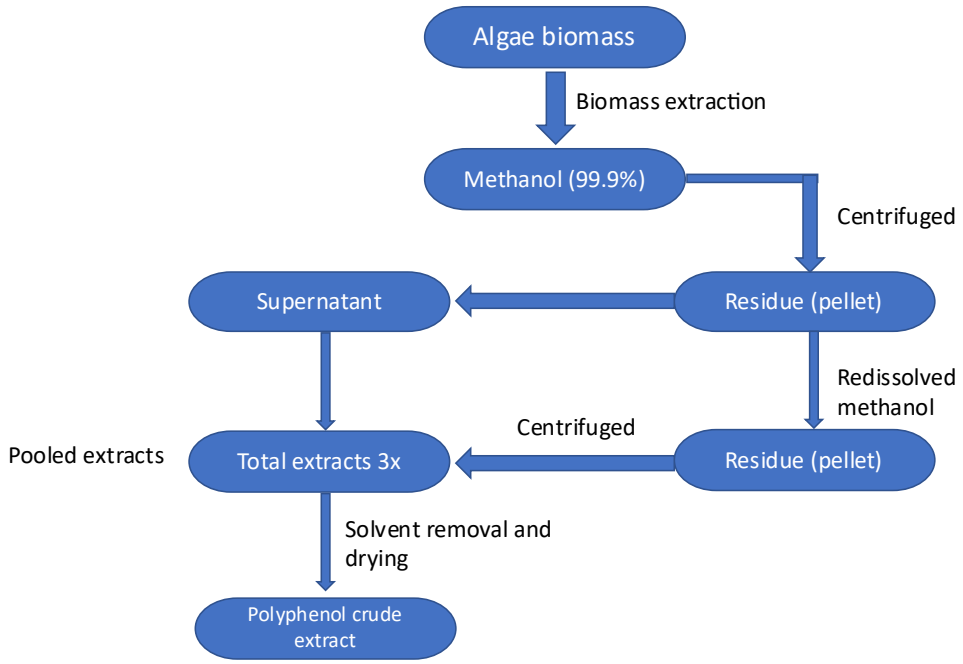

Figure 2.4 Schematic process of extraction polyphenols from microalgae biomass.

2.4.10 Extraction of polyphenols from mushroom exudate

100 mg of mushroom exudate (used substrate) was crushed and dissolved in 100 mL of 99.9% methanol with stirring, and the mixture was placed on a stirring plate for 24 hours. The extraction was then carried out using a centrifuge at 3000 *g* for 5 minutes, and the supernatant was collected through filtration. The residual exudate was resuspended in fresh solvent, and the extraction process was repeated twice (2x). The extracted solvents were then pooled together, and the solvent was collected using a rotary evaporator (Buchi-Rotavapor R-300) at 40°C under reduced pressure. After solvent extraction, the crude polyphenol extract was dried under a flow of nitrogen gas and the total polyphenol yield was determined from equation (2.15).

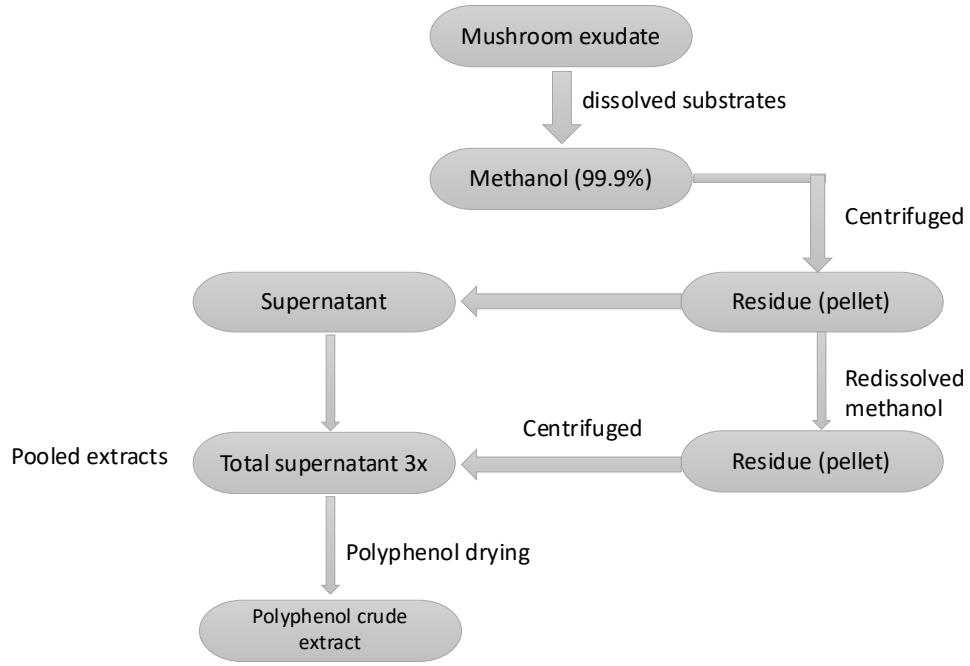

Figure 2.5 Schematic process of extraction polyphenols from microalgae biomass.

2.4.11 Estimated total extraction yield

Quantification of extraction yield from microalgae and mushroom exudate was estimated using the equation below:

$$\text{Total extraction yield } \% = \frac{\text{weight of dry extract (g)}}{\text{weight of sample (g)}} \text{ x } 100 \qquad (2.15)$$

2.4.12 Determination of total antioxidant capacity

The antioxidant capacity of the sample was measured by adding 1 mL of reagent solution, consisting of 0.6 M sulphuric acid (3.14 mL in 100 mL), 28 mM sodium phosphate (397.49 mg in 100 mL), and 4 mM ammonium molybdate (494.36 mg in 100 mL), to 1 mL of the sample extract (Bhatti *et al*., 2015a). The tubes were then sealed and incubated at 90 °C for 30 minutes. The absorbance was read at 695 nm using a reagent mixture as a blank, and ascorbic acid was used as a standard to determine the equivalent grams of total antioxidant capacity (AAE) per extract. For antioxidant activities such as Trolox equivalent antioxidant capacity (TEAC), 2,2-diphenyl-1-picrylhydrazyl (DPPH), total phenolic content, and 2,2-azinobis (3-ethylbenzothiazoline-6-sulfonic acid) (ABTS). There are several limitations: the chemistry and molecular targets of most *in-vitro* assays may not be suitable for the *in-vivo* assays, commonly used antioxidant assays may not be adequate in measuring the radical reactions in lipids, interference with other compounds not only to phenolic compounds but

other reducing agents including ascorbic acid, citric acid, and amino acids can interfere with the analysis for an overestimated result (Capanoglu *et al*., 2021).

2.4.13 Determination of total phenolic content (TPC)

The total phenolic content was determined using the modified Folin-Ciocalteu (FC) method described previously (Singleton and Rossi, 1965). To an aliquot of 1 mL of sample at 1 mg mL^{-1}, 1 mL of FC reagent diluted in water (1:9 v/v) was added. After 5 min, 1 mL Na_2CO_3 (7.5%) was added and incubated for 1 h. The absorbance was measured at 765 nm after incubation with the solvent as a blank. The results are expressed as gallic acid equivalents per gram of dry weight (GAE/g extract). However, the interactions of phenolic compounds and proteins are known to affect free polyphenols and antioxidant capacity. Polyphenols are very sensitive to light, pH, and temperature. For precise quantification polyphenolic extraction should be undertaken on freeze dried biomass with organic solvents and under subdued lighting to prevent degradation of the antioxidant properties (Ozdal *et al*., 2013).

2.4.14 ABTS radical scavenging activity

The ability of algal biomass to scavenge free radicals using ABTS test was evaluated using modified method from (Monteiro et al., 2019). The ABTS radical ($ABTS^{+*}$) was generated by 10 mL of 7 mM (2,2-azinobis (3-ethylbenzothiazoline-6-sulfonic acid) ABTS solution with 10 mL of 2.45 mM potassium persulfate solution. The reaction mixture is allowed to stand in the dark at room temperature for 12–16 h, then adjusted with ethanol to an absorbance of 1.0 at 734 nm before use. The lyophilised samples (algal biomass) were prepared in different concentrations of methanol. Then 100 µL sample was mixed with 200 µL ABTS solution and allowed to react for 10 min to subsequently measure their absorbances at 734 nm. Butylated hydroxyanisole (BHA) was used as a positive control of antioxidant activity. The radical scavenging capacity was calculated according to equation (2.16):

$$\% \text{ ABTS scavenging activity} = \frac{\text{Abs}_{\text{control}} - \text{Abs}_{\text{sample}}}{\text{Abs}_{\text{control}}} \text{ x } 100 \qquad (2.16)$$

where $abs_{control}$ is the absorbance of the control, and the abs_{sample} is the absorbance of the extract/standard.

2.4.15 Determination of Sun Protective Factor (SPF)

The sunscreen protective factor of each biomass was estimated by using the polyphenol extracts from a range of concentrations of their individual stock. The SPF values of each biomass were measured separately, and a mixture of both polyphenols was also tested at different ratios to determine their SPF values at 5 nm intervals from 290 to 320 nm using a Multiskan Go microplate spectrophotometer (1510-04220C Thermo Scientific, UK). In addition, the SPF values were estimated using a formula developed by Mansur *et al*. (1986) from table 2.5 and simplified by Sayre *et al*. (1979) through UV spectrophotometry in vitro.

$$SPF = CF_x \sum_{290\,nm}^{320\,nm} \mathrm{EE}(\lambda)\, x\, I(\lambda)\; x\, ABS(\lambda) \qquad (2.18)$$

CF, correction factor (10); EE, erythemal effect wavelength; I, solar intensity spectrum; Abs, absorbance of the sample at 290–320 nm. The values for each [EE(λ) × I(λ)] are constants normalised and reported by (Sayre *et al.* (1979).

Table 2.5 The normalised product function for SPF calculations (Mansur *et al*. 1986).

Wavelength (nm)	EE x I (normalized)
290	0.0150
295	0.0812
300	0.2874
305	0.3278
310	0.1864
315	0.0837
320	0.0180
Total	1

2.5 Statistical analysis

All the experiments were conducted in triplicates and results were expressed as mean value ± standard deviation. Statistical differences between experimental groups were defined using one-way analysis of variance (ANOVA) with post-hoc Tukey's test. All statistical analysis were conducted using OriginPro software (version 9.8, 2021).

CHAPTER 3

Comparing carbon capture efficiency and biochemical composition of five microalgal species in a bicarbonate-based system

3.1 Background

The emission of greenhouse gases, particularly CO_2, is globally acknowledged as a significant issue impacting the world's climate. This has led to extensive research in recent years to mitigate carbon dioxide emissions by employing different carbon capture techniques (Guo *et al*., 2019). Microalgae are photosynthetic organisms that exhibit high CO_2 fixation efficiency in both gaseous and soluble states in the form of bicarbonates and carbonates, up to 10 – 50 folds compared to terrestrial plants (Singh and Dhar, 2019). The process of CO_2 biofixation by microalgae is under thorough examination as a strategy to reduce greenhouse gas emissions (Cheah *et al*., 2015; Meylan *et al*., 2015). Microalgal growth is not solely dependent on CO_2 sequestration but also on the uptake of nutrients, photosynthetic light, and various enzymatic activities (Prasad *et al*., 2021a). The optimal pH condition for microalgal growth range between 6.5 to 8. Genetic engineering can help overcome the inherent limitation of metabolic capacity for higher accumulation of desired biomolecules. Moreover, acid-tolerant and acidophilic microalgae have been investigated, and it has been demonstrated that microalgae cultivated at pH below 3 can have biomass productivities compared to neutrophilic strains (Abiusi *et al*., 2022). Usually, acidic pH is beneficial for CO_2 sequestration as it leads to an increase in the concentration of free-CO_2, which is advantageous for acid-tolerant species such as *Scenedesmus* sp. and *C. sorokiniana* (Abiusi *et al*., 2022). Alkaline pH levels also increase the solubility of CO_2 in the form of CO_3^{2-} ions (Prasad *et al*., 2021b) which is beneficial for high-CO_2 and alkaline-tolerant species like *C. sorokiniana* str. SLA-04 and *Chlorella* sp. AT1 (Ighalo *et al*., 2022a; Tesson, 2023; Wu *et al*., 2022). The primary cause for the rise in culture pH is the dissolution of CO_2, which forms HCO_3^-. This HCO_3^- can rapidly move through the carbon concentrating mechanisms (CCMs) of microalgae, with cellular carbonic anhydrases facilitating the conversion of HCO_3^- to CO_2 and OH^- (Colman *et al*., 2002). A developed system called carbon concentrating mechanisms (CCM) in algae, which operates on the external bicarbonate (HCO_3^-) pool constitutes about 90% of the total dissolved inorganic carbon in their culture environment (Moulin *et al*., 2011). This CCM operates in three functional models mainly the active inorganic carbon (Ci) uptake systems, carbonic anhydrase (CA) for converting Ci, and CO_2 fixation system (Singh *et al*., 2016).

Different research findings have been undertaken with a concluding aim on the selection of appropriate strains, nutrient availability, and the technological cost which is a significant hurdle in the commercial development of microalgae-based CO_2 capture processes (Acién Fernández *et al*., 2012; Zhou *et al*., 2017). Microalgal species that can tolerate CO_2 concentrations greater than 20% are classified as CO_2-tolerant microalgae groups, while those that can only withstand 2-5% CO_2 concentration are classified as CO_2-sensitive (Morales *et al*., 2015; Wang *et al*., 2023). One of the major challenges in enhancing CO_2 capture processes is identifying microalgae strains that can tolerate high CO_2 concentrations. The significant characteristics of microalgae have led to their widespread use in sustainable biomass production, CO_2 sequestration, wastewater treatment, biofuel production by *Dunaliella salina* (Yimin Chen a and Changan Xu a, 2021), and industrial waste such as flue gases, biogas, agricultural waste products such as pig manure, brewery, and wastewater (Beigbeder *et al*., 2021). *Parachlorella kessleri,* achieved 97% inorganic carbon removal and 95% biofixation efficiency when cultivated in inorganic carbon derived from fermented sugar-beet molasses (Beigbeder and Lavoie, 2022). Microalgae convert CO_2 into molecules such as lipids, proteins, carbohydrates, and pigments which are commercially important through photosynthesis (Chen *et al*., 2017).

Interestingly, due to increased consumer awareness and demand, there is a significant growing pressure within the personal care products, cosmetics, foods, pharmaceuticals, and agricultural industries to use natural products instead of synthetic ones (Gernaey *et al*., 2012). Among the several strains of microalgae, *Parachlorella kessleri* and *Scenedesmus quadricauda* have been evaluated for their high value-added products for various industrial applications on wastewater treatment, CO_2 fixation, biofuel production, and pharmaceutical industries due to their high biomass productivity and biochemical composition. Although, Eustigmatophytes such as *Nannochloropsis* sp. and *Vischeria* sp. have gained industrial attention due to their great biotechnological potential for producing high value-added products such as polyunsaturated fatty acid (PUFAs), eicosapentaenoic acid (EPA), pigments, antioxidants, and ability to utilise NH_3 and CO_2 (Stoykova *et al*., 2019) which is a promising food constituent for nutraceutical values (Sinetova *et al*., 2021). *Phaeodactylum tricornutum,* and *Porphyridium purpureum* has the characteristic to meet several functional areas within these industries by possessing the ability to produce a broad range of commercial value-added products such as exopolysaccharides (EPS), polyunsaturated fatty acids (PUFAs), phycobiliprotein, antioxidants properties, and metabolic flexibility in response to light fluctuations (Castro-Ferreira *et al*., 2022; Coward *et al*., 2016). Strain such as *Phaeodactylum tricornutum,*

Scenedesmus quadricauda, and *Parachlorella kessleri* have been identified as potential strains for CO_2 sequestration, wastewater treatment, accumulate (carbohydrates, lipids, and antioxidants), and biofuels production by (Beigbeder *et al*., 2021; Song *et al*., 2014) *Porphyridium purpureum* produce valuable chemicals such as phycobiliprotein (which is a water-soluble protein of a complex light-harvesting pigments), polysaccharides, and polyunsaturated fatty acids (PUFAs) applied in food and drink and pharmaceutical industries (Coward *et al*., 2016). This strain is capable of accumulating about 43.7% of the total fatty acids, PUFAs such as eicosapentaenoic acid (EPA) and docosahexaenoic acid (DHA) for anti-inflammatory properties (Ryan *et al*., 2009). The selected microalgae species from table 2.1 were provided by AlgaeCytes Ltd (industrial partner) based on their value-added products and secondary metabolites below and throughout this section. In addition to their high biomass production rates, the species can accumulate a wide spectrum of valuable compounds such as lipids, carbohydrates, proteins, antioxidants, phycobiliproteins, eicosapentaenoic acid (EPA). The main objective of this study is to identify the best inorganic carbon tolerant strain for microalgae-based carbon capture and utilisation (CCU) and provide analysis its effect on microalgae growth and biochemical compositions.

3.2 Materials and Methods

3.2.1 Screening of inorganic carbon concentrations

The selected microalgal strains provided by AlgaeCytes Ltd were cultured in a BG11 media for freshwater strains table 2.1 and Guillard's *f/2* medium for marine strains table 2.2 following the recipes from the Culture Collection of Algae and Protozoa (CCAP). BG11 medium was prepared with a stock solution of 20 g L^{-1} $NaHCO_3$ for 1, 2, 4, and 6 g L^{-1} as well as *f/2* media. The BG11 culture medium autoclaved at 121 °C for 1 hour, *f/2* medium was filtered-sterilised, and pH was adjusted for all to 7.5 with 1 M NaOH or HCl using an electronic pH meter (Orion Star A211, Thermo Scientific).

3.2.2 Experimental setup

These microalgal species were inoculated in 250 mL conical flasks with 120 mL working volume of modified BG11 and *f/2* media with different $NaHCO_3$ concentrations. The flasks were incubated on a Stuart orbital shaker (Cole-Parmer 51900-22) at 120 rpm (unit too low to be converted into *g*) and illuminated with an intensity of light 200 µmol/m^2/s (ROHS, UK) for 24 h using a BT-881D lux meter (BT-Meter store, UK). Samples were taken every 2 days to measure the optical density. The experiments were performed in triplicates for a cultivation period of 14 days.

3.2.3 Microalgal analysis on specific growth rates

The OD_{680nm} of the cultures was continuously measured using a Multiskan Go microplate spectrophotometer (1510-04220C Thermo Scientific, UK). The specific growth rate (µ, d^{-1}) was calculated using the following equation (Beigbeder *et al*., 2021).

$$\mu = \frac{\ln (X_2 / X_1)}{t_2 - t_1} \qquad (3.1)$$

where X_2 and X_1 (dry weight) are the exponential phases at the end and beginning, respectively, and time (t_2) represents the end and start (t_1) of cultivation.

3.2.4 Quantification of inorganic carbon (HCO_3^-) utilisation by microalgae

The concentration of inorganic carbon was quantified using titrimetric methodology of the culture supernatant described in chapter 2, section 2.4.5

3.2.5 Pigment analysis on biomass composition

The harvested algal biomass was analysed for pigment content using reverse-phase high-performance liquid chromatography (C18-RP HPLC). Approximately 4 - 5 mg of lyophilised algal biomass sample was extracted using 1 mL of organic solvent (acetone: methanol, 7:3 v/v) containing an internal standard (α-tocopherol acetate, 100 mg L^{-1}) by homogenizing them in a VelociRuptor V2 Microtube Homo ™ (SLS1401) at 6.00 m/s for 15 seconds (3x cycles) described in chapter 2, section 2.4.6 (D. A. Wright *et al*., 1991).

3.2.6 Determination of total lipids (FAME) using GC-FID

The fatty acid composition was determined for each strain using a 52 CB GC column (Agilent 6890A, Germany). For each sample, 8-10 mg of the biomass was weighed into a 2 mL vial, and 50 µL of standard tridecanoic acid (TDA) was added as an internal standard described in chapter 2, section 2.4.7.

3.2.7 Quantification for biochemical composition using FTIR

The lipid, protein, and carbohydrate content of the freeze-dried microalgal biomass was determined using C630 Fourier Transform Infrared Spectroscopy (FTIR) described in chapter 2, section 2.4.8 by (Mayers *et al*., 2013).

3.3 Results and discussion

3.3.1 Effect of bicarbonate concentrations on cell growth and biomass production

In this study, the biomass production and productivity, inorganic carbon utilisation, and carbon uptake rate of five microalgal species were evaluated at different $NaHCO_3$ concentrations (1, 2, 4, and 6 g L^{-1}) for their growth profiles, carbon capture efficiencies, and biochemical composition (Figure 3.1). The above observations of all species were significantly affected by the concentration of $NaHCO_3$ ($p \leq 0.05$). The highest specific growth rate and biomass concentration of *P. kessleri* occurred at a $NaHCO_3$ concentration of 4 g L^{-1}, where the highest specific growth rate was 0.162 d^{-1} and the highest biomass production was 1.67 g L^{-1}, further increase in $NaHCO_3$ (6 g L^{-1}) resulted in decrease in biomass 1.59 g L^{-1} higher than the control (1.27 g L^{-1}) affecting the algal growth (Figure 3.2). This trend is similar to a recent study with *P. kessleri* that reported the maximum biomass productivity (1.54 g L^{-1}) at 3 g L^{-1} $NaHCO_3$ with a decrease in productivity beyond 5 g L^{-1} $NaHCO_3$ (Beigbeder *et al*., 2021) due to salt stress caused by high sodium ions, which affects photosynthesis by inactivation of

specific enzymes in cells (Sudhir and Murthy, 2004). The enzymatic activity of ribulose-1,5-biphosphate (RuBisCO) and carboxylase can be reduced by low temperature whiles high temperatures above 40^{o}C can alter photorespiration and the metabolic activity of microalgae (Prasad *et al*., 2021b). Meanwhile, *S. quadricauda, Vischeria* sp*.,* and *P. purpureum* had an increase in the specific growth rate, even at a $NaHCO_3$ concentration of 6 g L^{-1} (Figure 3.1a). Decrease in growth on day 12, was a result of temperature variation within the laboratory which resulted to fluctuations in growth. This suggests that these three species can sequester high levels of carbon dioxide in the form of $NaHCO_3$ to produce biomass. A recent study reported a significant increase in biomass productivity of *Scenedesmus* sp*.,* from 19.9 to 28.3 mg $L^{-1}d^{-1}$, as the concentration of $NaHCO_3$ was increased from 0 to 1.2 g L^{-1} (Pancha *et al*., 2015). Similarly, *Scenedesmus* sp*.,* cultured in BG11 medium for 14 days with an increasing carbon dioxide concentration from 0.03% to 10% showed higher growth (Tang *et al*., 2011a). These studies show similar trends to the present study with a positive correlation between the availability of carbon sources and biomass productivity. Growth in higher bicarbonate supplements promoted cell growth and photosynthetic pigments, however, higher concentrations can cause stress and increase the culture pH which can inhibit growth which is crucial for carbon sequestration can be influenced by temperature.

In the case of *P. tricornutum,* a peculiar trend was observed: the specific growth rate and biomass concentration decreased as $NaHCO_3$ concentration increased (Figure 3.2). The highest specific growth rate was 0.173 d^{-1} and biomass production (1.75 g L^{-1}) in the control (1 g L^{-1}) compared to the 6 g L^{-1} $NaHCO_3$ (1.51 g L^{-1}). A similar trend was reported in the literature, indicating the highest growth of *P. tricornutum* at a bicarbonate supplement of 2.7 g L^{-1} in *P. tricornutum* (Gardner et al., 2011). These results suggest that the optimal substrate ($NaHCO_3$) concentration for *P. tricornutum* was at 1 g L^{-1} (control). A study conducted by Song et al tested the carbon dioxide flow range of 0 – 2.5 vvm and found that the maximum specific growth rate and biomass concentration occurred at 1.5 vvm in the lowest flow (Song et al., 2014). Increasing the carbon dioxide flow beyond this point resulted in a decrease in both the specific growth rate and biomass concentration (Guo *et al*., 2019). A similar study by (Mirón *et al*., 2003) showed that an increase in the concentration of $NaHCO_3$ caused a decrease in the growth of *P. tricornutum.*

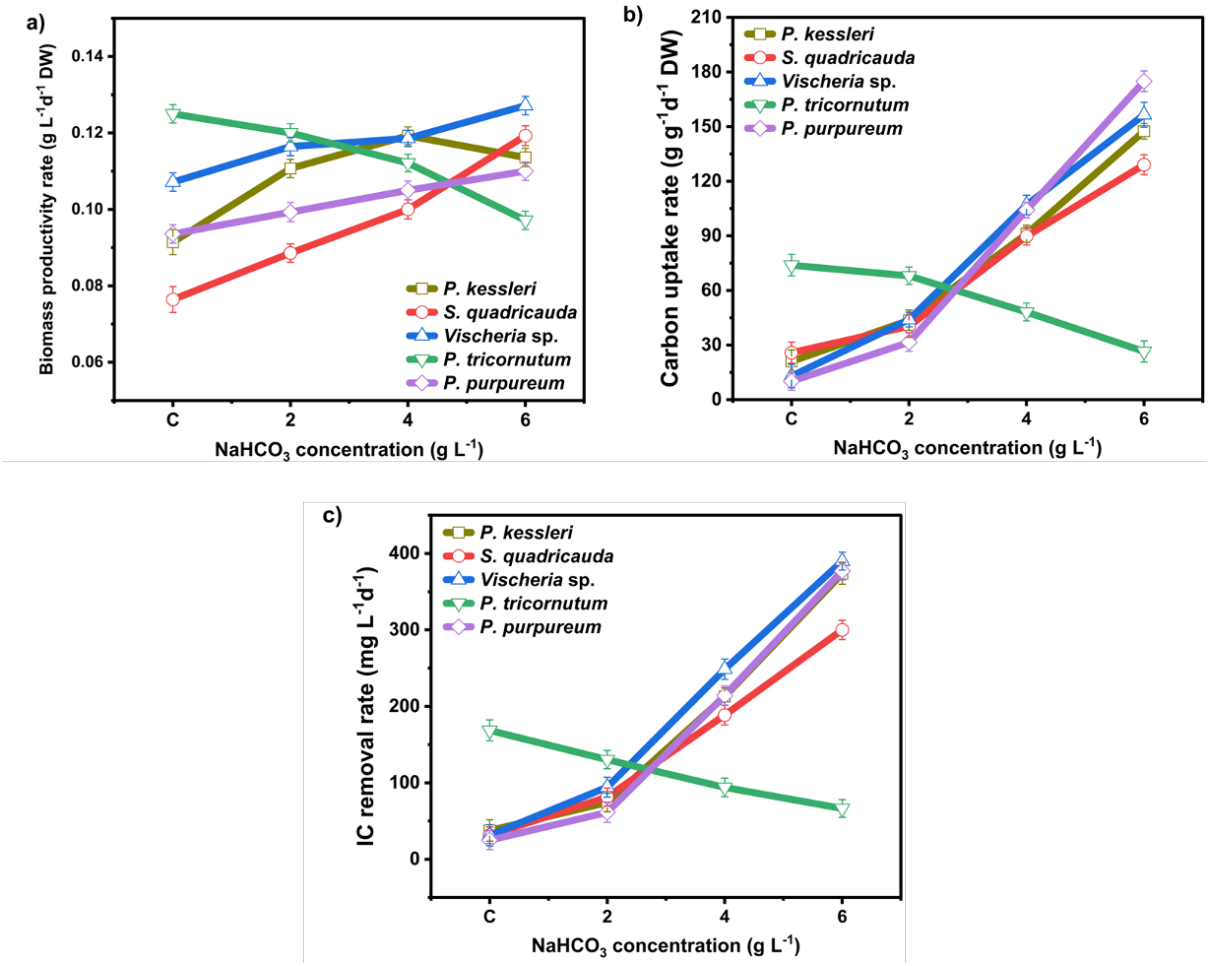

Figure 3.1 Represents the (a) biomass productivity rate, (b) carbon uptake rate, and (c) inorganic carbon removal rate levels in *Parachlorella kessleri, Scenedesmus quadricauda, Vischeria* sp.*, Phaeodactylum tricornutum,* and *Porphyridium purpureum*. These rates are measured after a 14-day cultivation period in the presence of varying concentrations of $NaHCO_3$, including a control (C) 1 g L^{-1} and additional 2, 4, and 6 g L^{-1}. Data values expressed as mean ± standard deviation, n=3.

The culture pH was measured at regular intervals throughout the experiment for each condition. An increase in pH (Figure 3.3) is due to the utilisation of HCO_3^- by microalgal cells by the enzyme carbonic anhydrase during photosynthesis, which resulted in the alkalisation of the medium (Li *et al*., 2018b). Other reports have also shown the effects of sodium bicarbonate on the increase in culture pH in *Tetradesmus* sp. (Umetani *et al*., 2021).

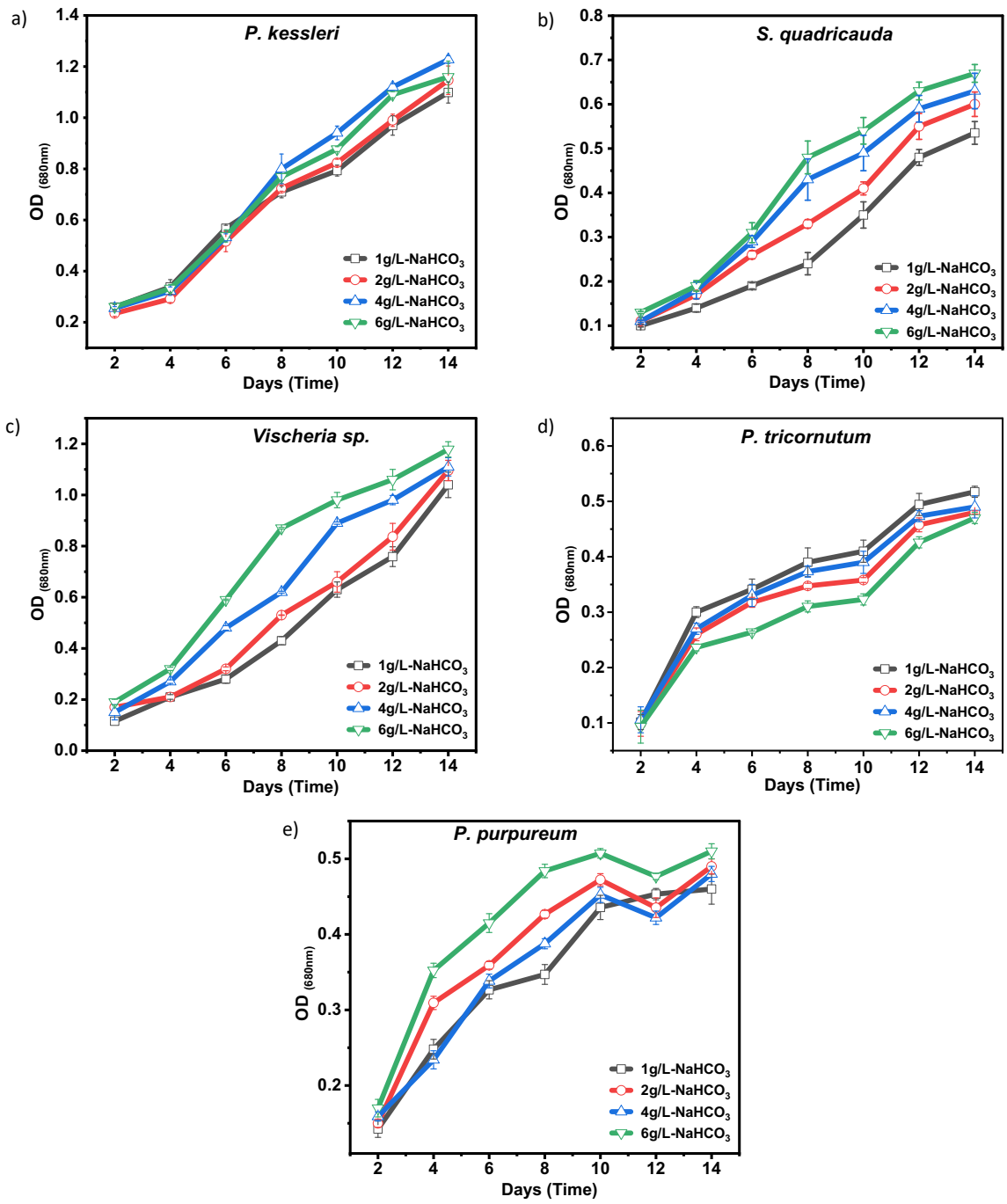

Figure 3.2 Growth curves of (a) *Parachlorella kessleri*, (b) *Scenedesmus quadricauda*, (c) *Vischeria* sp., d) *Phaeodactylum tricornutum*, and (e) *Porphyridium purpureum* cultivated in different sodium bicarbonate ($NaHCO_3$) supplements with similar growth trend at different concentration level and biomass. Data values expressed as mean ± standard deviation, n=3.

At the end of the experiment, the inorganic carbon removal achieved was beyond 87.1% at 6 g L^{-1} $NaHCO_3$ for *P. kessleri, Vischeria* sp., and *P. purpureum* (table 3.1). The exception was *S. quadricauda,* which achieved 70.2% removal under the highest supplement. As discussed previously, *P. tricornutum* demonstrated the highest inorganic carbon removal 93.1%. These

results show that inorganic carbon removal correspond to growth and biomass production in all algal species tested.

Table 3.1 Microalgal utilisation efficiency of inorganic carbon (IC) removal at different $NaHCO_3$ concentrations. Data values expressed as mean ± standard deviation, n=3.

	Total inorganic carbon removal (%)			
Parameters	1 g L^{-1}	2 g L^{-1}	4 g L^{-1}	6 g L^{-1}
P. kessleri	33.4 ± 0.18	52.3 ± 0.94	75.1 ± 0.12	87.1 ± 0.41
S. quadricauda	44.2 ± 0.08	57.2 ± 0.14	66.8 ± 0.21	70.2 ± 0.62
Vischeria sp.	47.2 ± 0.75	66.9 ± 0.30	87.6 ± 0.82	91.7 ± 0.73
P. tricornutum	93.1 ± 0.97	84.8 ± 0.67	59.4 ± 0.34	28.9 ± 0.37
P. purpureum	21.1 ± 0.49	43.5 ± 0.84	75.8 ± 0.92	88.2 ± 0.95

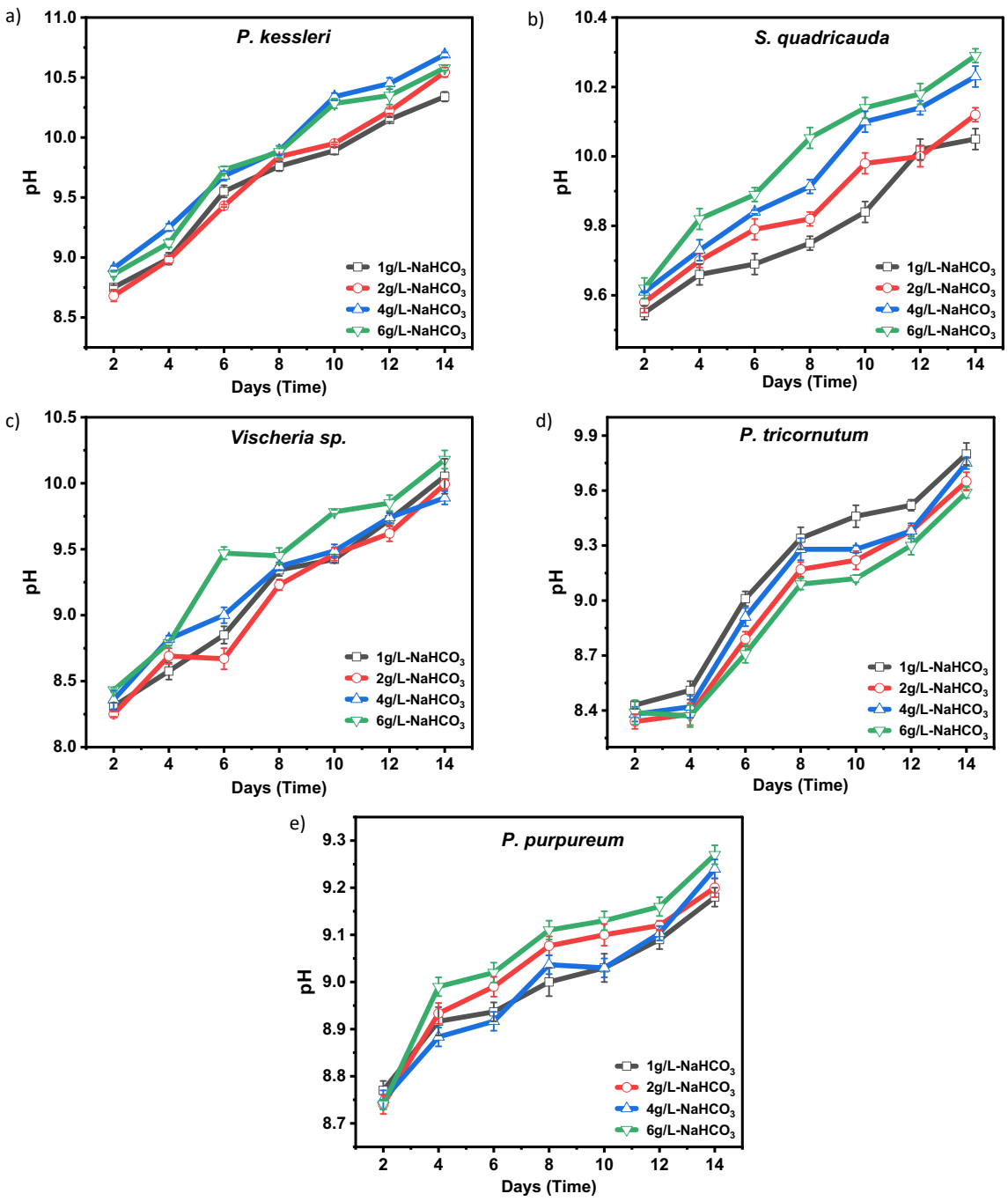

Figure 3.3 pH levels of (a) *Parachlorella kessleri*, (b) *Scenedesmus quadricauda*, (c) *Vischeria* sp. (d) *Phaeodactylum tricornutum*, and (e) *Porphyridium purpureum* cultivation in sodium bicarbonate ($NaHCO_3$) concentration of 1 g L^{-1} (black), 2 g L^{-1} (red), 4 g L^{-1} (blue) and 6 g L^{-1} (green) on a 14-day cultivation period. Data values expressed as mean ± standard deviation, n=3.

3.3.2 Impact of inorganic carbon on the biochemical composition

The biochemical compound varies depending on the microalgae specie but also on other process parameters such as inorganic carbon, pH, light, and nutrient availability. The harvested microalgal biomass was analysed by determining the content and biomass production of

carbohydrate, protein, and lipid. The protein content estimated from the microalgal biomass of *P. kessleri*, *S. quadricauda*, and *Vischeria* sp. ranged between 15 – 19%, 28 – 33%, and 33 – 36% respectively and the marine species *P. tricornutum* and *P. purpureum,* from 6 – 8% and 13 – 21% respectively depending on the $NaHCO_3$ supplement (Figure. 3.4). The addition of inorganic carbon to *P. kessleri* showed that, the accumulation of carbohydrate, protein, and lipid was statistically significant. The maximum protein and carbohydrate content was accumulated at 4 g L^{-1}, which demonstrated significant difference with the control ($p \leq 0.01$) except when varied between 4 and 6 g L^{-1}. From this study, a similar report on *P. kessleri* by (Beigbeder *et al*., 2021) supported this argument. Specifically, when the $NaHCO_3$ concentration reached 6 g L^{-1}, the biomass decreased which promoted other content such as lipid. The increase in $NaHCO_3$ concentration up to 6 g L^{-1} did not have any significant effect on the carbohydrate content by *S. quadricauda*. The control (1 g L^{-1}) $NaHCO_3$, the carbohydrate content of 33.28% was higher and decreases with increasing $NaHCO_3$ concentration (Figure 3.4b). From Figure 3.4c, increasing inorganic carbon concentration did not have significant difference on the biochemical composition of *Vischeria* sp. with increasing biomass production of 1.78 g L^{-1}. In *P. tricornutum,* the carbohydrate and lipid content were 61.67% and 22.43% respectively in the control (1 g L^{-1}) with a biomass production of 1.75 g L^{-1} compared to the remaining $NaHCO_3$ concentration which decreases with increasing concentration. An increase with the inorganic carbon concentration on biomass production and biochemical accumulation was due to osmotic stress reported by (Srinivasan *et al*., 2018).

Moreover, the addition of inorganic carbon promoted the biochemical contents of protein and carbohydrate in *P. purpureum* except lipid. (Yadav *et al*., 2019a) also reported an increase of the carbohydrate content of *Chlorella* sp. from 13.2% to 23.1% with increasing CO_2 concentration from 0.03% to 10% in the culture media. Comparably, the carbohydrate and protein content presented a different profile with different trend from *S. quadricauda* and *Vischeria* sp. respectively. The addition of inorganic carbon concentrations did not improve the biochemical content in *P. tricornutum* and *Vischeria* sp., likewise lipid content in *P. purpureum.* However, from the control (1 g L^{-1}) bicarbonate concentration resulted into metabolic regulation towards the production of lipids and carbohydrates than protein with increasing concentration from 2 - 6 g L^{-1}. Although, a study on nitrogen and phosphorus regulation promoted neutral lipid accumulation by shifting the enzymatic metabolism most used to stimulate lipid induction in microalgal cultivation (Guo *et al*., 2014). Under stress conditions, microalgae accumulate carbohydrate in the form of various molecules such as glycogen, triglycerides, and starch (Kandasamy *et al*., 2022). Similar trends have been reported

in another study, where lipid (TAG) accumulation was improved by the addition of bicarbonate (50 mM) under low nitrogen concentrations in *P. tricornutum* (Gardner *et al*., 2012). A similar study by (Song *et al*., 2014), confirmed that increasing carbon source up to 1 g L^{-1} resulted in an increase in growth rate and biomass concentration, but these values decreased beyond a carbon concentration of 2 g L^{-1}. Other studies have also reported that biomass productivity of *Phaeodactylum tricornutum* decreased at a gas-liquid ratio above 2.0 vvm (Mirón *et al*., 2003).

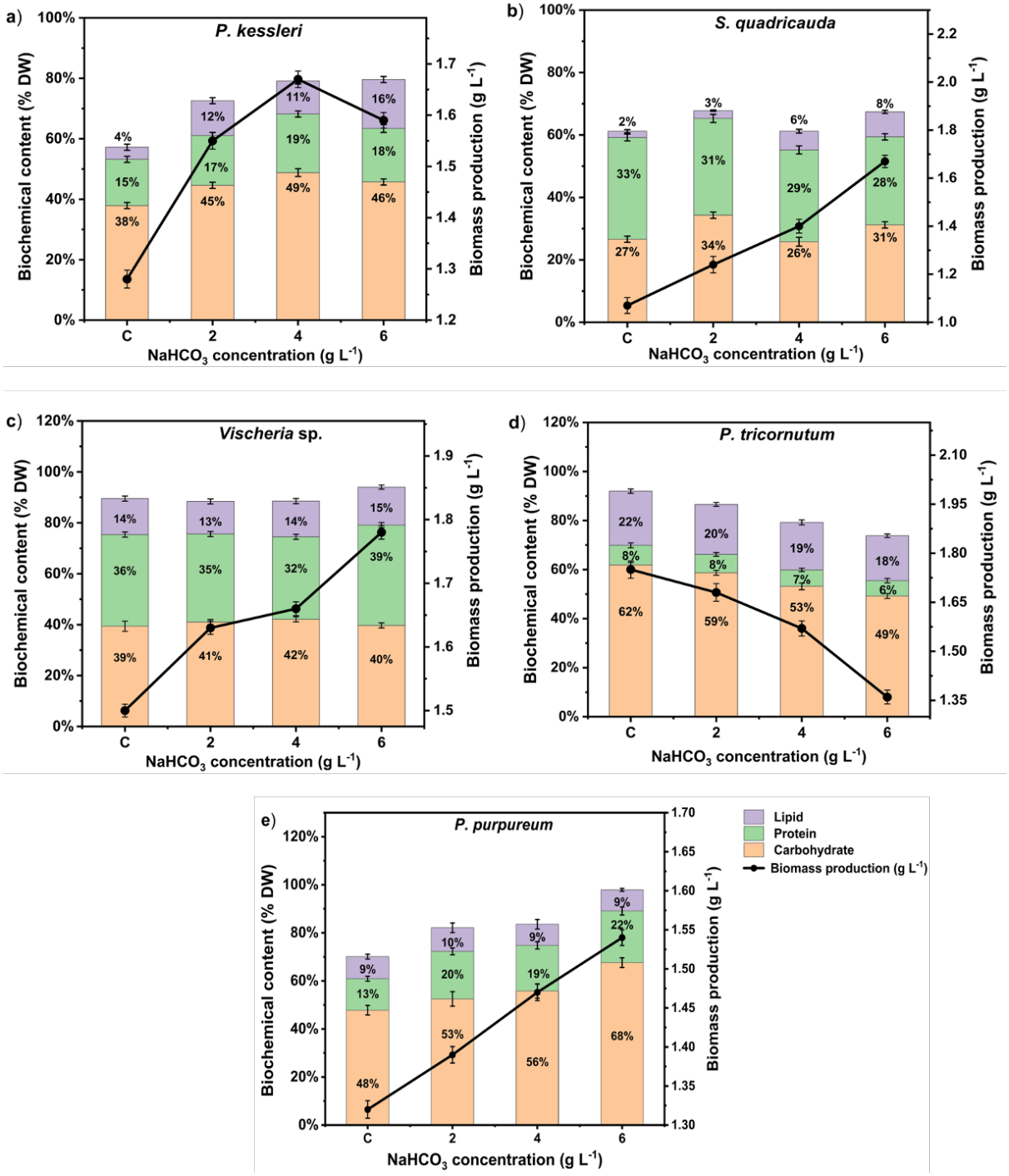

Figure 3.4 The biochemical content (bars) and biomass production (circle + lines) from (a) *Parachlorella kessleri*, (b) *Scenedesmus quadricauda*, (c) *Vischeria* sp. (d) *Phaeodactylum*

tricornutum, and (e) *Porphyridium purpureum* harvested after 14 days of cultivation at different bicarbonate ($NaHCO_3$) concentrations of 1, 2, 4, and 6 g L^{-1}. Data values expressed as mean ± standard deviation, n=3, and statistical analysis by one-way ANOVA with post-hoc test shown in Appendix A.

3.3.3 Effects of different inorganic carbon on fatty acid profiles

Microalgae can accumulate a high content of neutral lipids, particularly triacylglycerols (TAGs), which are mostly composed of saturated and monounsaturated fatty acids (Bigogno, 2002). some microalgae are rich in long-chain polyunsaturated fatty acids (LC-PUFAs) such as eicosapentaenoic acid (EPA) and docosahexaenoic acid (DHA), while others like arachidonic acid are relatively rare but strains of Rhodophyta such as *Porphridium cruentum* contains relatively high content (Gao *et al*., 2020). Under different inorganic carbon (Figure 3.5.), the change in the relative content of main fatty acids (total fatty acids %) under inorganic carbon concentrations were similar. For *P. kessleri*, the content of C18:3, C18:2, and C16:0 was increased cultivated under 1 - 4 g L^{-1} $NaHCO_3$ concentration for more than 80% of the total fatty acids (Figure 3.5a). Similar investigation on nutrient stimulation resulted in the overproduction of lipids in *P. kessleri* (Li *et al*., 2013) which is has been identified as a feedstock for biofuel production (Beigbeder *et al*., 2021). *Scenedesmus dimorphus* showed increased accumulation of polyunsaturated fatty acids, including alpha linoleic acid (C18:3), in response to elevated carbon dioxide levels (Vidyashankar *et al*., 2013). In *S. quadricauda,* the addition of sodium bicarbonate did not enhance the overall lipid content, there was no significant difference among various $NaHCO_3$ concentrations due to alkaline shift in pH with similar reports on *Scenedesmus* sp. (Singh *et al*., 2022). The fatty acid composition of Eustigmatophytes includes C14, C16, C18, and C20 (Xu *et al*., 2020). The total fatty acids of C16:0 and C16:1 accounted for about 58.78% under the varying $NaHCO_3$ (2-6 g L^{-1}) compared to 48.44% control (1 g L^{-1}) *Vischeria* sp. while the EPA accounted for 27.11% in the control with 5 folds higher than the other remaining treated concentration about 22.55% lower (Figure 3.5), similar results on *E. vischeri* JHsu-01 were reported by (Xu *et al*., 2020). The EPA content in Eustigmatophyceae vary among species such as *Nannochloropsis salina* which can account EPA content of 27.0% of TFA, similar to this study on *Vischeria* sp. (Solovchenko *et al*., 2008). The $NaHCO_3$ concentration promoted the C16:1 content, but decreased EPA (27.27 % - 21.29%) with no effect on C14:0, C16:0, C18:0, C18:1, C18:2, and C20:4. The maximum percentage of EPA was found in the control but substantially decreased with increasing $NaHCO_3$ concentration at the end of the cultivation Other studies on *Vischeria* sp. have shown increases in EPA content under salt stress (Sinetova *et al*., 2021).

Another report on *Vischeria stellata* showed an increase in EPA (C20:5) and arachidonic acid (C20:4) on nitrogen stress conditions (Gao *et al*., 2016). Interestingly, a different trend was observed in *P. tricornutum* with the addition of bicarbonate. As the $NaHCO_3$ increases, the content of C16:1 from each bicarbonate supplement was found to be similar with the maximum value 54.32% including the control but the content of C16:0 (27.69%) was 2 folds lower comparatively in *P. tricornutum*. The average EPA content was 9.83% constant at each $NaHCO_3$ condition but did not improve the C18:1 level. A study by (Peng *et al*., 2013) confirmed increased proportions in C16:0 (38.03%) and C16:1 (33.22%) and a decrease in EPA C20:5 (6.88%) under sufficient carbon (40 mM $NaHCO_3$) in *P. tricornutum*. Although, carbon metabolism promotes sufficient substrates for the synthesis of TAG but through nitrogen and phosphorus (Peng *et al*., 2013). High levels of inorganic carbon can promote lipid accumulation in microalgal cells but carbon to nitrogen/phosphate ratio has significant effects on lipid metabolism (Tang *et al*., 2011b). The reduction in the content of C16:0 and C18:0 could be attributed to the desaturation rate surpassing the elongation rate, ultimately leading to an increase in the production of C16:1 with similar results reported by (Song *et al*., 2014). In relation to the fatty acid composition in *P. purpureum*, as depicted in figure 3.5e, it's evident that varying concentrations of $NaHCO_3$ in the culture resulted in a distinct variation pattern for the primary fatty acids (C16:0, C18:2, C20:4, and C20:5). The arachidonic acid C20:4 of about 34.70% content was 2 folds higher than the EPA C20:5 of about 14.27% content under each bicarbonate concentration. The content of C16:0 constituted approximately 31.62%, and the C18:2 content 15.81% was decreased by $NaHCO_3$ (Figure 3.5). This suggests that the unsaturation index of the cellular fatty acids was enhanced by $NaHCO_3$, particularly in relation to the two primary beneficial polyunsaturated fatty acids in *P. purpureum*.

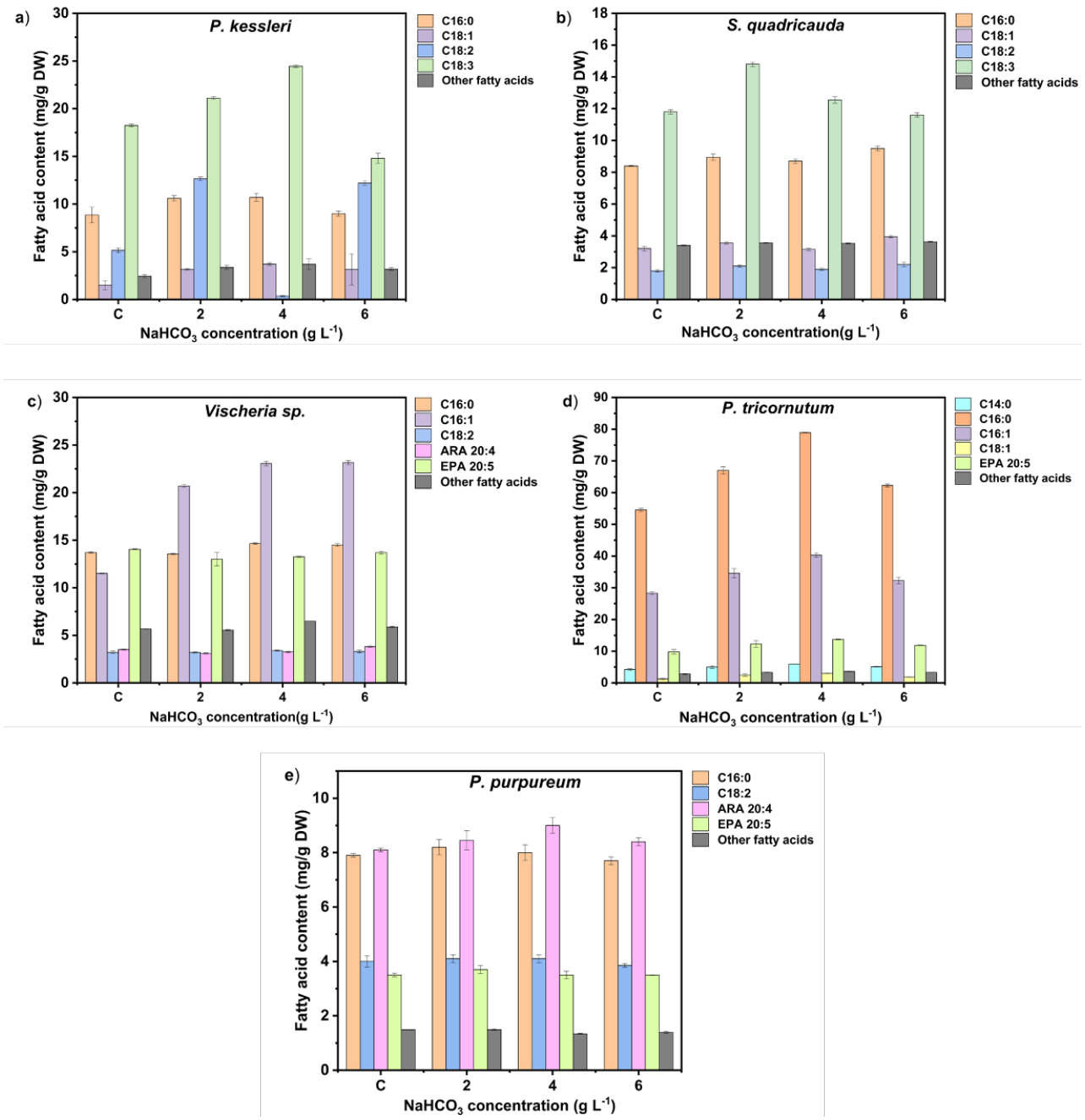

Figure 3.5 Represents the fatty acid contents from the biomass dry weight of (a) *Parachlorella kessleri*, (b) *Scenedesmus quadricauda*, (c) *Vischeria* sp., (d) *Phaeodactylum tricornutum*, and (e) *Porphyridium purpureum* under different inorganic carbon concentrations after a cultivation period of 14 days. Data values expressed as mean ± standard deviation, n=3.

3.3.4 Effects of inorganic carbon on photosynthetic pigment.

The growth response of the *P. kessleri, S. quadricauda, Vischeria* sp.*, P. purpureum,* and *P. tricornutum* was studied at different inorganic carbon concentrations on pigments from figure 3.6 with a chromatogram presented in Appendix D (Figure D.1). The addition of inorganic carbon contributed to the photosynthetic pigments of the chlorophyll-*a* and β-

carotene for each strain. There was significant difference of chlorophyll-*a* when the inorganic carbon concentration was increased from 1 – 4 g L^{-1} but insignificant between 4 and 6g L^{-1} ($p < 0.01$). The highest amount of chlorophyll-*a* (6.96 ± 0.07 mg g^{-1}) was found in 6g L^{-1} similar to 4 g L^{-1} which is about 1.8 folds higher than the control culture 3.86 ± 0.12 mg g^{-1} in *P. kessleri* higher than (Beigbeder et al., 2021; Beigbeder and Lavoie, 2022). From Figure 3.6b, the chlorophyll-*a* content (0.75 ± 0.01 mg g^{-1}) increases with increasing bicarbonate concentration but decreased in β-carotene (0.19±0.00 mg g^{-1}) at 6g L^{-1}. A similar report on *S. quadricauda,* the chlorophyll-*a* content was 2.14 folds higher than the control (1 g L^{-1}) with lower β-carotene content (Singh *et al*., 2022). The maximum chlorophyll-*a* content estimated in *Vischeria* sp. was 27.23 ± 0.6 mg g^{-1} (control) higher than the highest bicarbonate concentration 23.89 ± 0.40 mg g^{-1} (6 g L^{-1}). There was no significant difference in the chlorophyll-*a* content at each treatment condition. Another study on *Nannochloropsis salina* and *Tetraselmis suecica* was cultivated with 1 g L^{-1} bicarbonate supplementation, their chlorophyll-*a* concentration increased 1.9 and 2.2 times as compared to control grown culture (White *et al*., 2013). The improvement of β-carotene content was not dose dependent with addition of sodium bicarbonate. The highest amount of β-carotene (7.38 ± 0.26 mg g^{-1}) was found in 4 g L^{-1} sodium bicarbonate culture, the remaining bicarbonate concentration 2 and 6 g L^{-1} was averagely similar (6.7 ± 0.35 mg g^{-1}) and the lowest was found in the control (5.25 ± 0.21 mg g^{-1}) sodium bicarbonate cultures.

Furthermore, the addition of sodium bicarbonate (up to 6 g L^{-1}) did not increase the both the chlorophyll-*a* content and β-carotene content. The decreased pigment ratio can be explained by the fact that adding sodium bicarbonate of such amounts causes a rapid increase in pH, resulting in an alkaline environment, which is unfavourable for microalgal growth. Interestingly, different trend on growth has been on *P. tricornutum* growth, the chlorophyll-*a* and β-carotene increases with increasing bicarbonate concentration. At 6 g L^{-1}, the chlorophyll-*a* content 2.87 ± 0.09 mg g^{-1} was 3.6 folds higher than the control 0.79 ± 0.05 mg g^{-1} and β-carotene content were 0.86 ± 0.05 mg g^{-1} at 6 g L^{-1} higher than the control. In our study, *P. purpureum* grew optimally at each sodium bicarbonate concentration, however, there was no significant difference among the total chlorophyll and β-carotene content under the treatment condition. Both light intensity and the concentration of inorganic carbon have been demonstrated to impact the chlorophyll-*a* and β-carotene content relative to biomass composition in these species.

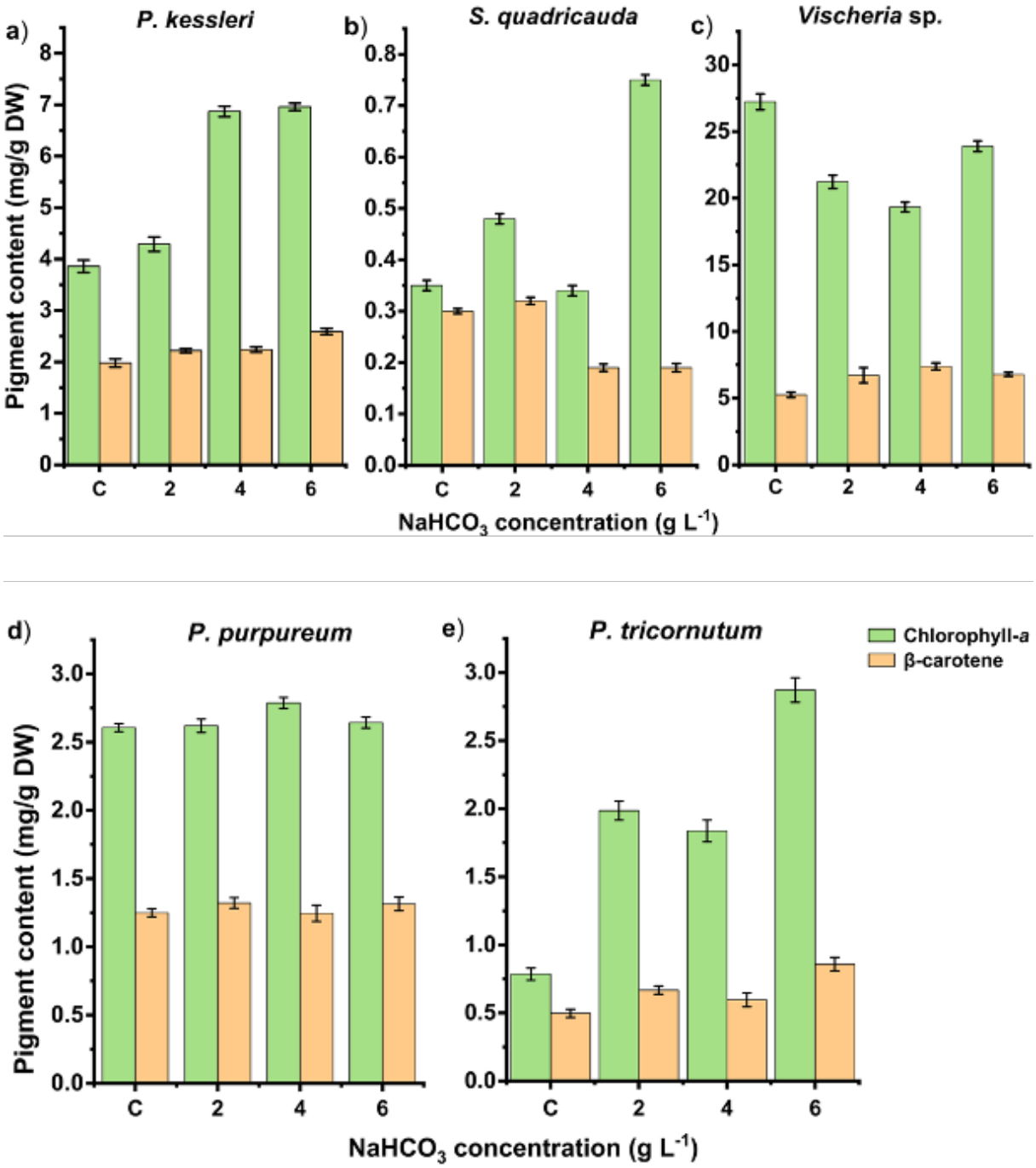

Figure 3.6 Represents chlorophyll-*a* content and β-carotene content from the dry weight of (a) *Parachlorella kessleri,* (b) *Scenedesmus quadricauda,* (c) *Vischeria* sp. (d) *Porphyridium purpureum,* and (e) *Phaeodactylum tricornutum* microalgal species at different sodium bicarbonate concentration for a cultivation period of 14 days. Data values expressed as mean ± standard deviation n=3, and statistical analysis by one-way ANOVA with post-hoc test show in Appendix A.

3.4 Conclusion

This study investigated the effects of bicarbonate concentration on the growth and biochemical composition of five microalgal species for carbon capture and value-added

product production. The results showed that each microalgal species had a different capacity to utilise bicarbonate and production of biomass. *P. kessleri*, *Vischeria* sp., and *P. purpureum* achieved the highest carbon removal efficiency and biomass production at 6 g L^{-1} $NaHCO_3$, while 1 g L^{-1} $NaHCO_3$ was more suitable for *P. tricornutum*. The biomass composition of the microalgae varied with bicarbonate concentration and species. The freshwater species had higher protein content compared to marine species, while the marine species had a higher carbohydrate content than the freshwater species in response to bicarbonate. The lipid content was highest in *P. tricornutum,* followed by *P. kessleri* and *Vischeria* sp. The fatty acid profiles of the microalgae were dominated by C16 and C18 fatty acids, with *P. purpureum, Vischeria* sp., and *P. tricornutum* having highest EPA content. Additional research is needed to optimise the pH of a bicarbonate supplemented medium and nutrient amendment to stimulate intracellular lipid synthesis, particularly by utilising dissolved inorganic carbon. This study demonstrates that bicarbonate can served as an alternative carbon source for microalgae cultivation and that different microalgal species can be selected for different applications based on their growth and biochemical compositions. However, in addition to the selection of appropriate microalgae strains with the highest growth properties, high inorganic carbon removal, biomass productivity, high biochemical compositions, and valuable metabolites such as phycobiliprotein, polysaccharides, eicosapentaenoic acid (EPA), and arachidonic acids from *Vischeria* sp. and *P. purpureum* was selected as a key aspect for the development and implementation of microalgae-based carbon capture and utilisation approach.

CHAPTER 4

Development of a bicarbonate-based integrated carbon capture and algal production system for mushroom cultivation using two microalgal species.

4.1 Background

The global mushroom market size is projected at a compound annual growth rate (CAGR) between 9.2 – 10.1% in the forecasted period between 2022 -2030 at USD 23.3 billion (Zion, 2021). Mushrooms are a relatively fast-growing crop (Girmay *et al*., 2016) and have emerged as one of the most profitable commercial agribusinesses across continents of North America, Europe, Asia Pacific, South America, Middle East, and Africa (Muswati *et al*., 2021). Mostly, edible mushrooms are commercially cultivated for medicinal and nutritional purposes. Cultivation of edible mushrooms requires critical environmental factors such as high humidity (80–90%), temperature (25-30°C), light, nutrients, and carbon dioxide throughout their cultivation phases (Kües and Navarro-González, 2015;Sakamoto, 2018). During mushroom growth, large amounts of oxygen are consumed, and carbon dioxide is released (Baumann *et al*., 2012; Hall *et al*., 2010). Elevated levels of carbon dioxide during mushroom-growing negatively affect the yield and quality through carbon dioxide poisoning. During the initial phases of growth, called the spawn run, the edible fungi can generate levels of carbon dioxide between 10,000 - 20,000 ppm depending on the inoculum size (Khanna, 2020). There have been a few recent reports on the use of carbon dioxide produced from mushroom farms to cultivate *C. vulgaris* (Širić *et al*., 2023) and the sustainable cultivation of lettuce by utilising carbon dioxide from mushroom production (Jung & Son, 2021). To tackle the carbon dioxide challenge, various carbon capture and conversion techniques have been suggested which are generally applied to concentrated carbon sources from steel, cement, power plants etc., using chemical absorption (solvents), physical adsorption, or cryogenic or membrane separations (Singh, J. & Dhar, 2019b). However, due to the low solubility for mass transfer (gas-liquid phase) in culture media, less than 10 % through direct sparging is being utilised (González-López *et al*., 2012). Therefore, it is necessary to develop a process that allows for the efficient capture of carbon dioxide from mushroom production in the form of inorganic carbon for algal cultivation. The application of amine-based solvents such as diethanolamine (DEA) and mono-ethanolamine (MEA) is currently the most commonly used commercialised process in post-combustion plants with high energy consumption (Sanna *et al*., 2014). However, MEA is a

corrosive amine that reacts with atmospheric oxygen to form reactive intermediates (Luis 2016; Zhao *et al*. 2011). Sodium hydroxide has been identified as an alternative solvent to MEA for carbon capture through aqueous solutions, due to its relatively non-corrosive and non-toxic properties (Stolaroff *et al*., 2008a). The use of highly efficient alkaline absorption methods such as NaOH have been evaluated for carbon capture to overcome the limitations of gas-liquid mass transfer (González-López *et al*., 2012). CO_2 can be introduced into the culture either through injection as a gas or it can be incorporated as bicarbonate in an alkaline solution (Chisti, 2016).

Moreover, pH of the cultivation is mostly affected by the carbon dioxide delivery system. Bicarbonate from CO_2 capture requires high pH level to sustain the bicarbonate in the solution without escaping from the system (Yadav *et al*., 2016). The optimal pH for microalgae cultivation is species dependent and the addition of CO_2 is a common method for pH control in microalgae cultivation systems (Moheimani, 2013). A significant disadvantage of controlling pH through direct CO_2 injection is the inefficient solubility and utilisation of CO_2. A considerable portion of the injected CO_2 escapes into the atmosphere, leading to environmental pollution. Hence, it's crucial to find an alternative method that ensures effective use of carbon dioxide in the form of a bicarbonate solution. Different microalgae strains such as *P. tricornutum* and *Chlamydomonas* sp., cultivated at pH 9 gave specific growth rates of 0.3 d^{-1} and 0.41 d^{-1} respectively reported to remove 50 - 60% CO_2 while other reports on *E. gracilis* (0.72 d^{-1}), *E. mutabilis* (0.58 d^{-1}) cultivated at pH 3 contributed to 10 – 24% CO_2 removal (Piiparinen *et al*., 2018). Microalgal species behaves differently at pH ranges which promotes photosynthetic growth leading to functional activities like the enzymatic activities of the cells and biomass production by (K. Li *et al*., 2020). The application of proportional integral with pH control improved microalgae production and CO_2 utilisation with pulse modelling in a tubular photobioreactor (Fernández *et al*., 2010). However, the bicarbonate ion (HCO_3^-) is highly soluble, which facilitates its use by microalgae through the carbon dioxide concentration mechanism (CCM). This process involves the enzyme carbonic anhydrase, which transforms bicarbonate (HCO_3^-) into carbon dioxide (CO_2) within the microalgae's intracellular membrane (Moroney and Ynalvez, 2007). Several reports on carbon capture and utilisation (CCU) have been studied on the utilisation efficiency of different microalgal species such as *Scenedesmus obliquus* on 10 % carbon dioxide removal from fermented brewery wastewater in a bubble column photobioreactor (Ferreira *et al*., 2017), *Arthrospira platensis* was evaluated for carbon dioxide fixation using carbon dioxide from fermented molasses in a tubular photobioreactor (Matsudo *et al*., 2011), and cultivation of *Spirulina* sp*.,* using carbon dioxide absorbents such

as monoethanolamine (MEA) and sodium hydroxide on their influence in growth and biomass production (Rosa *et al*., 2016). Hence, it is essential to examine the microalgae growth at different pH conditions on biomass productivity and inorganic carbon removal. From chapter 3, based on the effect of varying different $NaHCO_3$ concentration tolerance by different microalgal species, *Vischeria* sp., and *P. purpureum* were identified based on their growth, biomass production, carbon removal, and their valuable metabolites such as phycobiliprotein, eicosapentaenoic acid (EPA), long-chain polyunsaturated fatty acids, arachidonic acid, carbohydrates, proteins, and polysaccharides (Sánchez-Saavedra *et al*., 2018; Sinetova *et al*., 2021). This study hypothesised and aimed that, will the growth rate and CO_2 uptake ability be influenced by the pH of the culture medium and to assess their impact for *Vischeria* sp., and *P. purpureum* cultivation in synthetic media and mushroom-bicarbonate media.

4.2 Materials and methods

4.2.1 Mushroom growth and carbon dioxide capture

A closed growth system was designed using a transparent storage box (60 cm × 40 cm × 25 cm) from Figure 4.1. The system was equipped with a portable CM-501 GasLab monitor with a measurement range of 0 – 15,999 ppm with a sensitivity of ± 50 ppm, an air pump, air filters, a humidifier, and light. The carbon dioxide concentration in each chamber was measured every 10 min by using a CM-501 GasLab monitor. Furthermore, each box was outfitted (eight holes) with an air inlet and outlet around each box to ensure efficient airflow. The outlet was fitted with a one-way to allow excess carbon dioxide to flow into the absorption medium (NaOH-BBM) by continuous injection. An air pump (Pawfy MC-3000 pump, UK) was placed inside the growth box to remove the carbon dioxide generated by the mushrooms into the coupled culture medium (NaOH-BBM). The CM-501 GasLab monitor with a CSV file format was placed inside the box to measure parameters such as carbon dioxide coming the fungi, temperature, and relative humidity. From figure 4.2, a negative control of the atmospheric carbon dioxide concentration from the laboratory was measured in comparison with the carbon dioxide emitted from the mushrooms. A light source is provided during the pinhead phase which set to direct growth of the mushroom bodies. A beaker of water was placed in the box to create a humid environment that promoted the effective growth of mushrooms. The experiment was conducted on a small scale using a 1 L Schott bottle at a flow rate of 2.5 L/min using a Pawfy MC-3000 pump, UK.

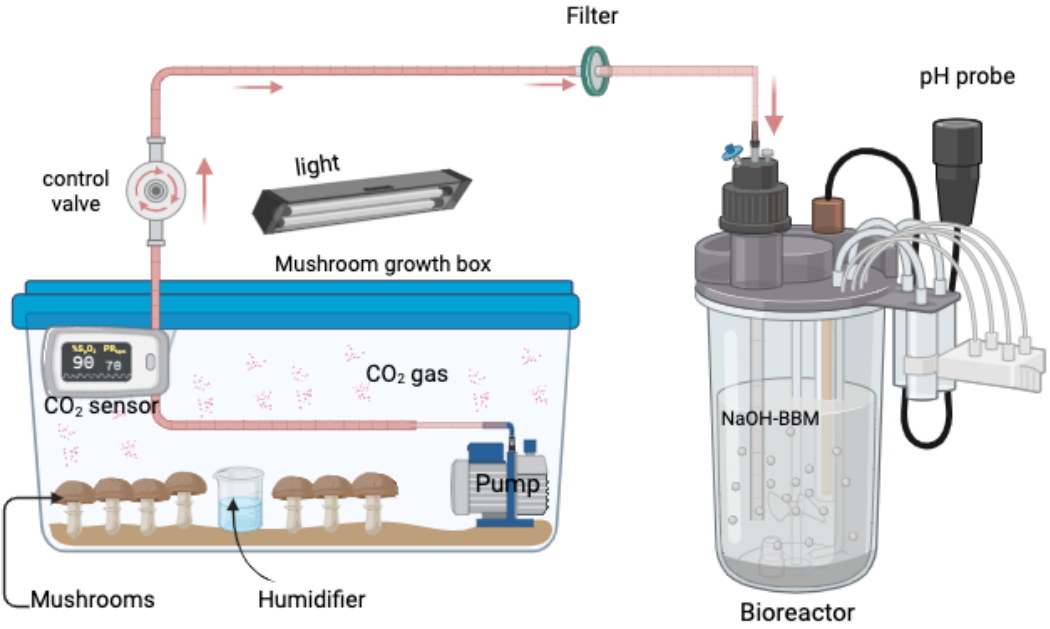

Figure 4.1 Schematic representation of carbon capture from mushroom cultivation chamber using an absorbing media coupled with microalgal growth media.

4.2.2 Microalgal inoculation preparation

The green microalgae *Vischeria* sp., (Eustigmatophyceae), and red microalga *Porphyridium purpureum* (Rhodophyta) used in this study were provided by AlgaeCytes Ltd., UK. A stock inoculum of 1 L was cultivated for *Vischeria* sp. in Bold's Basal Medium (Allen, 1968) and *P. purpureum* was cultivated in BBM with the addition 37 g L^{-1} of tropic sea salt of the supplemented with 1 g L^{-1} $NaHCO_3$. The culture media were autoclave and filtered to remove precipitates from the addition of sea salts. These cultures were incubated with a continuous intensity of light 150 μmol/m^2/s, aerated at a flow rate of 1 L/min, and under 120 rpm (unit too low to be converted into *g*) using a Cole-Parmer Stuart magnetic stirrer.

4.2.3 Screening of microalgae culture under different pH values

From the culture stocks in section 4.2.3, *Vischeria* sp. and *P. purpureum* strain was cultivated in 250 mL Erlenmeyer flasks. Microalgae strains were cultivated in Bold's basal medium (control) of 2.0 g L^{-1} $NaHCO_3$, and the captured carbon medium (NaOH-BBM) was used for the pH screening study with 2 g L^{-1} ($NaHCO_3$) captured carbon as an inorganic carbon source. An initial pH of 5, 7, and 9 was set for all the media using 0.1 M NaOH and HCl solutions. A medium of 150 mL was inoculated with 0.1 optical density of microalgae cells. For this screening, the pH of the reactors was monitored every 12 hours and regulated to their set culture conditions using a 0.1 M HCl solution. Cultures were incubated for eight days at room temperature under continuous illumination and agitation at 120 rpm (unit too low to be converted into *g*) on an Orbital Stuart shaker. All cultivation reactors were executed in duplicates. Duplicate cultures were pooled on day 8, harvested by centrifugation at 3000 g for 6 min, and dried. Marine species were desalinated using 20 mL of 0.5 M ammonium formate to remove salt traces and prevent spectra interferences before storing at -20 °C until further process.

4.2.4 Specific growth rates of microalgae

The specific growth rate (μ, d^{-1}) was estimated based on the optical density of the culture suspension at 680 nm (OD) using a microplate reader (Thermo Scientific, UK), as follows:

$$\mu\ (d^{-1}) = \frac{\ln (OD_2 / OD_1)}{t_2 - t_1} \qquad (4.1)$$

where "μ" is the specific growth rate (d^{-1}), "OD_2" on the final day "t_2", and "OD_1" is the OD on day "t_1". An aliquot of 10 mL of the culture suspension was sampled from the photobioreactor, centrifuged at 3000 *g* for 5 min (washed twice with distilled water for freshwater species and ammonium formate for the marine species), and filtered through a pre-weighed Whatman GF/C glass microfiber filter (pore size 0.22 µm). Biomass content was quantified by determining the dry weight difference after drying at 105°C for 24 hours.

4.2.5 Phycobiliprotein extraction and analysis

The freeze-thaw method was used for the extraction of phycobiliprotein (PBP) from *P. purpureum* freeze-dried biomass, using a modified method by (Mc Gee *et al*., 2020b) from section 2.4.4.

4.2.6 Biochemical composition analysis using FTIR spectroscopy

FTIR attenuated total reflectance (ATR) spectra were collected using a Cary 630 PerkinElmer Model Spectrum two instrument equipped with a diamond crystal ATR reflectance cell with a DTGS detector scanning over the wavenumber range of 4000–450 cm^{-1} at a resolution of 4 cm^{-1} as described by McGee *et al*.(2020) in Chapter 2 section 2.4.8.

4.2.7 Pigment extraction

Pigment extraction was carried out under ice-cold acetone with approximately 4 - 5 mg lyophilised biomass (n=3) transferred into a 2 mL tube by adding two scoops of glass beads (~500 mg) were added. The samples were extracted using 1 mL of organic solvent (acetone: methanol, 7:3 v/v) containing an internal standard (α-tocopherol acetate, 100 mg L^{-1}) by homogenising them in a VelociRuptor V2 Microtube Homo^{TM} (SLS1401) at 6.00 m/s for 15 seconds (9x cycles). The extracts were filtered through a 0.2 µm PTFE syringe filter transferred into 2 mL RP-HPLC vials and stored at -80^{o}C before HPLC analysis (S. Wright *et al*., 1991).

4.2.8 High-pressure liquid chromatography analysis

The purified extract stored at -80^{o}C from section 4.3.4 was analysed using a Hewlett Packard instrument with a Nova-Pak C18 4um, 3.5 × 150 mm column with a guard column. Mobile phase A consisted of methanol:0.5 M ammonium acetate (80:20 v/v), mobile phase B consisted of acetonitrile and deionised water (90:10 v/v), and mobile phase C consisted of 100% ethyl acetate (D. A. Wright *et al*., 1991). The injection volume was 25 µL with 1 mL/min

flow rate and a run time of 24 min. The pigments were identified based on their retention times, and the UV-vis spectral fine structures were compared to standards.

4.3 Results and Discussion

4.3.1 Carbon dioxide generation during mushroom growth

The concentration of carbon dioxide produced from the mushroom cultivation chamber was monitored for 48 h from the primordia (pinning) phase. From this phase onwards, the carbon dioxide levels from the mushroom increased from 680 ppm (optimum) to more than 10000 ppm after 24 hours (Figure 4.3). From the continuous observation of carbon dioxide production, the level of production fluctuated between 10,000 ppm and 15,000 ppm within the instrumental range. A diaphragm pump with a flow rate of 16 L/min placed inside the growth box with a suction filter helped remove approximately 13,565 ppm of carbon dioxide from the chamber into the absorption media for carbon dioxide absorption continuously until the required inorganic carbon was captured for microalgae cultivation. However, figure 4.3 represents the mushroom fruiting bodies cultivated at an optimum carbon dioxide concentration level (≤ 1000 ppm). Figure 4.4 represents the fruiting yield and quality of mushroom growth under optimum carbon dioxide concentration condition.

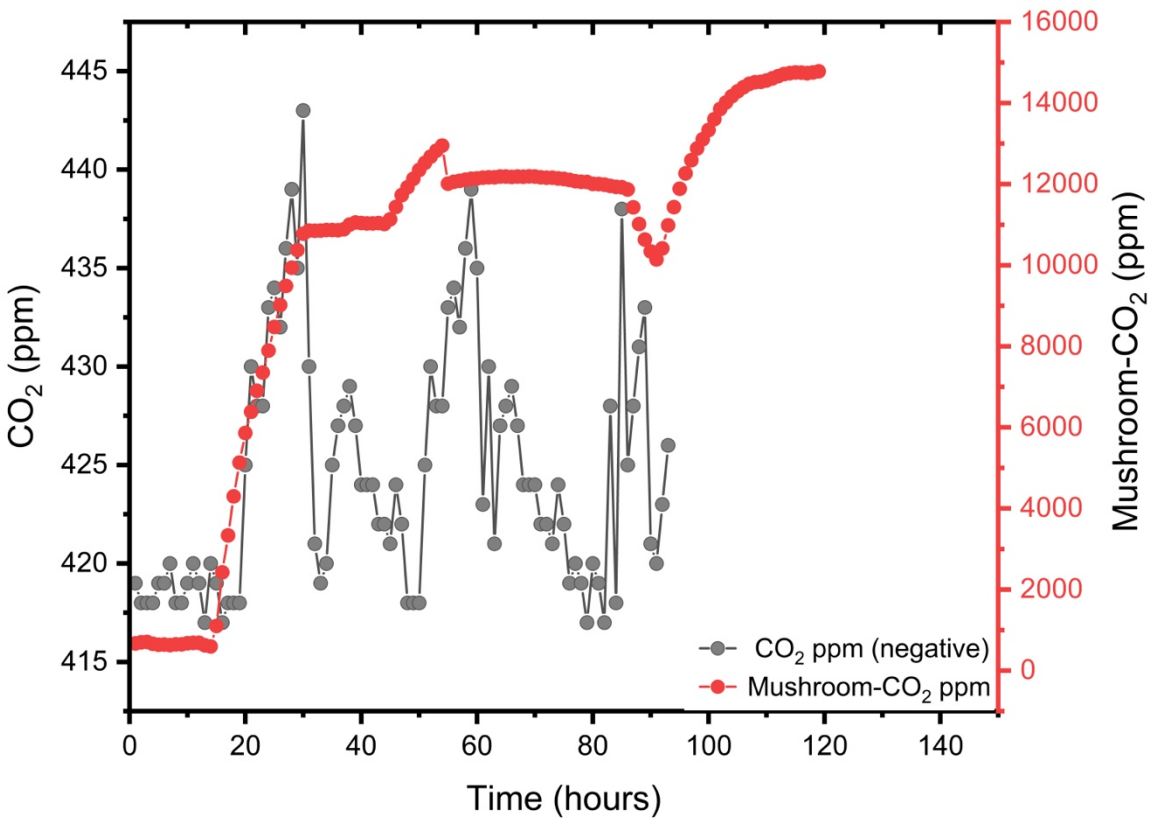

Figure 4.2 Comparison of accumulated carbon dioxide concentrations by mushrooms from the chamber (red circle) and carbon dioxide concentration within the laboratory workspace (control - grey circle) measurement using CM501-GasLab monitor for about 120 hours continuous observation.

4.3.2 Physiological effect of carbon dioxide on *Pleurotus ostreatus*

Figure 4.3. represents the effect of carbon dioxide on *P. ostreatus* fruiting bodies at different carbon dioxide concentration levels observed from four different set of boxes at set ppm. The development of the mushroom fruiting bodies was observed at elevated carbon dioxide concentration (Figure 4.3a-b) and optimal (Figure 4.3c-d) carbon dioxide conditions. These analyses were conducted in four separate growth boxes with a CM-501 GasLab monitor. The stipes from figure 4a-b were longer (8 cm-a, 12 cm-b) and thinner at higher carbon dioxide concentrations (≥ 3000 ppm) than the fruiting bodies between 3cm – 7cm from figure 4c-d at lower CO_2 concentration (≤ 1000 ppm). High levels of carbon dioxide during cultivation can result in longer stipes in certain mushroom species, particularly in controlled environment mushroom cultivation (Ho *et al*., 2020). To optimise stipe length, a multifaceted approach is necessary, involving the control of various factors such as fresh air exchange, humidity levels, temperature stability, light exposure, and carbon dioxide levels, which collectively contribute to achieving the desired morphology of the fruiting bodies (Sakamoto, 2018). Carbon dioxide (CO_2) is a metabolic product in mushrooms. During the initial phases of growth, the spawn

run, and the fruiting bodies require elevated levels of carbon dioxide (≥ 5000 ppm). After the growth becomes evident, the optimum requirements change, therefore farmers need to maintain the carbon dioxide concentration in the growth rooms between 800 to 1500 ppm, depending on the species of the mushroom. At a concentration of less than 800 ppm, the mushrooms become too small and numerous. At levels exceeding 2000 ppm, the quality of mushrooms is deplorable. In this case, the stem height is very long, and the cap is too small. A higher concentration of 4000 - 5000 ppm hinders the development of the mushrooms. The precise and oscillating optimal values make mushroom farming a challenging task. The mushrooms that do not meet the quality parameters have to be thrown away, resulting in economic loss for the farmer.

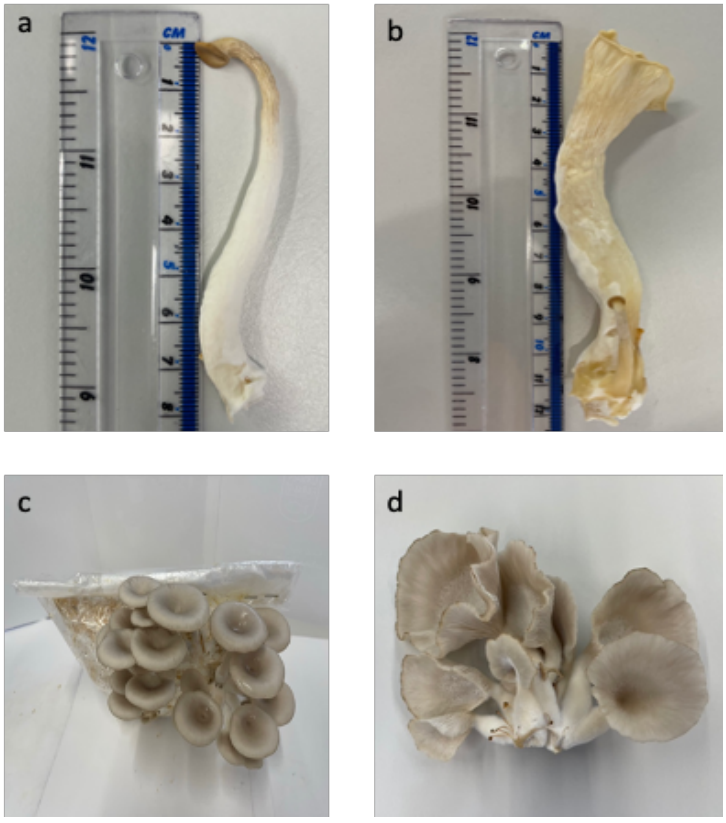

Figure 4.3 Physiological impact of optimised and elevated carbon dioxide on the fruiting bodies of mushrooms a) CO_2 level ≥ 9000 ppm, b) between 3000 ppm and 9000 ppm, c) less than 600 ppm and d) ≤ 1000 ppm.

4.3.3 Microalgal proliferation in a bicarbonate media at different pH conditions

The effect of bicarbonate medium from both synthetic and carbon capture from mushroom production was evaluated on their impact on growth for *Vischeria* sp. and *P. purpureum* at different pH conditions. From Figure 4.4a, the microalgal growth for *Vischeria* sp. in synthetic media and mushroom-bicarbonate media at different pH shows that, in the

synthetic media at pH 7 and 9, microalgal cells were able to thrive compared to the mushroom-bicarbonate media at the same pH conditions. The highest growth rate achieved was 0.201 d^{-1} at pH 9 in the synthetic media than the specific growth rate in mushroom-bicarbonate with 0.166 d^{-1} at pH 9. The growth rate in the mushroom-bicarbonate at pH 7 and 9 was similar. Growth in the synthetic media increased with increasing initial pH with a final biomass of 1.69 g L^{-1} at pH 9 followed by 1.03 g L^{-1} at pH 7 and the lowest at pH 5 as 0.701 g L^{-1}. In the mushroom-bicarbonate media, the highest growth rate was observed at pH 7 with the maximum biomass production of 1.178 g L^{-1} 1.2 folds higher at pH 9 with a biomass of 0.998 g L^{-1}. This is because the algal growth was sufficient in the synthetic media due to less salt stress. The highest specific growth rate in the mushroom-bicarbonate culture was 0.168 d^{-1} at pH 7 compared to the growth rate with 0.142 d^{-1} at pH 9. Comparison of growth in both media shows that bicarbonate provided sufficient inorganic carbon for algal growth and higher biomass production, while pH 5 response with low growth is due to acidic conditions for the cells. In a similar study, the effect of bicarbonate and pH on *Chlorella sorokiniana* was investigated with an average of 0.353 g $L^{-1}d^{-1}$ as the maximum rate at pH 7 by (Qiu *et al*., 2017). However, the optimisation of induced salt in *C. reinhardtii* at 200 mM NaCl suppressed the growth rate but significantly increased the biomass productivity to 0.028 g $L^{-1}d^{-1}$ (Fal *et al*., 2022). In addition, under salt stress of 0.5 M NaCl, the biomass accumulation in *Vischeria punctata* was inhibited (Sinetova *et al*., 2021), which confirms the results seen with *Vischeria* sp. in the present study.

However, the growth of *P. purpureum* was better in mushroom-bicarbonate media with a specific growth rate of 0.247 d^{-1} at pH 7 compared to that in the synthetic media with 0.123 d^{-1} at pH 9. The final biomass production in the mushroom-bicarbonate media at pH 7 was 1.972 g L^{-1} 2 folds higher than the synthetic media of 0.983 g L^{-1}. The growth response in Figure 4.6b showed similar trend except pH 7 in the bicarbonate media which gave the highest growth rate with respect to the biomass productivity. Although, at lower pH 5, there was no inhibition in growth with low inorganic carbon removal. This may be because microalgae are tolerant to pH changes and tend to have increased growth at higher pH levels due to their ability to metabolise inorganic carbon (Singh and Singh, 2015). However, both strains responded differently to increasing pH conditions.

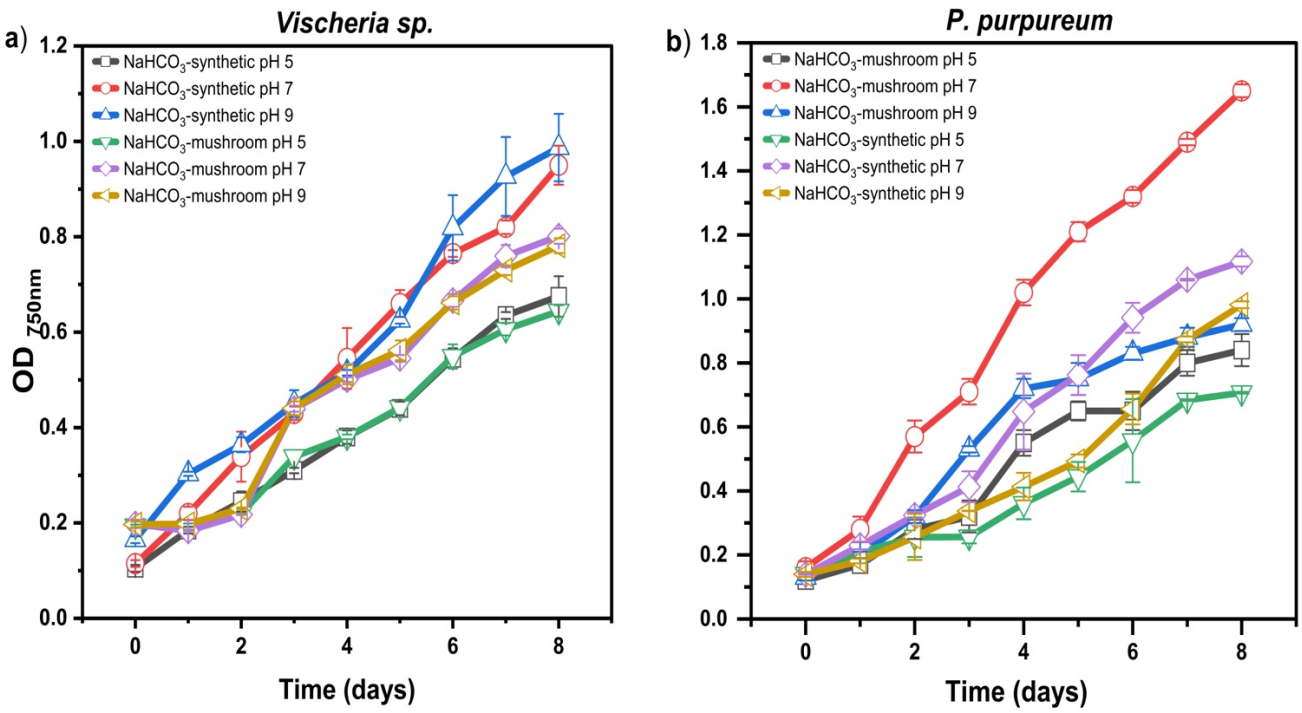

Figure 4.4 Microalgal growth levels for *(*a) *Vischeria* sp. and *(*b) *Porphyridium purpureum* cultivated in synthetic media and mushroom-bicarbonate media at different conditions of pH 5, 7, and 9 for a period of 8 days. Data values expressed as mean ± standard deviation, n=3.

4.3.4 Inorganic carbon utilisation at different pH conditions

The availability of inorganic carbon in both synthetic and mushroom-bicarbonate media at varying pH levels ensured uniform carbon source supply under each pH condition. The utilisation of bicarbonate through the carbon dioxide concentration mechanism via carbonic anhydrase in the microalgae cells was observed. From table 4.1, it was found that the inorganic carbon utilisation efficiency increased with increasing pH in the synthetic media compared to the mushroom-bicarbonate culture. The highest carbon utilisation in the synthetic media was achieved at pH 9, while in the mushroom-bicarbonate media, it was found to be at pH 7. The average total inorganic carbon removal obtained from the mushroom-bicarbonate media was higher compared to the synthetic media. It was observed that adjusting the culture media at different pH levels improved the inorganic carbon removal depending on the microalgal species and bicarbonate media, leading to varying removal rates. The adjustment of pH had a positive effect on the growth properties of *Vischeria* sp. and *P. purpureum* and resulted in increased biomass production under different bicarbonate conditions. Additionally, consistent adjustment of pH under each bicarbonate condition led to higher carbon dioxide removal, with 76.57% and 87.33% removed in synthetic media at pH 9 and mushroom-bicarbonate media at pH 7, respectively. However, it is hypothesized that most of the inorganic carbon was converted

into carbon dioxide from the bicarbonate species (HCO_3^-) by the carbon anhydrase, but a portion of the carbon dioxide may have escaped due to mechanical agitation of the culture media which relates when shaking was applied during this study. Similar study was reported during screening of *P. kessleri* in bicarbonate under regulated pH condition by (Beigbeder *et al*., 2021). The maximum inorganic carbon removal efficiency was reported in the latter study. A study on *Chlorella* sp. and *Tetraselmis* sp. reported that microalgal cells were able to grow at higher pH in a bicarbonate supplement (Moheimani, 2013).

Table 4.1 Microalgae growth parameters and inorganic carbon removal efficiency of *Vischeria* sp. and *P. purpureum* for the investigated bicarbonate concentrations at different pH conditions. Data values expressed as mean ± standard deviation, n=3.

Strain	***Vischeria* sp.**		***P. purpureum***	
	Synthetic media	Mushroom-bicarbonate	Synthetic media	Mushroom-bicarbonate
		Total inorganic removal (%)		
pH 5	44.8 ± 0.01	42.5 ± 0.03	40.5 ± 0.03	47.9 ± 0.01
pH 7	72.6 ± 0.03	67.3 ± 0.01	76.4 ± 0.01	87.3 ± 0.02
pH 9	76.6 ± 0.02	65.6 ± 0.01	65.7 ± 0.01	71.0 ± 0.01

4.3.5 Effect of inorganic carbon on photosynthetic pigment at different pH conditions

The impact of different pH conditions on the pigment content from *Vischeria* sp. and *P. purpureum* has been described in figure 4.5. There was a significant difference in pigment content cultured at different pH condition in mushroom-bicarbonate and synthetic media in figure 4.5. Comparatively, the chlorophyll-*a* content of 37.31 mg g^{-1} in the synthetic media was 1.4 folds higher than the chlorophyll-*a* content 26.18 mg g^{-1} of the mushroom-bicarbonate media by *Vischeria* sp. ($p \leq 0.01$) at pH 9 (Figure 4.5a). The β-carotene content showed statistical difference at pH 5 and 7 but not at pH 9. The difference in chlorophyll-*a* and β-carotene content between the bicarbonate culture and synthetic media was significant (Figure 4.5b), which might be due to the oxidative stress caused by sodium (Na^+) that promotes chlorophyllase activity and leads to chlorophyll degradation, as reported in *C. reinhardtii* by (Ji *et al*., 2018a). A decrease in the activity of carbonic enzyme due to low carbon dioxide

utilisation which is a key factor led to the reduction in chlorophyll production at pH 5 (Hounslow *et al*., 2021). Under unfavourable conditions, microalgae and cyanobacteria mostly accumulate carotenoids due to oxidative and lipid peroxidation damage caused by antioxidative molecules (Rezayian *et al*., 2019). In *P. purpureum*, there was a significant difference between the synthetic media and mushroom-bicarbonate media of chlorophyll-*a* content which was 13.47 mg g^{-1} and 7.93 mg g^{-1} respectively at pH 5. At pH 9, the chlorophyll-*a* content were 16.49 mg g^{-1} and 3.89 mg g^{-1} in the synthetic media and mushroom-bicarbonate media respectively ($p \leq 0.001$). There was no significant difference between the chlorophyll-*a* and β-carotene concentrations in the bicarbonate media (Figure 4.5d). The obtained results were similar in both the synthetic media and mushroom-bicarbonate media at pH 7, with a concentrations of 22.67 mg g^{-1} chlorophyll-*a* and 4.48 mg g^{-1} β-carotene which was statistically insignificant (Figure 4.5d). The importance of photosynthesis and plant development is directly affected by β-carotene content, which was found to be 2.6 ± 0.242 mg L^{-1} in sodium stress response. This confirms our study on β-carotene content which gave a concentration of 4.48 mg g^{-1}, which is approximately 2 folds high than the concentration reported by (Rezayian *et al*., 2019).

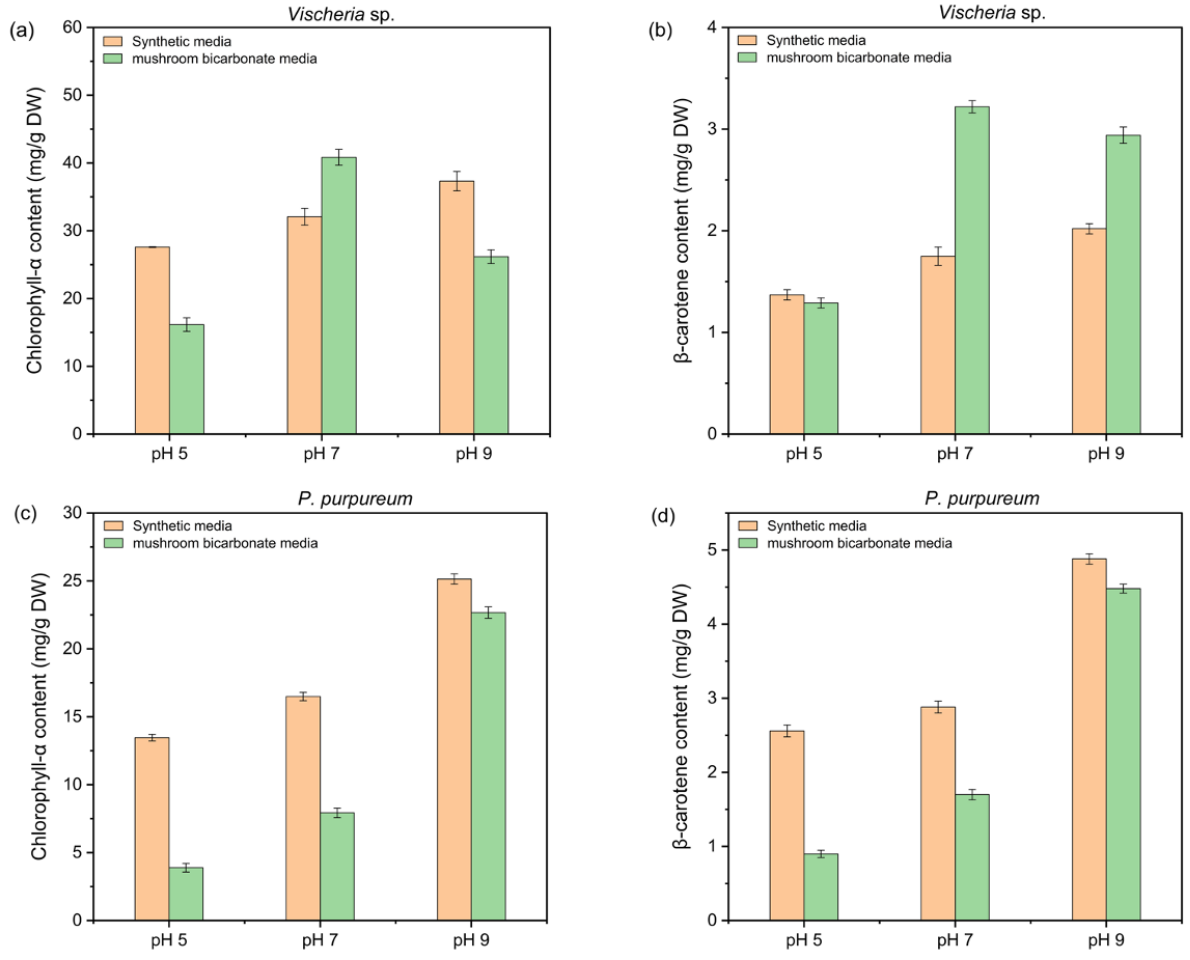

Figure 4.5 Describes the effect of inorganic carbon on the photosynthetic pigments of (a, c) chlorophyll-*a* and (b, d) β-carotene from the dry weight of *Vischeria* sp. and *Porphyridium purpureum* in synthetic media and mushroom-bicarbonate media at a pH of 5, 7, and 9 measured using HPLC. Data values expressed as mean ± standard deviation n=3, and statistical analysis by one-way ANOVA with post-hoc test shown in Appendix B.

4.3.6 Effect of bicarbonate on phycobiliproteins content at different pH conditions

The phycobilisome is a flexible structure that can modify the cell's light absorption abilities based on the available light intensity, quality, nutrient availability with the capacity to adjust the production of phycoerythrin and phycocyanin according to the spectral characteristics of their cultivation conditions (Johnson *et al*., 2014b). Comparative study of phycobiliproteins yield in synthetic media and mushroom-bicarbonate from Figure 4.6. Synthetic media was found more suitable for phycobiliprotein content (1.75 mg g^{-1}) at pH 7 compared mushroom-bicarbonate media with 1.13 mg g^{-1} at pH 7 ($p \leq 0.01$). Changes in pH affected the phycobiliprotein content in both bicarbonate media. In addition, *P. purpureum* was found comfortably growing at pH 7 and 9. However, at pH 5, the phycobiliprotein was lower and started to bleach out. Growth study by *Nostoc* sp. at pH 8 grew well but bleached out at pH 3 according to (Johnson *et al*., 2014b). Most studies have reported the optimum alkaline conditions between pH 8 – 10 to be appropriate for phycobiliprotein synthesis (Zeng *et al*., 2012). A study on *Gloetrichia natans* under pH adjustment did not affect growth but significantly changed the phycobiliprotein synthesis according to (Boussiba, 1991). In *Arthrospira* sp. optimisation of single freeze-thaw process yielded (219.87 mg g^{-1}) maximum phycobiliprotein (Tan *et al*., 2020).

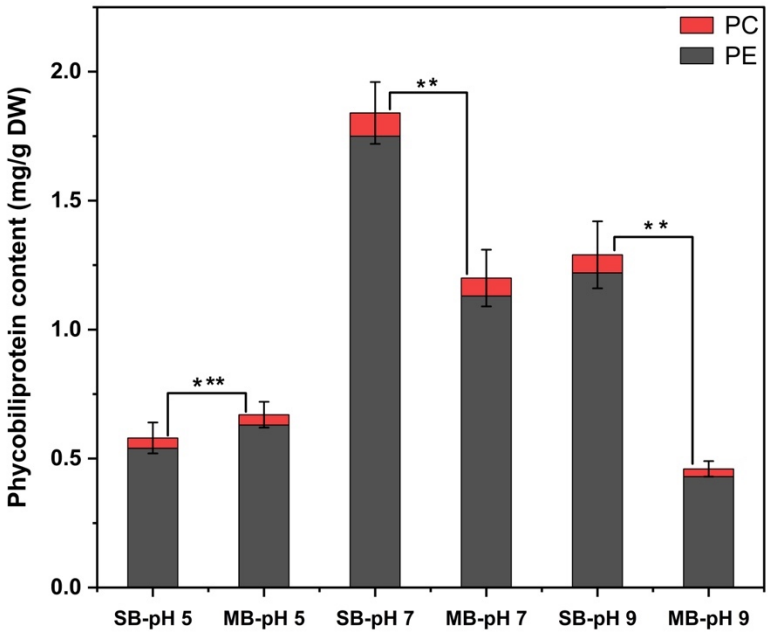

Figure 4.6 Describes the phycobiliprotein (PB) content of phycoerythrin (PE) and phycocyanin (PC) extracted from *Porphyridium purpureum* under synthetic media and mushroom-bicarbonate media at different pH levels. SB-pH and MB-pH represents synthetic media and mushroom-bicarbonate media. Data values expressed as mean ± standard deviation, n=3 and statistical analysis by one-way ANOVA with post-hoc test.

4.3.7 Effect of bicarbonate media on the biochemical composition as a function pH

The composition of biochemical compounds in microalgae varies based on the species and other parameters like pH and salinity. To analyse the biochemical composition of harvested microalgal biomass, the content of carbohydrates, proteins, and lipids were determined. In the synthetic media culture of *Vischeria* sp. the amount of carbohydrates in the final microalgal biomass ranged from 43.9 % to 48.7 % at varying pH conditions (Figure 4.7c). The estimated carbohydrate content at each bicarbonate media (synthetic and mushroom-bicarbonate) were insignificant at different pH condition. The estimated carbohydrate contents were similar except at pH 5 in the mushroom-bicarbonate which was about 1.3 folds lower than the synthetic media in *Vischeria* sp. The amount of protein content in *Vischeria* sp. accumulated was about 40% from both media which was statistically significant at pH 5 and 7 ($p \leq 0.008$). The protein content in the mushroom-bicarbonate media increases with increasing pH. The regulation of pH contributed protein accumulation in the synthetic media than the mushroom-bicarbonate media. However, the lipid content showed varied response when cultivated both bicarbonate medium. From the synthetic media of *Vischeria* sp. the highest lipid content was estimated to be 13.1% higher than the mushroom-bicarbonate media with 8.45%. Statistically, there was a

significant difference on the lipid content among the synthetic and mushroom-bicarbonate media ($p \leq 0.05$) within each varied pH condition.

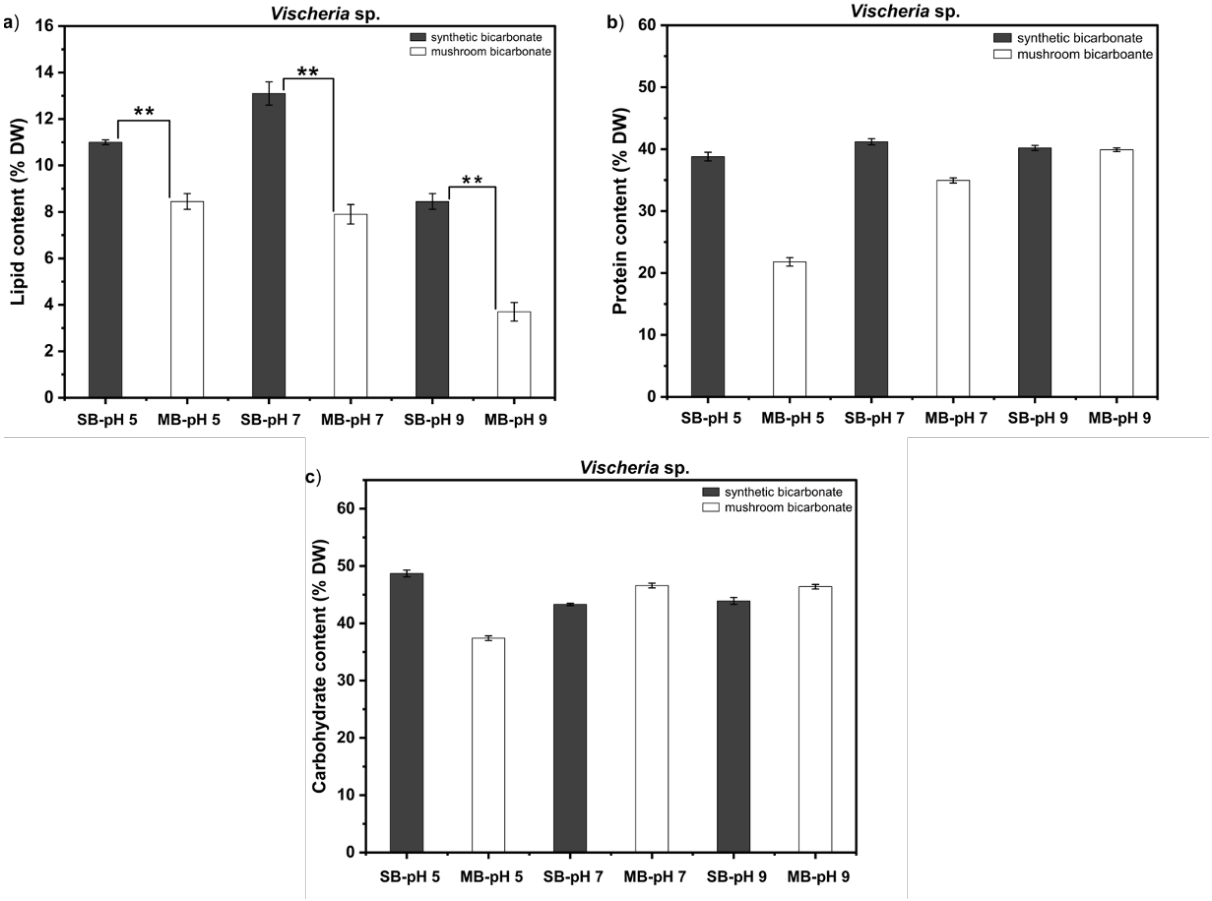

Figure 4.7 Represents biochemical composition of (a) lipid, (b) protein, and (c) carbohydrate in synthetic media and mushroom-bicarbonate media at different pH cultivation conditions for *Vischeria* sp. was measured using FTIR spectroscopy. Data values expressed as mean ± standard deviation, n=3 and statistical analysis by one-way ANOVA with post-hoc test (**$p \leq 0.01$). SB-pH and MB-pH represents synthetic bicarbonate media and mushroom-bicarbonate media respectively.

However, in *P. purpureum*, the highest carbohydrate content in the mushroom-bicarbonate media was 39.5% compared to synthetic media with 25.3% at pH 9 from figure 4.8. There was no statistical difference between the synthetic and mushroom-bicarbonate on carbohydrate content at pH 5 and 7. The cultivation of *Chlorella* sp. in a regulated pH between 8 and 9 accumulated carbohydrate content from 13.2% to 23.1% under bicarbonate culture (Yadav *et al*., 2019b). However, in the present study, the carbohydrate content was found to be higher, possibly due to differences in algal strains and growth properties in the mushroom-bicarbonate. A study on *P. purpureum* cultivated under pH 8 and bicarbonate yielded about 40% carbohydrate content, which agreed with our experimental findings of 39.5% (Lu *et al*., 2020). The highest protein content of 22.6% in the synthetic media was similar under pH 7 and

9. The total lipid content in the synthetic media decreases with increasing pH from 4.2% – 2.65%. There was no statistical difference between both bicarbonate media on lipid production, therefore the regulation of pH did not improve the lipid content in both bicarbonate cultures. Moreover, high salinity level resulted into lower accumulation of composition levels such as carbohydrate and lipid content in *P. purpureum*. These results suggest that the estimated content of the biochemical composition from the dry weight did not show significant differences, contrarily to what was observed in *P. purpureum* at difference pH and bicarbonate media which was in agreement with literature (Ferreira *et al*., 2021). This can be a result of metabolic regulation which was affected by the salinity modulation of the media which triggered specific biosynthetic pathways of the biochemical content (Zhang *et al*., 2022).

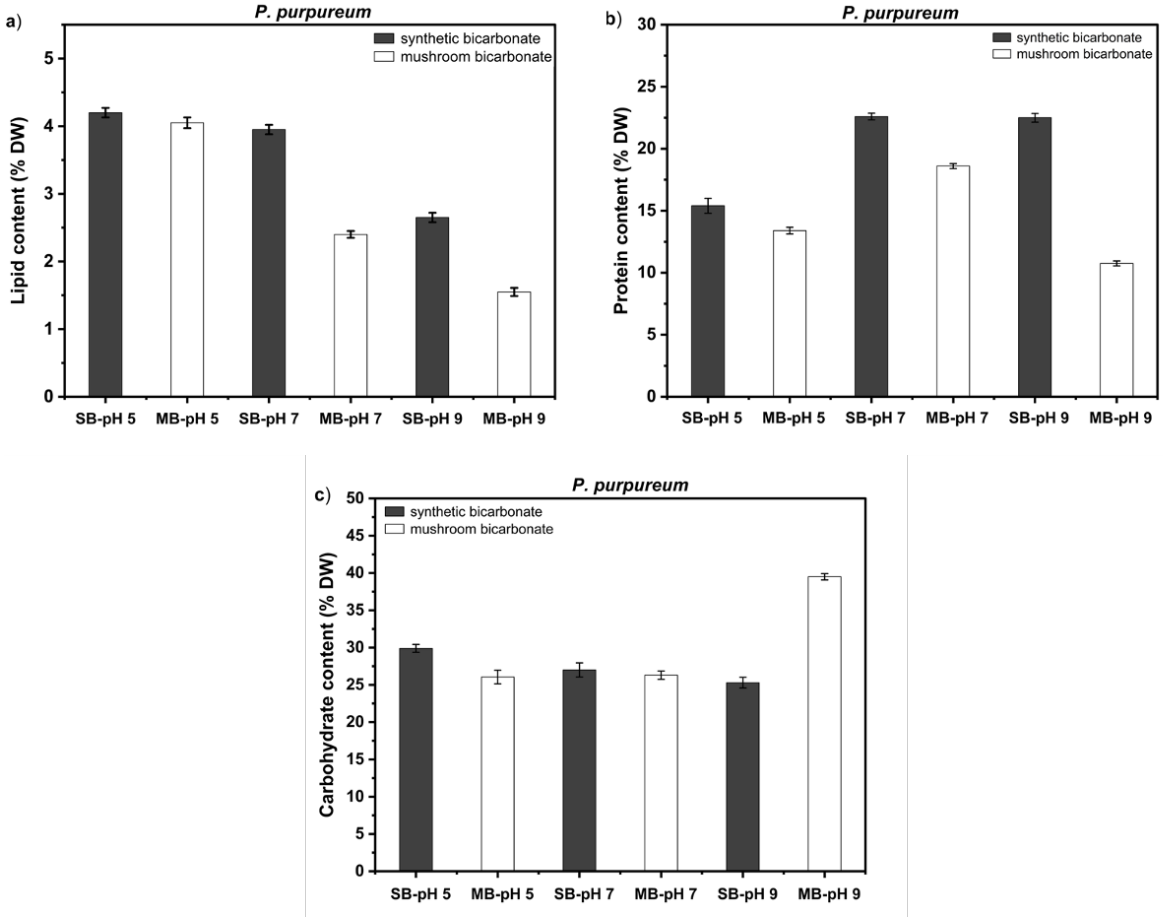

Figure 4.8 Represents the biochemical composition of (a) lipid, (b) protein, and (c) carbohydrate from synthetic media and mushroom-bicarbonate media at different pH (5, 7, and 9) cultivation conditions for *Porphyridium purpureum* was measured using FTIR spectroscopy. SB-pH and MB-pH represents synthetic bicarbonate media and mushroom-bicarbonate media respectively. Data values expressed as mean ± standard deviation, n=3.

4.3.8 Effect of different pH conditions on fatty acids

The primary fatty acids in *Vischeria* sp. are palmitic acid (C16:0), palmitoleic acid (C16:1), oleic acid (C18:1), arachidonic acid (C20:4), and eicosapentaenoic acid (C20:5). A study was conducted to assess the impact of synthetic media and mushroom-bicarbonate media on the fatty acid methyl ester (FAMEs) profile of *Vischeria* sp. and *P. purpureum*, as shown in Figure 4.9. The main fatty acids, ranging from C14:0 to C20:5, were found to be similar in both treatments under different pH conditions. The percentages of palmitic acid (C16:0), palmitoleic acid (C16:1), and arachidonic acid (ARA20:4) did not increase with a rise in pH (5, 7, and 9) in both types of media. However, the EPA content did increase from 17.0% to 22.0% as pH rose from 5 to 9 in each bicarbonate media. These changes in fatty acid compositions were seen as a defensive response to bicarbonate stress and pH conditions. In the synthetic media, the total EPA content was between 25.4% and 26.43% of the total fatty acids (TFAs) under each pH condition. Meanwhile, the total EPA in the mushroom-bicarbonate media was between 24.33% and 29.35% of the total fatty acids content. There was no significant difference between the synthetic and mushroom-bicarbonate cultivation conditions in terms of pH. The physiological state and fatty acid profile vary among different algae species (Juneja *et al*., 2013b). The overall major fatty acids, which accounted for at least 80% of the total fatty acids, were similar to those found in other groups of Eustigmatophyceae. These included palmitic acid C16:0, palmitoleic acid C16:1, oleic acid C18:1, arachidonic acid C20:4, and eicosapentaenoic acid C20:5.

In *P. purpureum*, the primary fatty acids are palmitic acid (C16:0), linoleic acid (C18:2), arachidonic acid (C20:4), and eicosapentaenoic acid (C20:5). When these fatty acids were compared in bicarbonate media, the average percentages of palmitic acid (39.03%) and linoleic acid (6.17%) in synthetic media were found to be similar to the percentages of palmitic acid (40.33%) and linoleic acid (8.16%) in mushroom-bicarbonate media. There was no significant difference in the percentages of arachidonic acid (26.36%) and eicosapentaenoic acid (25.63%) of the total fatty acids in synthetic media compared to the percentages of arachidonic acid (24.96%) and eicosapentaenoic acid (23.93%) in mushroom-bicarbonate media. As the pH increased, the EPA and ARA content in synthetic media showed a significant increase. The highest EPA and ARA content in *P. purpureum* was observed in synthetic media. Moreover, the stimulation of EPA content is not only due to inorganic carbon but also due to the optimisation of nitrate levels, leading to the accumulation of polyunsaturated fatty acids, as reported by (Remias *et al*., 2020). A study on the effect of adding bicarbonate to *Chlorella sorokiniana* at different pH levels reported high proportions of C16:1 and C18:1 when

cultivated at pH 6.5 (Qiu *et al*., 2017). Similarly, the regulation of pH in bicarbonate conditions led to an increase in the major fatty acid compositions in *Chlorella sorokiniana* (Qiu *et al*., 2017), which aligns with the findings of this study.

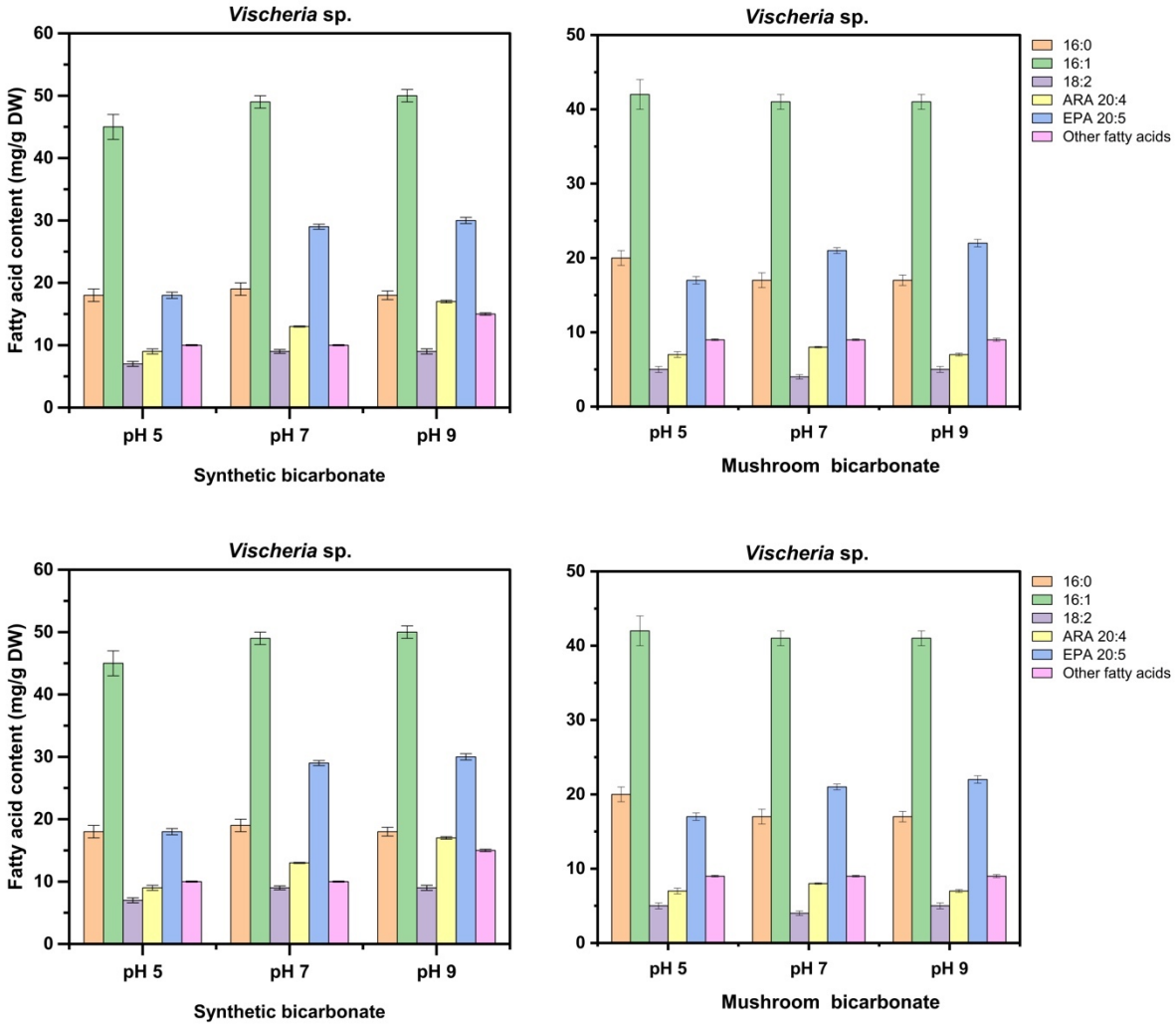

Figure 4.9 Represents the fatty acid content of *Vischeria* sp. and *Porphyridium purpureum* cultivated in synthetic media and mushroom-bicarbonate media at pH 5, 7, and 9. Data values expressed as mean ± standard deviation, n=3.

4.4 Conclusion

In this work, a sequential optimisation for *Vischeria* sp. and *P. purpureum* cultivation in a generated inorganic carbon media from mushroom production at different pH treatment conditions was conducted to analyse the influence of culture pH at different range was investigated to observe their utilisation capacity. Comparison between *Vischeria* sp. and *P. purpureum* on both synthetic media and mushroom-bicarbonate at different pH levels suggested that the best pH condition for inorganic carbon removal was 76.6% *Vischeria* sp. at pH 9 in the synthetic media and 67.3% in the mushroom-bicarbonate culture at pH 7. The

highest inorganic carbon removal from *P. purpureum* was 87.3% from mushroom-bicarbonate and 76.4% in the synthetic media at pH 7. The results showed that bicarbonate stimulated the lipid content at pH 7 in the synthetic media by *Vischeria* sp. pH variations distinctively affected inorganic carbon removal and biomass accumulation in both strains but did not cause any variation in biochemical composition. Inhibition on cell growth was insignificant during pH variations but resulted into maximum inorganic carbon utilisation. Since this series of experiment is in progressive stage for photobioreactor scale-up. This study will provide more information on how the cells will respond to sodium ions on scale-up process during carbon capture processes.

CHAPTER 5

Demonstration of the scalability of the bicarbonate-based integrated algal production system for carbon capture during mushroom cultivation and assessment of valuable products from microalgal biomass and mushroom exudate.

5.1 Background

In agricultural settings, mushroom cultivation in a controlled environment is designed to yield high quality mushrooms. The level of carbon dioxide builds up in mushroom growth environment has detrimental effects on the quality of mushroom yield. For high quality mushroom fruits, the excess carbon dioxide build ups are degassed from the mushroom farm to provide the optimal growth conditions, which contributes to the rising levels of carbon dioxide in the atmosphere. Besides industrial production of carbon dioxide from cement, metals, and fossil fuel combustion, mushroom farming has been identified as a potential contributor to greenhouse gas. Microalgae-based carbon capture and utilisation technology has been identified as an alternative method. However, chemical absorption of carbon dioxide from point sources requires extensive technology involving the use of amines such as monoethanolamine (MEA) and diethanolamine (DEA) and requires significant energy input for their regeneration (Beigbeder *et al*., 2021; González-López *et al*., 2012). A more cost-effective alternative is the use of absorbents such as sodium hydroxide for carbon capture to produce useful sodium bicarbonate ($NaHCO_3$) for industrial purposes including biological application as an inorganic carbon source for microalgae cultivation (Stolaroff *et al*., 2008b; Yoo *et al*., 2013). The direct utilisation of gaseous carbon dioxide by biological systems such as microalgae has also been extensively explored, although this depends on the adequate design and operations of the cultivation systems (Beigbeder and Lavoie, 2022; Kordylewski et al., 2013). A study carried out on *P. kessleri* and *Scenedesmus obliquus* demonstrated as a promising strain for various waste cultivation media such as wastewaters, pig manure, brewery waste (Beigbeder *et al*., 2021; Beigbeder and Lavoie, 2022). The ability to fix CO_2 by microalgae is indicative of the productivity of the biomass. Many species of microalgae possess carbon concentrating mechanisms, which allow them to thrive and store carbon even under fluctuating CO_2 concentrations. They achieve this by using bicarbonate transporters and CO_2 receptors to create high internal concentrations of dissolved inorganic carbon. As discussed in Chapter 3, high biomass production, biochemical composition (protein, lipid, and

carbohydrate) and the production of secondary metabolites and valuable products such as antioxidants, phycobiliprotein, and polysaccharides are important considerations for the implementation of microalgae-based carbon capture and utilisation techniques.

Recent studies have explored the important of antioxidant properties from microalgal extracts in cosmetic and nutraceutical applications (Liang *et al*., 2019; Salami *et al*., 2021). Algal antioxidants such as carotenoids, vitamin E (α-tocopherol), phycobiliproteins, and polyphenols (Shalaby, 2015). Today, industries isolate valuable compounds like fatty acids such as polyunsaturated fatty acids (PUFAs), eicosapentaenoic acid (EPA), and docosahexaenoic acid (DHA) from microalgae can prevent many diseases such as cardiovascular diseases and cancer (Cichoński and Chrzanowski, 2022a; Mata *et al*., 2010). Moreover, among the antioxidant compounds isolated from marine sources, phenolic and polyphenolic compounds are secondary metabolic products from microalgae, which are natural sources of these molecules (Albuquerque *et al*., 2021; Freile-Pelegrín and Robledo, 2013). Several classes of flavonoids, such as flavonols, flavanones, isoflavones, and dihydrochalcones were found in microalgae and cyanobacteria (Cichoński and Chrzanowski, 2022a). Furthermore, phenolic acids such as gallic, protocatechuic, caffeic, chlorogenic, vanillic, and salicylic acids, were found in different species of marine algae (Goiris *et al*., 2015; Klejdus *et al*., 2010). The concentration of algal polyphenols within algal cells varies according to the habitat, and factors such as UV irradiation, light, nutrient availability, and salinity (Freile-Pelegrín and Robledo, 2013). Phenolic content evaluated on 13 microalgal species by (Almendinger *et al*., 2021) reported that *Neochloris oleobundans* and *Wilmottia murravi* surpassed 20 mg gallic acid equivalents per gram. Although, a study on high intensity of light exposure on *Chlorococcum* sp., *Chlamydomonas reinhardtii,* and *Scenedesmus* sp., produced higher concentrations of phenolic compounds (Vignaud *et al*., 2023).

This work aims to demonstrate the scalability of microalgal carbon capture process described in Chapter 3 and to evaluate the value-added products generated from the spent biomass and mushroom waste. To simulate the captured carbon dioxide through enriched bicarbonate culture media, the culture media was supplemented with $NaHCO_3$ (1-6 g L^{-1}) in the first part of this study to evaluate the tolerance of the five selected microalgal strains (Chapter 3). In the second part of this study described in the present chapter, the two best performing strains were further cultivated in the captured carbon dioxide media to better examine the effect of pH regulation microalgae growth and inorganic carbon removal. Finally, the microalgal proliferation, inorganic carbon removal, biomass production, carbon mass balance analysis, the biochemical composition, and bioactive contents were evaluated. To the

best of my knowledge, this work represents the first study focusing on the capture of carbon dioxide generated from mushroom production and its subsequent assimilation by *Vischeria* sp.*,* and *P. purpureum* cultivation. Furthermore, this work demonstrates the scalability of the microalgal carbon capture system and explores the antioxidant and photoprotective properties of microalgal biomass and mushroom exudates thereby contributing to the development of a cost-effective and sustainable microalgae biosystem.

5.2 Materials and methods

5.2.1 Mushroom growth box for carbon capture

The mushroom cultivation and the measurement of carbon dioxide from the growth box were continued from the same process described in Chapter 4, section 4.2.1 and this was integrated with the photobioreactor for scale-up cultivation.

5.2.2 Microalgal inoculum preparation

Vischeria sp*.,* and *P. purpureum* were obtained from AlgaeCytes Ltd, UK. The seed culture for *Vischeria* sp. was cultivated in a 1 L round bottom flask using modified Bold's Basal medium (BBM) (Allen, 1968) and *P. purpureum* was cultivated in the same medium with tropic sea salt. The seed cultures were supplemented with 1 g L^{-1} $NaHCO_3$ inorganic carbon, cultivated at ambient temperature with continuous illumination 150 µmol/m^2/s (LED) and aerated at a flow rate of 1.8 L/min (LPM). The cultures were monitored for growth from the lag phase to their exponential phase before inoculating into the bubble column photobioreactor.

5.2.3 Photobioreactor (PBR) set-up and operation

The scale-up studies were carried out in glass bubble column photobioreactors (PBR) of 8-10 L capacity with 5 L working volume (length 100 cm, 110 mm OD, 104 mm ID) with an inlet/outlet port for sparging and sampling. The photobioreactors were kindly supplied by AlgaeCytes Ltd. A pH controller monitor (Up-aqua, UK) probe was placed in the photobioreactor to monitor pH drop through the bubble of carbon dioxide. The absorbing reagent (3 g L^{-1} NaOH) was added to the culture medium (BBM) of 5 L. The air pump placed inside the mushroom was connected with a check valve to prevent back-flow of the gas and medium to keep the reaction process of carbon dioxide with the sodium hydroxide to produce forms of sodium bicarbonate ($NaHCO_3$). The fully constructed photobioreactor was integrated with the mushroom growth box (as described in Chapter 4, section 4.1.2). These CO_2 absorption reactions can be expressed by the following equations:

$$2NaOH_{(aq)} + CO_2(q) \rightarrow Na_2CO_{3(aq)} + H_2O_{(l)} \quad (5.1)$$

$$Na_2CO_{3(aq)} + H_2O_{(l)} + CO_{2(q)} \rightarrow 2NaHCO_{3(aq)} \quad (5.2)$$

$$2NaOH_{(aq)} + CO_{2(q)} \rightarrow 2NaHCO_{3(aq)} \quad (5.3)$$

A sparger was placed at the bottom of the reactor for the effective distribution of carbon dioxide into the medium to increase resistance and improve the reaction efficiency of carbon dioxide and sodium hydroxide. The reaction time varied due to slow kinetic reactions. After the reaction, the bicarbonate-based medium (NaOH-BBM) was transferred into the bubble column photobioreactor for microalgal cultivation (Figure 5.1). The bubble columns were inoculated with *Vischeria* sp. and *P. purpureum* on the same day. The total inorganic carbon was estimated using titrimetric methods and the final pH of 7.5 was adjusted for microalgae cultivation. The bubble columns were illuminated with an intensity of 150 µmol/m^2/s (LED) with a BT-881D lux meter (BT-Meter store, UK). The photobioreactors were aerated with air from the laboratory with a flow rate of 5 L/min from the air pump. The set up was designed in a batch process with generated media but not in a continuous process of carbon dioxide injection from the mushroom growth box.

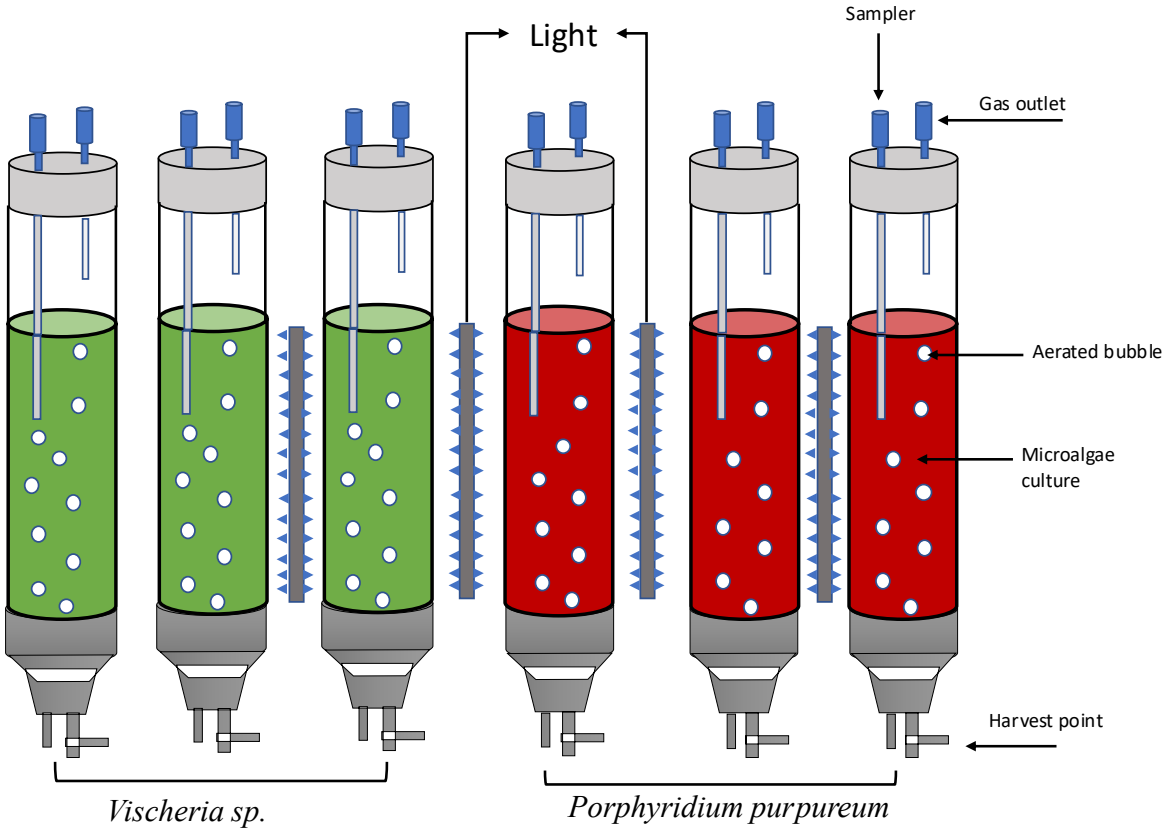

Figure 5.1 Schematic representation of microalgal cultivation system of *Vischeria* sp. and *Porphyridium purpureum* cultivated in inorganic carbon generated from mushroom production in a bubble column photobioreactor with triplicate experiments conducted for each strain.

5.2.4 Specific growth rates of microalgae

The specific growth rate (μ, d^{-1}) was estimated based on the optical density of the culture suspension at 750 nm (OD) using a microplate reader (Thermo-Scientific, UK) and was determined by:

$$\mu\ (d^{-1}) = \frac{\ln (OD_2 / OD_1)}{t_2 - t_1} \quad (5.4)$$

Where μ is the specific growth rate (d^{-1}), OD_2 on the final day t_2 and OD_1 is the OD on day t_1. An aliquot of 10 mL of the culture suspension was sampled from the photobioreactor was centrifuged at 3000 *g* for 5min (washed twice with distilled water) and filtered using a pre-weighed Whatman GF/C glass microfiber filter (pore size 0.22 μm) to measure the biomass productivity (g $L^{-1}d^{-1}$).

5.2.5 Phycobiliprotein extraction and analysis

Freeze-thaw method was used in the extraction of phycobiliprotein (PBP) from *P. purpureum* using a modified method by (Coward et al., 2016). Briefly, 6 mg of lyophilised was dissolved in 1.5 mL of 0.1 M L^{-1} phosphate buffer (pH 6.8) and frozen at −20°C for 24 hours and thawed at room temperature (2 hours) subject to vortex for 5 min. The samples were repeated three times and centrifugated at 3000 *g* for 5 min to remove cell debris. The absorbance of the supernatant at 455, 564, 592, 618 and 645 nm using Multiskan Go microplate spectrophotometer (1510-04220C Thermo Scientific, UK). The total phycobiliprotein content (PB, mg g^{-1}) was estimated by adding values of phycoerythrin (mg mL^{-1}) and phycocyanin (mg mL^{-1}) from the following equation by (Beer and Eshel, 1985).

$$PE = [(OD_{564\ nm} - OD_{592\ nm}) - (OD_{455\ nm} - OD_{592\ nm}) \times 0.2] \times 0.12 \quad (5.6)$$

$$PC = [(OD_{618\ nm} - OD_{645\ nm}) - (OD_{592\ nm} - OD_{645\ nm}) \times 0.51] \times 0.15 \quad (5.7)$$

$$\text{PB yield (mg g}^{-1}) = PE * V / DW_{(g)} \quad (5.8)$$

where PE is phycoerythrin concentration (mg mL^{-1}), volume (mL), and dried weight (g).

5.2.6 Estimation of inorganic carbon utilisation by microalgae

To measure the levels of inorganic carbon in the culture medium, a titrimetric-based alkalinity method was used with slight modification in the volume of supernatant. Samples were centrifuged, and the supernatants were titrated with 0.02 N standardised sulfuric acid (H_2SO_4) to obtain the total alkalinity. The inorganic carbon removal in culture media was calculated using the equation from Chapter 2, section 2.4.5.

5.2.7 Determination of biochemical composition by FTIR spectroscopy

The protein, lipid and carbohydrate composition of the freeze-dried biomass was analysed using Cary 630 Fourier Transform Infrared spectroscopy described in Chapter 2, section 2.4.8.

5.2.8 Pigment extraction and analysis

Extraction was carried out under ice-cold acetone. Approximately 4 - 5 mg of lyophilised biomass was extracted with 1 mL organic solvent (acetone: methanol, 7:3 v/v) containing an internal standard (α-tocopherol acetate, 100 mg L^{-1}) with glass beads (~100mg) were added and homogenized using a VelociRuptor V2 Microtube (Homo^{TM} SLS1401) at 6.00 m/s for 15 seconds (9x cycles). After, homogenisation, the extracts were filtered through a 0.2 µm PTFE syringe filter into 2 mL RP-HPLC vials and analysed using a Hewlett Packard instrument with a Nova-Pak C18 4um, 3.9x150mm column with a guard column. The mobile phase and elution gradient programme employed has been described in Chapter 2, section 2.4.6.

5.2.9 Fatty acid analysis using GC-FID

Fatty acid composition was determined for all treatments at the end of the cell culture using a 52 CB GC column Agilent 6890A (Agilent Technologies, Germany). The fatty acids were identified by comparing the obtained retention times with that of internal standards from AlgaeCytes Ltd with profile analysis described in Chapter 2, section 2.4.7.

5.3 Antioxidant activities

5.3.1 Total antioxidant assay (TAC)

Total antioxidant capacity was tested using modified (Bhatti *et al*., 2015b). Phosphomolybdate reagent was prepared from 0.6 M sulfuric acid, 28 mM sodium phosphate, and 4 mM ammonium molybdate. 1 mL of the reaction reagent was added to 0.5 mL aliquot of sample prepared from different concentrations (100 – 300 µg/mL). the sample mixture was incubated at 90^{o}C for 60 min. After incubation, the samples were allowed to cool at room temperature before measurement. The antioxidant capacity was estimated using a Multiskan Go microplate spectrophotometer (1510-04220C Thermo Scientific, UK) against a reagent blank measured at 695nm.

5.3.2 Determination of total phenolic content (TPC)

The total phenolic content in the microalgae extracts was evaluated by using the Folin-Ciocalteu method with slight modifications (Rahman *et al*., 2015). Folin-Ciocalteu reagent (diluted with distilled water in 1:9 v/v) and 75% sodium carbonate were prepared. To each 0.25 mL sample extract, 1 mL of Folin-Ciocalteu and kept in the dark for 5 mins. After that, 0.1 mL sodium carbonate was added to each extract and incubated for 30 mins. The absorbance of the reaction mixture was measured at 765 nm using a spectrophotometer. The total phenolic content was expressed in gallic acid equivalent to the sample dry weight.

5.3.3 ABTS scavenging assay

The ability of algal biomass to scavenge free radicals was determined by an ABTS assay with few modifications according to radical was generated by preparing 7 mM ABST stock solution and 2.45 mM potassium persulfate, 50 mL prepared in ratio was prepared from the stock and left in the dark for 24 hours. The absorbance of the ABTS was adjusted to 1.0 at 734 nm working OD. 1.75 mL of ABTS was reacted with 0.25 mL of sample extract and incubated in the dark for 10 min. The absorbance of the mixture was measured at 734 nm using Multiskan Go microplate spectrophotometer (1510-04220C Thermo Scientific, UK) and butylated hydroxyanisole (BHA) as standard reference expressed in equivalent in mg BHAE/g of dry weight.

$$\% \text{ Inhibition activity} = \frac{Ab_0 - Ab_1}{A_{b0}}\ x\ 100 \qquad (5.9)$$

Where Ab_0 is the absorbance of the control and Ab_0 is the absorbance of the sample extract.

5.3.4 Sunscreen Protective Factor

Estimation of sun protection factor (SPF) on the phenolic extracts from microalgae and mushroom exudate was calculated using the universal formula by Mansur *et al*. (1986) for describing the efficiency of sunscreen products against sunburn caused by UVB and short wavelength UVA (320–340 nm). In-vitro extracts were assaying from the following equation to evaluate the SPF value:

$$\text{SPF} = \text{CF}_x \sum_{290\text{ nm}}^{320\text{ nm}} \text{EE}(\lambda)\ \text{x}\ \text{I}(\lambda)\ \text{x}\ \text{ABS}(\lambda) \qquad (5.11)$$

CF, a correction factor (10); EE, erythemal effect wavelength; I, solar intensity spectrum; Abs, absorbance of the sample at 290–320 nm. The values for each [EE(λ) × I(λ)] are constants normalised and reported by (Sayre *et al*. (1979).

5.4 Results and Discussion

5.4.1 Effect of inorganic carbon on microalgae growth

Microalgal growth was measured to study the growth pattern of both species in asynthetic media (control) compared with mushroom-bicarbonate culture generated through carbon capture (NaOH-BBM) from mushroom production. From Figure 5.2a, *Vischeria sp.,* growth in the bicarbonate culture was slow for the first 10 days compared to control. The specific growth rate in the control was 0.367 d^{-1} which was 2.3 folds higher than the bicarbonate medium with a growth rate of 0.203 d^{-1}. The final biomass production in the control culture was 6.612 g L^{-1} which was 1.8 folds higher compared to 3.655 g L^{-1} in the mushroom-bicarbonate culture. Comparatively, the bicarbonate culture was not able to yield enough biomass than achieved in the control due to their intolerance to high salt stress which led lower biomass production. The addition NaOH further increase sodium ions (Na^{+}) concentration in the culture causing stress or becoming harmful which might have affected the enzymatic activities of the RuBisCO (ribulose biphosphate carboxylase) which plays a significant role during photosynthesis by inhibiting growth with similar report on *Nannochloropsis* sp. by (Yustinadiar *et al*., 2020). The study on the integration of bicarbonate-based carbon capture for *Neochloris oleoabundans* was observed to be slow when cultivated in 0.3 mol L^{-1} bicarbonate for the first few days (Zhu *et al*., 2018). Cultivation of *Scenedesmus* sp. in the presence of different alkanolamine carbon dioxide absorbents reported similar trends in growth under monoethanolamine, diethanolamine, and triethanolamine (Chi *et al*., 2013). However, in *P. purpureum,* comparing the growth in both media, the specific growth rate in the mushroom-bicarbonate culture 0.182 d^{-1} 1.9 folds higher compared to the control with 0.092 d^{-1}. The final biomass production from mushroom-bicarbonate culture gave significant increase compared to the control (3.292 g L^{-1} and 1.672 g L^{-1} respectively). Figure 5.2b shows that microalgal growth in the mushroom-bicarbonate culture was better than growth in the control. This shows that *P. purpureum* show its tolerance level for sodium ions in the mushroom-bicarbonate compared to the control with less sodium ions. The tolerance of *Chlorella vulgaris* under 160 mM $NaHCO_3$ and NaCl was reported by (Li *et al*., 2018c; Luangpipat and Chisti, 2017). Similar results were presented in

C. vulgaris cultivated in a high bicarbonate dose of 3 g L^{-1} owing to high biomass and growth (Yeh *et al*., 2010).

These results indicate that *P. purpureum* can tolerate extremely high salinity, unlike *Vischeria* sp. Comparing the impact of bicarbonate in both species with the synthetic media, growth, and biomass production were improved in the mushroom-bicarbonate media for *P. purpureum* compared to *Vischeria* sp. under the same cultivating conditions with a greater growth and biomass response in the control. Results obtained in the control of *Vischeria* sp. were doubled relative to the bicarbonate results and vice versa, in *P. purpureum*, results were in favour of the mushroom-bicarbonate culture compared to the control. The benefit from the synthetic media for *Vischeria* sp. is that it contains fewer sodium ions which in terms benefited growth and inorganic carbon utilisation compared to the mushroom-bicarbonate culture with high sodium ions.

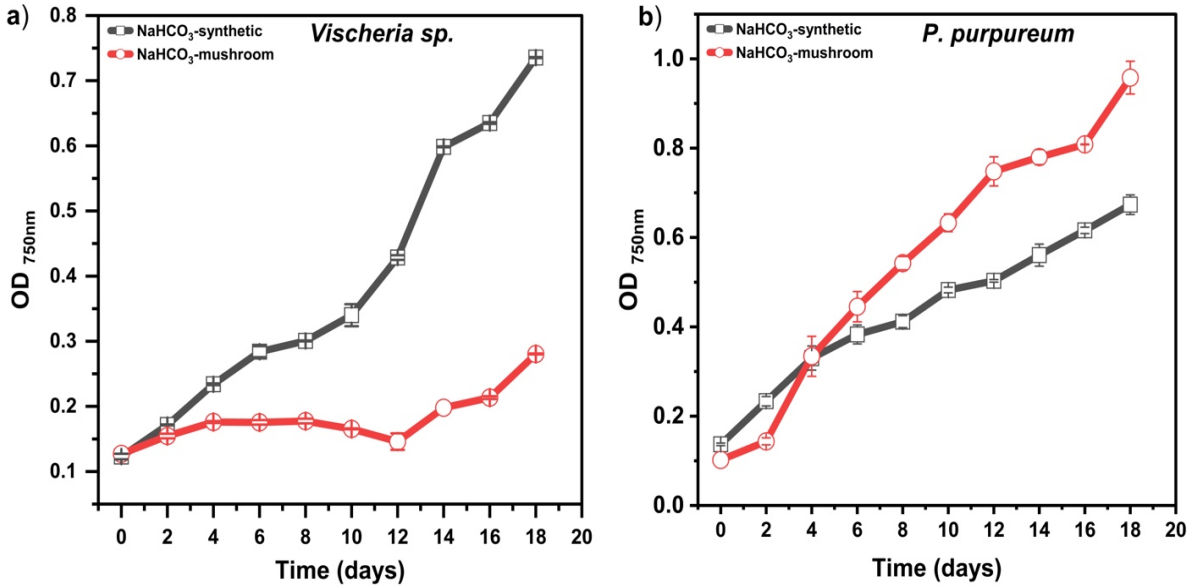

Figure 5.2 Microalgal growth trend for (a) *Vischeria* sp. and (b) *Porphyridium purpureum* cultivated in synthetic media (black square) and mushroom-bicarbonate media (red circle) for a period 18 days. Data values expressed as mean ± standard deviation, n=3.

5.4.2 Inorganic carbon utilisation by microalgae

Inorganic carbon utilisation was significantly affected by the type of growth media (synthetic media and mushroom-bicarbonate) in both *Vischeria* sp. and *P. purpureum*, although contrasting effects were observed in both species. From table 5.1, the inorganic carbon utilisation rate for *Vischeria* sp. was significantly higher in the synthetic media ($p \leq 0.001$) compared to the mushroom-bicarbonate, with an overall inorganic carbon utilisation rate of 134.44 mg $L^{-1}d^{-1}$ and 43.33 mg $L^{-1}d^{-1}$ respectively. A higher removal rate was achieved in the

synthetic media while a lower removal rate was observed in the mushroom-bicarbonate due to slow growth because of high sodium concentrations causing osmotic stress on the microalgal cells in *Vischeria* sp. (Figure 5.2a). however, total inorganic carbon removal was 94.90% in the synthetic media 3 folds higher than the bicarbonate from the mushroom media at 30.59%. Inorganic carbon removal was observed to be low due to slow growth in *Vischeria* sp. from table 5.1, within the first 12 days before the cells were able to adapt to the mushroom-bicarbonate culture media. This can be a high concentrations of sodium (Na^+) ions in the media from sodium hydroxide coupled with the culture media. However, in *P. purpureum,* the inorganic carbon utilisation rate in the mushroom-bicarbonate culture (53.61 mg $L^{-1}d^{-1}$) was significantly higher than the synthetic media culture with 25.55 mg $L^{-1}d^{-1}$ utilisation rate ($p \leq 0.001$). After cultivation, the total inorganic carbon removal was estimated at 85.40% in the bicarbonate culture from the mushroom carbon 2.1 folds more than the synthetic media with a 40.71% estimate. This indicates that the marine strain *P. purpureum* had a high tolerant adaptivity in a bicarbonate media with high sodium concentrations compared to the *Vischeria* sp. although carbon utilisation was lower in the synthetic media due to low sodium ions present in the media. Inorganic carbon utilisation was also improved by culture pH. The maximum inorganic carbon removal by *Vischeria* sp. in the synthetic media was 94.90% and *P. purpureum* 85.40% in the mushroom-bicarbonate explains the tolerance of different algae species in different conditions before bicarbonate-based cultivation system microalgae growth. The integration of bicarbonate-based integrated carbon capture and algae production system on an alkalihalophilic strain (*N. oleoabundans*) reported slow growth when cultivated in high bicarbonate 0.7 mol L^{-1} (Zhu *et al*., 2018). Microalgal strains with high tolerance for sodium and bicarbonate concentration which are more favourable for bicarbonate-based system should be studied for inorganic carbon utilisation efficiency. Screening of microalgae strains for bicarbonate-based cultivation system was studied on strains under different concentrations of 0.3 M for *Synechocystis* sp., 0.6 M for *Dunaliella salina,* 0.1 M *Chlorella sorokiniana* which exhibited high tolerance for bicarbonate study (Chi *et al*., 2014).

Table 5.1. Microalgal inorganic carbon removal efficiency, removal rate, and biomass production by *Vischeria* sp. and *P. purpureum* cultivated in synthetic media and mushroom-bicarbonate media for a period of 18 days. Data values expressed as mean ± standard deviation, n=3.

Strain	***Vischeria* sp.**		***P. purpureum***	
	Synthetic media	Mushroom-bicarbonate	Synthetic media	Mushroom-bicarbonate
Total IC removal (%)	94.90 ± 0.34	30.59 ± 0.14	40.71 ± 0.12	85.40 ± 0.62
IC removal rate (mg $L^{-1}d^{-1}$)	134.44 ± 0.58	43.33 ± 0.11	25.55 ± 0.13	53.61 ± 0.39
Biomass production (g L^{-1})	6.61 ± 0.04	3.66 ± 0.02	1.67 ± 0.01	3.29 ± 0.01

In the presence of four different concentrations of $NaHCO_3$, *Vischeria* sp. and *P. purpureum* exhibited distinct growth patterns (as discussed in Chapter 3). The daily adjustment of pH levels to 5, 7, and 9 during cultivation in both synthetic media and mushroom-generated bicarbonate media significantly promoted microalgal proliferation and biomass production. A similar trend was observed in a recent study where *C. vulgaris* microalgae were grown at varying initial pH levels (7.5, 8.5, and 9.5) using a modified Bristol medium enriched with 1.9 g L^{-1} of $NaHCO_3$ (Li *et al*., 2018a). The maximum dry cell weight of 1.972 g L^{-1}, indicating the highest microalgal biomass, was achieved after eight days of cultivation at pH 7. However, synthetic media cultivation greatly enhanced overall microalgal growth, resulting in a 2 folds increase in biomass production to 6.612 g L^{-1} in *Vischeria* sp., compared to mushroom-bicarbonate 3.655 g L^{-1} at the scale-up stage. The pH increases to 7 was generally linked to the utilisation of HCO_3^- by *P. purpureum* during the scale-up cultivation, which resulted in a twofold increase in biomass under mushroom-bicarbonate. This led to the release of OH^- anions into the culture media, raising the overall pH of the solution and inhibiting microalgae proliferation and biomass generation during the scale-up of *Vischeria* sp. under mushroom-bicarbonate. The most recent findings showed that *Vischeria* sp. and *P. purpureum* microalgae cells were efficient in utilising the inorganic carbon source during photoautotrophic cultivation. However, the growth parameters and inorganic carbon removal were significantly higher than those observed in the cultivation experiments conducted in the Erlenmeyer flask under different pH regulation conditions (Table 4.1). These results can also be attributed to the different mixing rates used between Chapters 3, 4, and 5, as Erlenmeyer flasks were agitated by an orbital shaker, while bubble column photobioreactors were mixed through aeration from air pumps.

5.4.3 Effect of inorganic carbon on biochemical composition

Based on the development of bicarbonate-based applications for microalgae cultivation processes. The harvested biomass from the scale-up experiment was quantified for its accumulated content of lipids, protein, carbohydrates, and pigments. For *Vischeria* sp. from Figure 5.3a, there was a significant difference between the biochemical composition of lipids and protein in the synthetic media compared to the mushroom-bicarbonate media. The highest amount of carbohydrates accumulated was slightly similar in the synthetic media and the mushroom-bicarbonate media was 47.6% and 48.85% respectively of the total dry weight which was statistically insignificant ($p \leq 0.28$). In addition, the protein content of 31.50% was 1.7 folds higher in the synthetic media compared to the mushroom-bicarbonate media with a total of 18.25% ($p \leq 0.003$). Similar differences of 1.6 folds were observed in the lipid content of the synthetic media which was found to be significantly higher than the bicarbonate media from the mushroom production ($p \leq 0.001$). Interestingly, the inorganic carbon source from the mushroom-bicarbonate media did not have a significant impact on the biochemical composition due to salt stress which could not trigger the carbon dioxide concentration mechanism (CCM) for *Vischeria* sp. compared to the synthetic media. However, lower biomass production and biochemical composition in the carbon-captured media were found to be lower in our study, maybe due to inefficient inorganic carbon utilisation and adaptability of the algal strain to high sodium concentrations or salt stress (Beigbeder and Lavoie, 2022). In a similar study on *C. vulgaris* high bicarbonate and NaCl of 160 mM was reported to have a significant effect on biomass accumulation by stimulating lipid content (Li *et al*., 2018c). However, in *P. purpureum*, the lipid content of 17.15 % was about 5 folds higher in the mushroom-bicarbonate media than in the synthetic media with 3.05% ($p \leq 0.01$). There was a significant difference ($p \leq 0.05$) in the protein (6.75 % and 13.7%) but not the carbohydrate content (47.7% and 51.65%) in the synthetic media and mushroom-bicarbonate media respectively. The overall biochemical accumulation in the mushroom-bicarbonate media was higher compared to the synthetic media.

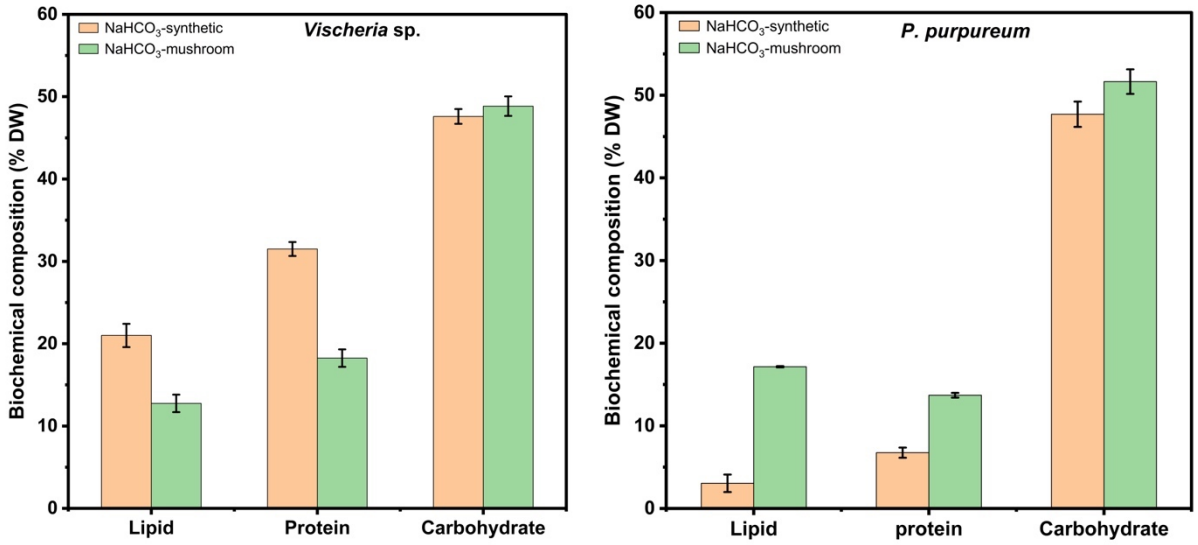

Figure 5.3 The impact of inorganic carbon source from synthetic media and mushroom-bicarbonate media on biochemical composition quantified in the harvested biomass of *Vischeria* sp. and *Porphyridium purpureum* cultivated for a period 18 days. Data values expressed as mean ± standard deviation, n=3 and statistical analysis by one-way ANOVA with post-hoc test.

Photosynthetic pigments were quantified in both microalgal strains for chlorophyll-*a* and ß-carotene. The chlorophyll-*a* and ß-carotene content in the synthetic media was 33.16 mg g^{-1} and 4.01 mg g^{-1} respectively in *Vischeria* sp. while in the mushroom-bicarbonate media, the chlorophyll-*a* content was 29.84 mg g^{-1} and 2.83 mg g^{-1} ß-carotene (Figure 5.4). From the results, the chlorophyll-*a* and ß-carotene contents in the synthetic media was higher than the bicarbonate media from the mushroom. There was no statistical difference in the photosynthetic pigments from *Vischeria* sp. cultivated in both culture media. However, there was a significant difference in the chlorophyll-*a* and ß-carotene content in *P. purpureum* cultivated in the synthetic media and bicarbonate media ($p \leq 0.05$). The maximum chlorophyll-*a* content was 11.78 mg g^{-1} and ß-carotene of 2.16 mg g^{-1} in the synthetic media compared to the chlorophyll-*a* 7.20 mg g^{-1} and ß-carotene content of 1.38 mg g^{-1} in the bicarbonate media from the mushroom production. One of the effects contributing to low total chlorophyll content can be oxidative stress which results in chlorophyll-*a* degradation but rather promotes chlorophyllase activities (Ji *et al*., 2018b). In *C. reinhardtii* cultivation under salt stress, the osmotic and ionic stress altered the photosynthetic rate which lowered the chlorophyll-*a* content (Fal *et al*., 2022).

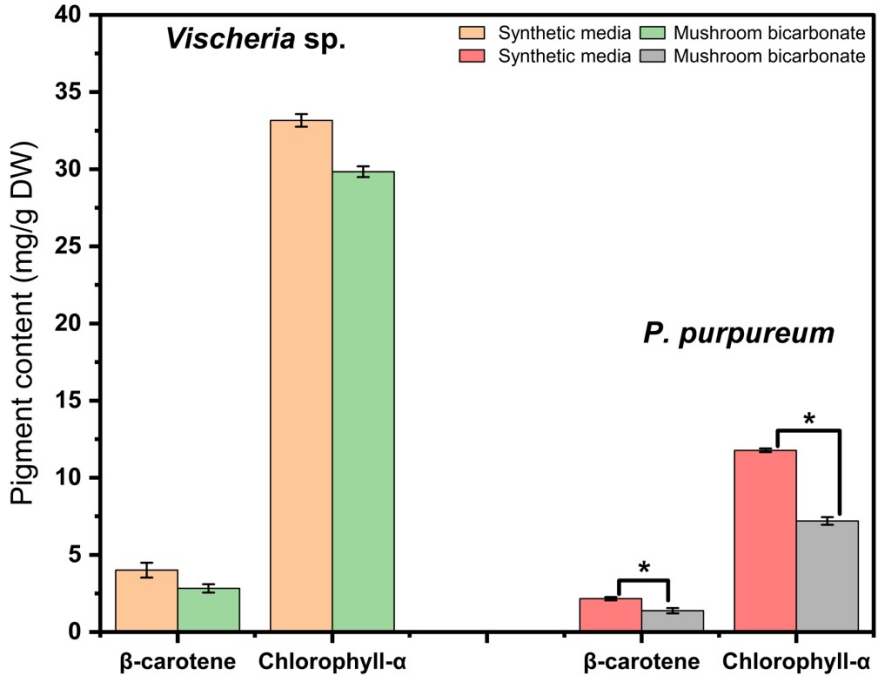

Figure 5.4 The effect of synthetic media and mushroom-bicarbonate media on chlorophyll-*a* (orange and green) and ß-carotene (orange and green) in *Vischeria* sp. and chlorophyll-*a* (red and grey) and ß-carotene (red and grey) in *Porphyridium purpureum* cultivated for a period 18 days. Data values expressed as mean ± standard deviation, n=3 and statistical analysis by one-way ANOVA with post-hoc test.

5.4.4 Estimation of phycobiliprotein from *P. purpureum* in bicarbonate media

Phycobiliproteins are a crucial component of cyanobacteria and their changes under various culture conditions provide valuable insights into the chromatic adaptation abilities of these organisms in extreme conditions. However, the quantification of phycobiliproteins was conducted by comparing their levels in synthetic and mushroom-bicarbonate media in Figure 5.5. The results revealed that the phycobiliprotein from the mushroom-bicarbonate culture were higher in content compared to the synthetic media, with an average of 0.429 mg g^{-1} compared to 0.325 mg g^{-1} respectively. As shown in Figure 5.5, the variation of phycobiliproteins in the cultivation medium where salt stress is maximum, the mushroom-bicarbonate culture has a higher concentration of phycobiliproteins than the synthetic media medium due to the contribution of sodium hydroxide for carbon capture. This is supported by the finding of (Y. Li *et al*., 2020) that reported a higher phycobiliprotein content in *S. platensis* when cultivated in a high sodium chloride concentration. However, the same study also reported a reduction in chlorophyll content under the same conditions, which is consistent with the observation that high sodium concentrations in the mushroom-bicarbonate culture reduced the chlorophyll

content in *Nannochloropsis oculata, Vischeria punctata*, and *Eustigmatos vischeri* as reported by (Y. Li *et al*., 2020).

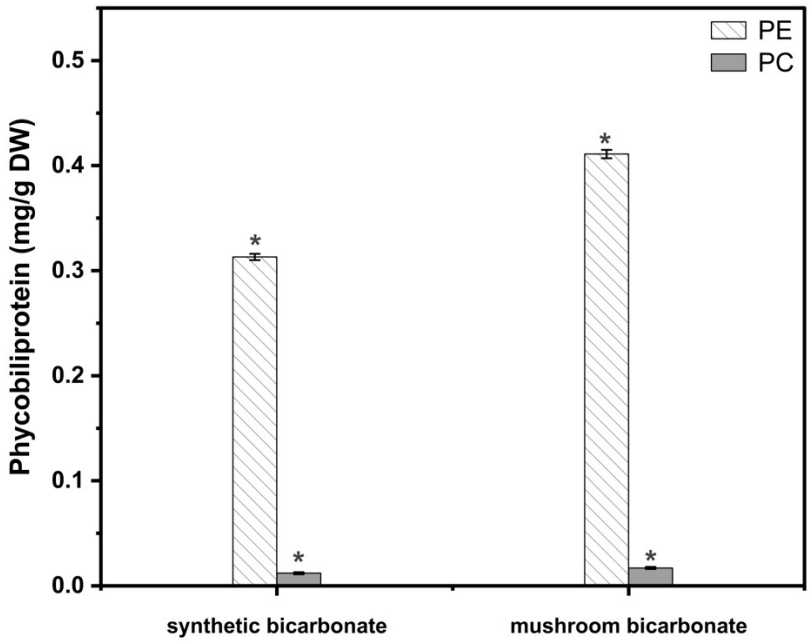

Figure 5.5 Changes of Phycobiliprotein content (PB, mg g^{-1} DW) and composition (phycoerythrin, PE and phycocyanin, PC) in *Porphyridium purpureum* cultivated in synthetic media and mushroom-bicarbonate media under 18 days of cultivation period. Data values expressed as mean ± standard deviation, n=3 and statistical analysis by one-way ANOVA with post-hoc test.

5.4.5 Effect of bicarbonate-media type on fatty acid composition

In Eustigmatophyceae, the primary fatty acids present are myristic acid (C14:0), myristoleic acid (C14:1), palmitic acid (C16:0), palmitoleic acid (C16:1), steric acid (C18:0), oleic acid (C18:1), linoleic acid (C18:2), arachidonic acid (C20:4), and eicosapentaenoic acid (EPA20:5) (Wang *et al*., 2018). However, in *Vischeria* sp. the major fatty acids were found to be palmitic acid (C16:0), palmitoleic acid (C16:1), arachidonic acid (ARA20:4), eicosapentaenoic acid (EPA20:5), and other fatty acids when cultivated in synthetic and mushroom-bicarbonate media (Figure 5.6). The synthetic media contained 24.5% and 37.8% of palmitic acid and palmitoleic acid respectively, while arachidonic acid and eicosapentaenoic acid accounted for 7.8% and 11.3% of the total fatty acids in *Vischeria* sp. In the mushroom-bicarbonate media, palmitic acid was 19.1% and palmitoleic acid 43.6%, while arachidonic acid and eicosapentaenoic acid were present at 5.9% and 16.1% respectively. The difference in total fatty acid composition between the synthetic and mushroom-bicarbonate media were similar except for the EPA content. It is worth noting that different Eustigmatophyceae species have varying fatty acid compositions, with *Nannochloropsis salina* showing a higher EPA

content (27% of the total fatty acid) compared to *E. vischeri* (5.3 – 20.6%) (Xu *et al*., 2020). The mushroom-bicarbonate culture demonstrated the highest estimated percentage of EPA (16.1% of TFA), leading to a substantial reduction in EPA content (11.3%) in the synthetic media. Similar results were observed in *V. stellate*, where elevated salt conditions resulted in an increase in the percentage of EPA (C20:5) and C20:4, with a decrease in the percentage of C18:1 compared to limited conditions (Xu *et al*., 2020). In *Vischeria punctata* cultivated in salt stress, higher palmitoleic acid (46.9%) and lower EPA (2.3%) content was reported, while the high salt stress from mushroom-bicarbonate led to changes in the fatty acid composition, with palmitic acid (C16:0) and stearic acid (C18:0) decreasing, and oleic acid (C18:1) increasing (Sinetova *et al*., 2021). A similar distribution of these fatty acids was also reported in freshwater *Monodus subterraneus* (Khozingoldberg & Cohen, 2006). One study found that the total fatty acids of *Vischeria* sp. strain E71.10 contained high levels of eicosapentaenoic acid (EPA) when grown in the presence of 68 mM NaCl (Remias *et al*., 2020), while a different yield was observed in eustigmatophytes, which demonstrated a decrease in EPA proportion in total fatty acids as sodium chloride (NaCl) concentration increased (Pal *et al*., 2013; Solovchenko *et al*., 2014). There was no significant difference in the EPA and arachidonic acid (ARA) content per dry weight in both synthetic and mushroom-bicarbonate cultures.

In *P. purpureum*, the major fatty acids were C16:0, C18:2, ARA20:4, and EPA20:5. Comparing the fatty acid compositions between synthetic media and mushroom-bicarbonate media, the maximum C16:0 and C18:2 in the synthetic media were 38.9% and 6.6%, respectively. These values were significantly different from those in the mushroom-bicarbonate media, which had C16:0 at 39.5% and C18:2 at 7.9% ($p \leq 0.001$). The EPA and ARA content in the synthetic media increased significantly compared to the mushroom-bicarbonate media ($p \leq 0.001$). The maximum EPA and ARA content in the mushroom-bicarbonate media were 11.05 mg g^{-1} and 13.75 mg g^{-1}, respectively, which were higher than the values in the synthetic media culture (9.6 mg g^{-1} and 11.95 mg g^{-1}, respectively). However, a study on *P. cruentum* using different carbonate sources showed that EPA and ARA content of approximately 9.9% and 26.2%, respectively, could be achieved under different carbon sources (Asgharpour *et al*., 2015). Additionally, (Su *et al*., 2016) reported that the accumulation of total fatty acids in *P. purpureum* increased under high carbon levels of 30-50%.

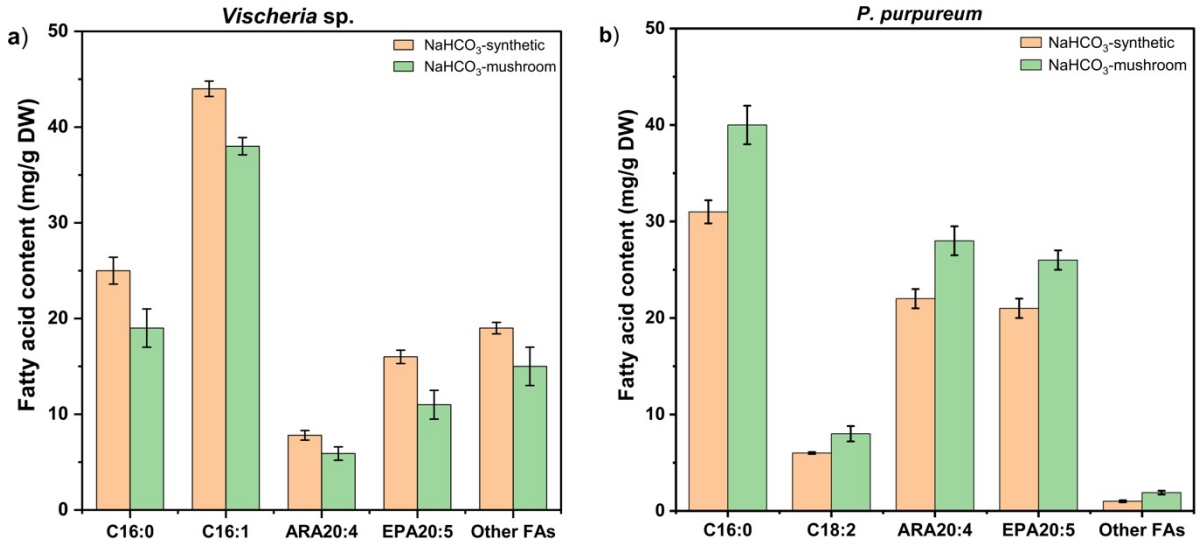

Figure 5.6 Effect of synthetic media and mushroom-bicarbonate media on the fatty acid compositions of (a) *Vischeria* sp. and (b) *Porphyridium purpureum* under each condition for a cultivation period of 18 days. Data values expressed as mean ± standard deviation, n=3.

5.4.6 Total antioxidant capacity

The antioxidant capacity evaluated in the dry weight of *Vischeria* sp. and *P. purpureum,* and mushroom exudate was 255.36 ± 3.34, 89.18 ± 2.33, and 108.05 ± 2.21 mg AAE/g respectively. The values obtained for *Vischeria* sp. cultivated in the synthetic media culture was 2 folds high compared to the mushroom-bicarbonate media of the same strain. The difference of 89.18 ± 2.33 and 76.77 ± 2.01 mg AAE/g of *P. purpureum* from the synthetic media and mushroom-bicarbonate respectively did not indicate any significant relation for their antioxidant capacity. The mushroom exudate indicated the potential of antioxidant capacity of potential application from their used substrate. The studied Rhodophyte (*P. purpureum*) showed low values of antioxidant capacity compared to eustigmatophyte, which corresponds with similar results from *Vischeria Helvetica* ACOI 299 (258.20 ± 0.65 TE/g) and *Porphyridium aerugineum* achieving 67.95 ± 0.36 mg TE/g (Assunção *et al*., 2017). Although, several studies reveals that the antioxidant properties are due to a high phenolic content from ketones, vitamin C, flavonoids, ellagic acid, anthocyanins and *Porphyridium* sp. are known for their low antioxidant capacity (Gülçin *et al*., 2011; Sariburun *et al*., 2010). The presence of bioactive compounds such as polyphenols, carotenoids, vitamin E, and vitamin C in the microalgae cells plays a crucial role in determining the antioxidant activity of a species.

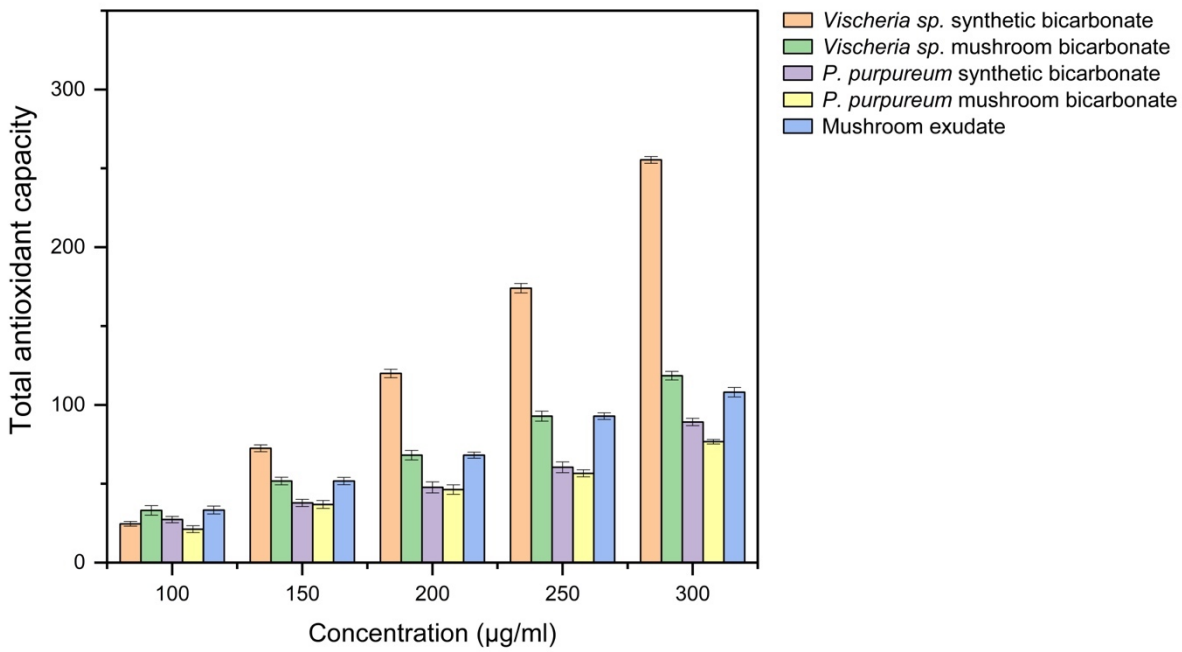

Figure 5.7 Represents values for relative antioxidant capacity estimated in the polyphenol extract from *Vischeria* sp. and *Porphyridium purpureum* cultivated in both synthetic and mushroom-bicarbonate media and mushroom exudate (used substrate). Data values expressed as mean ± standard deviation, n=3.

5.4.7 Total phenolic content

Phenolic compounds, such as catechin and gallic acid, act as antioxidants due to their capability for single electron transfer and hydrogen atom transfer reactions (Goiris *et al*., 2012). Under physiological conditions marine algae are exposed to environmental stressors, for example UV-light, which results in an accumulation of reactive oxygen species as by-products of the electron transport system in photosynthesis and enzymatic processes (Freile-Pelegrín and Robledo, 2013). A study by (Jerez-Martel *et al*., 2017), demonstrated that biomasses of various microalgae and cyanobacteria contain simple phenolic compounds like gallic acid, chlorogenic acid, and syringic acid, as well as flavonoids. The total phenolic content in the dry weight of *Vischeria* sp. and *P. purpureum* was evaluated using the Folin-Ciocalteu method. The highest phenolic content was found in *Vischeria* sp. cultivated in synthetic media (219.59 ± 1.12mg GAE/g) followed by *P. purpureum* 195.22 ± 0.92 mg GAE/g cultivated in synthetic media and the maximum phenolic content was 144.35 ± 0.21 mg GAE/g for the mushroom exudate. The total phenolic content in the *Vischeria* sp. under mushroom-bicarbonate was lower than that of the synthetic media. There was no significant difference between the phenolic content of synthetic media and mushroom-bicarbonate *P. purpureum*. It

is worth nothing that the polyphenolic composition and content can substantially vary as a function of microalgae growth conditions (stress, temperature, pH, and nutrients supplement) as well as the extraction solvents. However, (Bulut *et al*., 2019) reported a total phenolic content of *Scenedesmus* sp. was 5.40 ± 0.28 mg GAE/g with ethanol/water (3:1 v/v) and methanolic extraction of *Chlorella minutissima* was 9.04 ± 0.68 mg GAE/g dry weight. (Ferda Yylmaz *et al*., 2017) reported a higher amount of the total phenolic content of 62.45 ± 2.0 mg GAE/g.

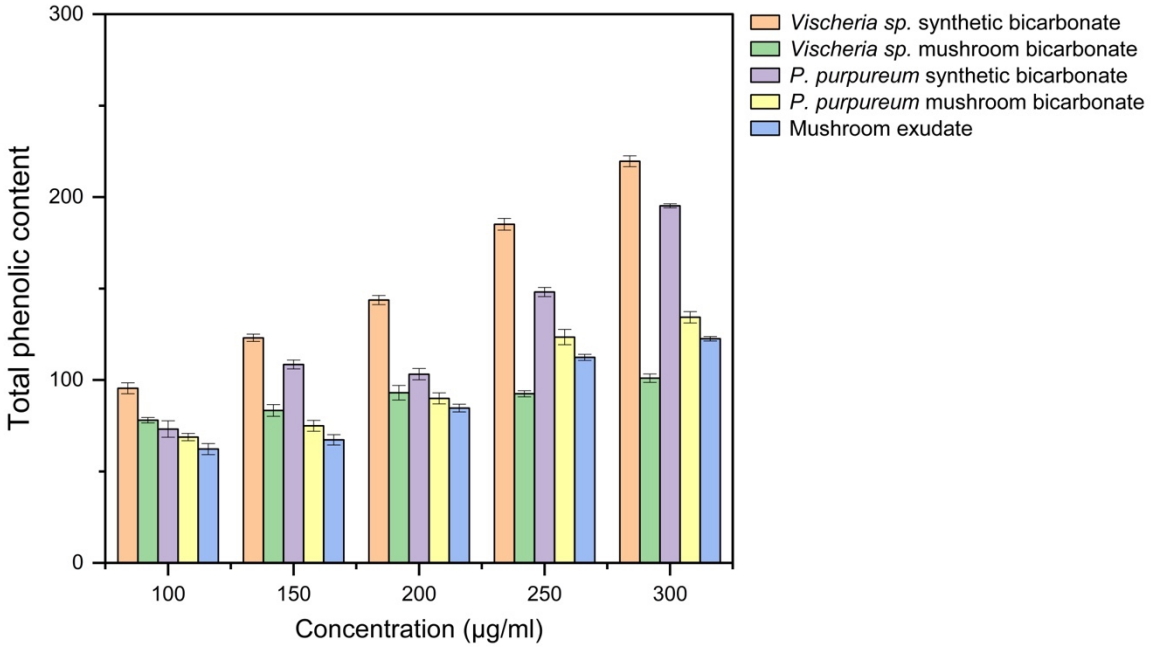

Figure 5.8 Represents values for relative total phenolic content estimated in the polyphenol extract from *Vischeria* sp. and *Porphyridium purpureum* cultivated in both synthetic and mushroom-bicarbonate media and the phenolic mushroom exudate (used substrate). Data values expressed as mean ± standard deviation, n=3.

The types of phenolics found in algae varies depending on the type of algae. The largest proportion of phenolic compounds in green and red algae is represented by bromophenols, phenolic acids, and flavonoids. Phlorotannins are found mainly in brown algae and, in lesser amounts, in red algae; even fewer polyphenols are contained in green algae. Several classes of flavonoids, such as flavonols, flavanones, isoflavones, and dihydrochalcones, were found in microalgae and cyanobacteria (Cichoński and Chrzanowski, 2022b). Regarding the phenolics assay, the Folin-Ciocalteu method is commonly used to measure total phenolic content. However, this method has limitations, one of them is the interference of non-phenolic compounds like tyrosine, which can lead to overestimation of phenolic content (Davies *et al*.,

2020; Pérez *et al*., 2023). An adjustment of PVPP (Polyvinylpolypyrrolidone) can be used to separate phenolics and non-phenolic reducing compounds from their original food matrix (Davies *et al*., 2020). This adjustment can help to provide a more accurate estimate of phenolic content. Furthermore, when measuring phenolic content, it's crucial to consider potential interferences by making necessary adjustments to ensure accurate results.

5.4.8 ABTS radical scavenging activities

There is no single antioxidant assay that can define the total antioxidant capacity of all compounds in the extracts because different compounds have different sensitivity to different assays such as hydroxyl radical, ferrous reducing capacity, and lipid peroxidation (Gündüz *et al*., 2023). The highest ABTS scavenging activity expressed in percentage of inhibition capacity estimated in *Vischeria* sp. extract was 58.66 ± 0.45 % in the synthetic media higher than the mushroom-bicarbonate with an inhibition capacity of 36.96 ± 0.34 %. In *P. purpureum* the inhibition capacity was 33.11 ± 0.63 % lower than mushroom-bicarbonate of 38.89 ± 0.34 %. According to (Foo *et al*., 2015), the stereoselectivity of the solubility concentrations of the extracts affects the capacity of the extracts to scavenge or react with the free radicals. A study on *Porphyra columbina* findings showed the variability in antioxidant activity depends on the algae species and solvent extract (Cian *et al*., 2014). The scavenging activity evaluated on *C. vulgaris* gave a higher capacity of 81.29 ± 0.09 % when cultivated in BBM (Mtaki *et al*., 2020). These results differ from the findings on *Nannochloropsis oculata* of 70.3 ± 0.6 % scavenging capacity by (Custódio *et al*., 2012). This method has been used extensively to predict antioxidant activities because of their relative short time analysis. Our results showed that the methanolic extract of *Vischeria* sp. demonstrated a scavenging activity when compared with standard BHA (Figure 5.9). These results indicated that both extracts have a noticeable effect on scavenging free radicals by donating proton scavenging free radicals making them potential antioxidants. The polyphenol content in the extracts from *Vischeria* sp. and *P. purpureum* was found to be responsible for the scavenging of ABTS radicals by their ability to donate electrons or hydrogen (Huang *et al*., 2005). However, this *in vitro* assay indicates that these microalgal strains are a significant source of natural antioxidants which requires further investigations on other antioxidant assays and compounds present in their biomass.

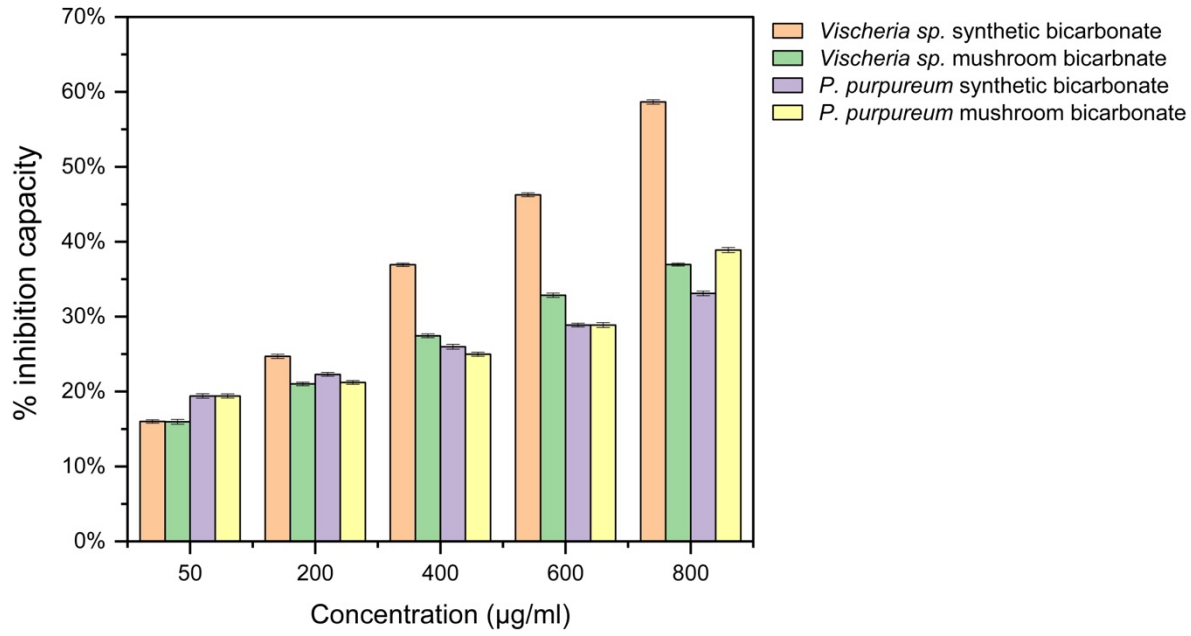

Figure 5.9 ABTS radical scavenging activity of *Vischeria* sp. and *Porphyridium purpureum* cultivated in both synthetic and mushroom-bicarbonate media. Data values expressed as mean ± standard deviation, n=3.

5.4.9 Sunscreen protective factor (SPF)

The SPF, or sun protection factor, evaluates the degree of sunburn protection provided by a product. To be considered effective, a sunscreen should have an absorption range of between 290 and 400 nm. During the development process of a product, the *in-vitro* SPF measurement is helpful, serving as a complement to the in vivo SPF determination. In this research, the effectiveness of polyphenol extracts from microalgae was examined using UV spectrophotometry and Mansur's mathematical equation. The SPF values of polyphenols extracted from *Vischeria* sp. and *P. purpureum,* and mushroom exudate (used substrate) were tested for their protective factors in Figure 5.10. below. The photoprotective characteristics of these bioactive compounds were evaluated for potential applications in the cosmetic industry. The highest SPF value ranged from 9.67 – 38.15 respectively with 0.4 mg mL^{-1} – 2 mg mL^{-1} concentrations of *Vischeria* sp. followed by *P. purpureum* with 11.92 – 35.45 respectively at a concentration from 0.4 mg mL^{-1} to 2 mg mL^{-1}, and the mushroom exudate at a concentration from 0.4 mg mL^{-1} to 2 mg mL^{-1} gave 7.78 – 34.04 respectively. A study by (aslani *et al*., 2021) on the evaluation of UV protection factor (SPF) on *Spirulina platensis* showed a higher SPF value of 11.94 comparably lower from our study. From Figure 5.10, polyphenols from microalgae and mushroom exudate at the highest concentration exhibited the best SPF values

which will be helpful in the selection of bioactive compounds from microalgae and mushroom substrates during the formulation of sunscreens. Although to develop and produce quality and safe sunscreen products with high SPF values, the formulator must understand the physicochemical principles and not solely rely on the UV absorbance of the bioactive extracts from these organisms and waste products. The polyphenols from microalgae and mushroom exudate showed their tolerance and resistant to UV-B (290-320 nm) with similar reports on *Scenedesmus* sp. by (Kováčik *et al*., 2010), and the effects UV stress on the fatty acids and lipids of *Odontella aurita* and *Diacronema lutheri* by (Guihéneuf *et al*., 2010).

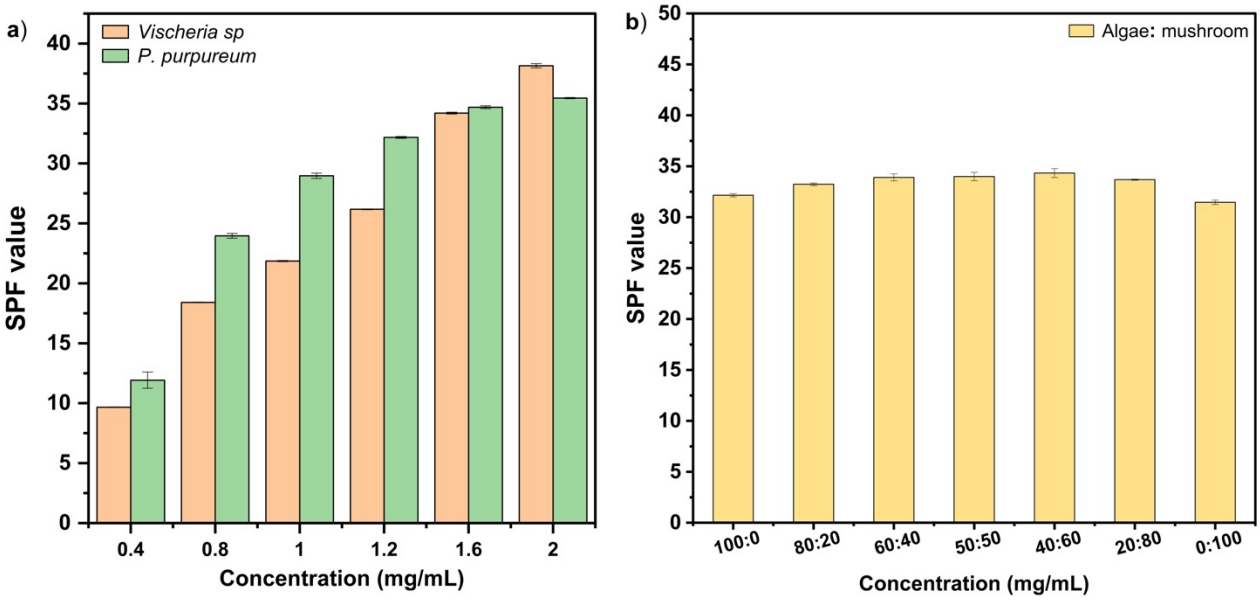

Figure 5.10 Determination of (a) sunscreen protective factor (SPF) values for polyphenols from *Vischeria* sp. and *Porphyridium purpureum* extracts using methanol and (b) sunscreen protection factor (SPF) value for mixture of algae and mushroom exudate polyphenols. Data values expressed as mean ± standard deviation, n=3.

5.5 Conclusion

Based on the findings of this study, it can be concluded that *Vischeria* sp. and *P. purpureum* exhibited distinct growth responses to bicarbonate-based and synthetic media. *Vischeria* sp. displayed slower growth and reduced biomass production in the bicarbonate medium, likely due to its sensitivity to high sodium concentrations resulting from the use of NaOH for carbon capture. *P. purpureum* showed improved growth and biomass production in the bicarbonate medium, indicating its high tolerance for bicarbonate salt. The differential responses can be attributed to the levels of sodium ions, with lower levels favouring growth and inorganic carbon utilisation in *Vischeria* sp. and higher concentrations promoting growth in *P. purpureum*. The study also highlights the importance of considering species-specific

responses when implementing bicarbonate-based cultivation systems and the potential of *P. purpureum* for high salinity environments. Additionally, the study suggests that culture pH can play a role in improving inorganic carbon utilisation and highlights the importance of considering the carbon dioxide concentration mechanism in response to salt stress. However, the importance of species-specific responses in bicarbonate-based cultivation systems and highlight the potential of *P. purpureum* for high-salinity environments. These results demonstrated variations in the biochemical composition of microalgae grown in synthetic media and mushroom-bicarbonate media. Specifically, *Vischeria* sp. showed lower levels of protein and lipid in the carbon captured medium, while *P. purpureum* demonstrated elevated lipid content in the mushroom-bicarbonate medium. These findings suggest that optimising cultivation conditions through tailored media and carbon capture strategies can enhance biomass production and biochemical composition in microalgae cultivation.

CHAPTER 6

6.1 Development of a bicarbonate-based microalgal carbon capture process

Several technological methods for carbon capture and storage have been implemented to reduce carbon dioxide emissions from various industrial plants. Carbon capture and utilisation using biological sequestration has been identified as one of the most promising methods for the reduction of carbon dioxide emissions in the energy sector, both from the cost and environmental points of view. The introduction of microalgae-based utilisation in particular, can help reduce the negative impact of carbon dioxide on the environment as well as generate biomass that can be used to produce useful, value-added products. This work arose from the real-world need to mitigate carbon emissions from mushroom farms. The overall aim of this research was to develop a bicarbonate-based microalgal process to capture and utilise the carbon dioxide produced during mushroom growth, in order to reduce the carbon footprint of mushroom farms. Furthermore, this work evaluated the properties of the spent algal biomass as well as the mushroom exudate for potential applications in the nutraceutical and cosmetic industries in order to promote a circular economy. The novelty of this work lies in the successful integration of mushroom growth and microalgae cultivation through the application of bicarbonate-based carbon capture and algae production systems.

The objectives of the thesis were achieved as follows:

Objective 1: Selection of the most suitable microalgal species in a bicarbonate-based system based on the carbon capture efficiency and biochemical composition. To develop any microalgae-based process, suitable strains must be selected based on the final objective. In the case of CO_2 capture, robust and highly productive strains tolerant to alkaline media must be used. This research highlighted the potential of *P. kessleri, S. quadricauda, Vischeria* sp., *P. tricornutum,* and *P. purpureum* microalgae system of cultivation for the sequestration of inorganic carbon present in absorption solutions, strains such as *P. kessleri, S. quadricauda,* and *P. tricornutum* previously used to capture residual CO_2. The first results obtained with different synthetic $NaHCO_3$ (1, 2, 4, and 6 g L^{-1}) showed that four out of five strains with an average biomass production (≥ 1.51 g L^{-1}) combined with efficient inorganic carbon removal (≥ 70.17 %) except *Phaeodactylum tricornutum* which showed the opposite trend in terms of growth but gave high inorganic carbon removal at different lower concentration. Uncontrolled pH negatively affected microalgal proliferation due to a quick increase of pH and the predominance of dissolved carbonate species which could not be assimilated by microalgae

cells. Out of the strains examined, *Vischeria* sp. and *P. purpureum* were the most productive with high biochemical and metabolite compounds such as protein, carbohydrate, lipid content, eicosapentaenoic acid, antioxidants, and photoprotective properties evaluated from their biomass. These two species were taken forward for the remaining objectives.

Objective 2: To design a two-step integrated bicarbonate-based system for capturing carbon dioxide generated during mushroom growth and estimate the carbon utilisation efficiency of microalgae species. This study showed that that bicarbonate feeding is a highly effective method for achieving high levels of carbon dioxide utilisation from gaseous mushroom effluents, even under varying pH conditions. Regularly adjusting the pH at 5, 7, and 9 contributed to the overall inorganic carbon removal and microalgal growth for *Vischeria* sp. (31%) and *P. purpureum* (85%). The high pH observation in cultures from the first objective without pH regulation (beyond 9.5) could explain the lowering microalgal growth and inorganic carbon removal observed in those cultures. The two-step process designed for capturing CO_2 during mushroom cultivation and converting it into microalgal biomass resulted in high removal rate for *P. purpureum*. The integrated microalgae-based CO_2 treatment process demonstrated the potential for simultaneous CO_2 capture and the production of microalgal metabolites in mushroom farming. These findings suggest that maintaining the pH at 7 during microalga cultivation is beneficial for inorganic carbon removal and the overall growth of *Vischeria* sp. and *P. purpureum* under inorganic carbon conditions.

Objective 3: To demonstrate the scalability of the bicarbonate-based integrated algal production system for carbon capture during mushroom cultivation and assess the properties of valuable products extracted from microalgal biomass and mushroom exudate for potential applications. This study showed that *Vischeria* sp. and *P. purpureum* exhibited distinct growth responses to bicarbonate-based and synthetic media. *Vischeria* sp. displayed slower growth and reduced biomass production in the bicarbonate medium, likely due to its sensitivity to high sodium concentrations resulting from the use of NaOH for carbon capture. On the other hand, *P. purpureum* showed improved growth and biomass production in the bicarbonate medium, indicating its high tolerance for bicarbonate salt. The differential responses can be attributed to the levels of sodium ions, with lower levels favouring growth and inorganic carbon utilisation in *Vischeria* sp. and higher concentrations promoting growth in *P. purpureum*. Scale-up experiments were performed in 8 L bubble column photobioreactors using inorganic carbon generated from the CO_2 produced during the mushroom cultivation. After 18 days of

cultivation, *P. purpureum* was able to assimilate up to 85% respectively of the inorganic carbon initially present in the mushroom-bicarbonate media while accumulating about 54% of carbohydrates and about 24% EPA content than 16% EPA from *Vischeria* sp. of the total fatty acids. Furthermore, *P. purpureum* was able to tolerate high sodium ions present in the media compared *Vischeria* sp. which induced both microalgal growth properties as well as CO_2 capture performances.

6.1.1 Wider scope and practical considerations

Integrating carbon capture from mushroom production with microalgae cultivation is an innovative approach that can enhance sustainability and environmental benefits. Algae growth media is a promising and environmentally friendly method for capturing and utilising carbon, especially in applications where high-value products can be characterise form their biomass effectively. Most algae production industries focus on production for animal feed and value- added products for industrial purposes using compressed carbon dioxide as a carbon source for cultivation (Gerardo *et al*., 2015). Agricultural sectors such as mushroom production also contributes to carbon emission, however, this should be considered as an alternative source for inorganic carbon production through the implementation of bicarbonate-based carbon capture and algae production systems (Zhu *et al*., 2018). Microalgae-based carbon capture has several advantages, it also comes with challenges, such as optimising growth conditions, selecting the right algal species, scaling up production, and addressing downstream processing issues. Integrating carbon capture from mushroom production with microalgae cultivation is a promising approach but involves technical, logistical, and economic challenges that require careful consideration and planning (Zhang *et al*., 2018). The potential environmental benefits and sustainability improvements make it an exciting area for exploration in agriculture and carbon mitigation efforts (Chandra *et al*., 2019). Implementing and managing an integrated system require expertise in mushroom cultivation, microalgae cultivation, bioenergy production, and carbon mass balance. Some of the challenges include designing greenhouse for mushroom production, constructing and integrating a photobioreactor for scale up production. Other challenges include connecting a desiccator or moisture absorber to remove water molecules from the transferred gas.

6.2 Future recommendations

Future recommendations on scale-up for carbon capture from mushroom farming using microalgae, here are some parameters that can be optimised for this process such as temperature

and reactor design. Temperature plays a crucial role in the growth and productivity of microalgae. It is important to study the optimal temperature range for the specific strain of microalgae used in the carbon capture process. This will ensure maximum efficiency in carbon sequestration. Additionally, understanding how temperature fluctuations affect the process can help in designing robust systems that can withstand variable environmental conditions. This process has been successfully scaled up from 100 ml to 8 L, demonstrating its potential for larger scale applications. However, before commercial implementation, a further pilot scale evaluation is recommended. This will help in identifying and addressing any challenges that might arise during the scale-up process. The design of the reactor should also be optimised to ensure efficient light penetration and nutrient distribution, which are critical for the growth of microalgae. Once the pilot scale evaluation is successful, the next step would be the implementation of the process in a real mushroom farm. This will provide valuable insights into the practical aspects of the process, such as the integration with existing infrastructure, the management of the microalgae biomass, and the actual amount of carbon captured. A lifecycle analysis (LCA): Lastly, a comprehensive LCA should be conducted to evaluate the environmental impact of the process. It will be valuable to perform a techno-economic assessment and lifecycle analysis (LCA) on the process of an integrated bicarbonate-based carbon capture system for mushroom farms. The lifecycle analysis serves as a standardised methodology which has been effectively employed to evaluate and acknowledge the environmental implications of utilising algae as a source of food or feed for animal, nutraceuticals, and pharmaceutical industries (Ighalo *et al*., 2022b; Kushwaha *et al*., 2022). Based on the international standard organisation ISO 14040 series (ISO, 2014) which outlines the process for LCA, the first step would be to define a system boundary. In this case, the system would include both the mushroom farm and the microalgal cultivation system.

The next step would be to perform an inventory analysis which involves data collection on the inputs and outputs of the system design. In the present context, this would involve (1) data for mushroom growth, including the energy consumption and CO_2 emissions from mushrooms and (2) data for microalgal growth involving CO_2, water, nutrients, and energy consumption as inputs and biomass yields and other products as the outputs (Garcia *et al*., 2020). Once all the key data has been collected, the next step would involve impact assessment, which could point to the factors that can significantly reduce the production costs and lower overall environmental impacts (Cole *et al*., 2023). Lastly, interpretation of results would involve determining the most effective methods for microalgae cultivation and carbon capture identifying areas for improvement. In this concluding phase, the results of the lifecycle

inventory and lifecycle impact assessment would be categorised, quantified, and analysed to formulate relevant conclusions and recommendations. Going forward, carrying out a techno-economic feasibility study would also be important to evaluate the technical performance of this process and evaluating its economic feasibility for implementation in real-world settings (de Souza Celente *et al*., 2023). The LCA will provide a holistic view of the process and help in identifying areas where environmental performance can be improved. These recommendations aim to ensure the successful implementation of carbon capture in mushroom farming using microalgae, contributing to the fight against climate change.

CHAPTER 7

7.1 Research activities arising from this thesis

7.1.1 Manuscript under review

1. Philip Asare Kusi[1], Donal McGee[2], Shamas Tabraiz[1], and Asma Ahmed[1*]: Comparing Carbon Capture Efficiency and Biochemical Composition of Five Microalgal Species in a Bicarbonate-Based System. [1] Canterbury Christ Church University, North Holmes Road, Canterbury, Kent, CT1 1QU, UK. [2] AlgaeCytes Ltd., Discovery Park House, Ramsgate Road, Sandwich, Kent CT13 9ND UK.

2. Philip Asare Kusi, Donal McGee, Asma Ahmed: Demonstration of the Scalability of the Bicarbonate-Based Integrated Algal Production System for Carbon Capture during Mushroom Cultivation

7.1.2 Presentations

1. **Philip Asare Kusi,** Dr Asma Ahmed, Donal McGee. Carbon capture efficiency and biochemical composition of five microalgal species in a bicarbonate-based system: A comparative study. International Conference on Algal Biomass, Biofuels and Bioproducts, June 2023, Hawaii, USA – Poster Presentation accepted.
2. **Philip Asare Kusi**, Dr Asma Ahmed. Development of a natural bio-based sunscreen product from an algal-mushroom biorefinery. Postgraduate conference of the School of Psychology and Life Sciences. June 2022 - Oral Presentation.
3. **Philip Asare Kusi**, Dr Asma Ahmed. Microalgae-based carbon capture from agricultural sector to combat climate change. High Value Biorenewables for academia and industry on bioeconomic challenges, King Manor in York, United Kingdom, December 2021 – ECR seminar.

Co-ordinated project

4. UKBBSRC and High Value Biorenewables (HVB) project on: Development of a natural bio-based sunscreen product from an algal-mushroom biorefinery. Canterbury Christ Church University, and AlgaeCytes Ltd, Sandwich, UK, and Edible Kingdom Ltd. 2022.

CHAPTER 8

References

Abiusi, F., Trompetter, E., Pollio, A., Wijffels, R.H., Janssen, M., 2022. Acid Tolerant and Acidophilic Microalgae: An Underexplored World of Biotechnological Opportunities. Front Microbiol 13. https://doi.org/10.3389/fmicb.2022.820907

Acién Fernández, F.G., González-López, C. V., Fernández Sevilla, J.M., Molina Grima, E., 2012. Conversion of CO2 into biomass by microalgae: how realistic a contribution may it be to significant CO2 removal? Appl Microbiol Biotechnol 96, 577–586. https://doi.org/10.1007/s00253-012-4362-z

Ahmad, A., W. Hassan, S., Banat, F., 2022. An overview of microalgae biomass as a sustainable aquaculture feed ingredient: food security and circular economy. Bioengineered 13, 9521–9547. https://doi.org/10.1080/21655979.2022.2061148

Airs, R.L., Temperton, B., Sambles, C., Farnham, G., Skill, S.C., Llewellyn, C.A., 2014. Chlorophyll *f* and chlorophyll *d* are produced in the cyanobacterium *Chlorogloeopsis fritschii* when cultured under natural light and near-infrared radiation. FEBS Lett 588, 3770–3777. https://doi.org/10.1016/j.febslet.2014.08.026

Albuquerque, B.R., Heleno, S.A., Oliveira, M.B.P.P., Barros, L., Ferreira, I.C.F.R., 2021. Phenolic compounds: current industrial applications, limitations and future challenges. Food Funct 12, 14–29. https://doi.org/10.1039/D0FO02324H

Allen, M.M., 1968. SIMPLE CONDITIONS FOR GROWTH OF UNICELLULAR BLUE-GREEN ALGAE ON PLATES1, 2. J Phycol 4, 1–4. https://doi.org/10.1111/J.1529-8817.1968.TB04667.X

Almendinger, M., Saalfrank, F., Rohn, S., Kurth, E., Springer, M., Pleissner, D., 2021. Characterization of selected microalgae and cyanobacteria as sources of compounds with antioxidant capacity. Algal Res 53, 102168. https://doi.org/10.1016/J.ALGAL.2020.102168

Amini Khoeyi, Z., Seyfabadi, J., Ramezanpour, Z., 2012. Effect of light intensity and photoperiod on biomass and fatty acid composition of the microalgae, Chlorella vulgaris. Aquaculture International 20, 41–49. https://doi.org/10.1007/s10499-011-9440-1

Asgharpour, M., Rodgers, B., Hestekin, J., 2015. Eicosapentaenoic Acid from Porphyridium Cruentum: Increasing Growth and Productivity of Microalgae for Pharmaceutical Products. Energies (Basel) 8, 10487–10503. https://doi.org/10.3390/en80910487

Aslan, S., Kapdan, I.K., 2006. Batch kinetics of nitrogen and phosphorus removal from synthetic wastewater by algae. Ecol Eng 28, 64–70. https://doi.org/10.1016/J.ECOLENG.2006.04.003

aslani, leila, Shabanpour, B., Pourashouri, P., payamnoor, vahide, Adeli, A., 2021. Comparison of UV absorption potential and phycobiliproteins amount extracted with the help of solvent and ultrasound from (Spirulina platensis) microalgae. Journal of Utilization and Cultivation of Aquatics 10, 81–96. https://doi.org/10.22069/japu.2021.18708.1566

Assunção, M.F.G., Amaral, R., Martins, C.B., Ferreira, J.D., Ressurreição, S., Santos, S.D., Varejão, J.M.T.B., Santos, L.M.A., 2017. Screening microalgae

as potential sources of antioxidants. J Appl Phycol 29, 865–877. https://doi.org/10.1007/s10811-016-0980-7
Atkinson, N., Leitão, N., Orr, D.J., Meyer, M.T., Carmo-Silva, E., Griffiths, H., Smith, A.M., McCormick, A.J., 2017. Rubisco small subunits from the unicellular green alga *Chlamydomonas* complement Rubisco-deficient mutants of Arabidopsis. New Phytologist 214, 655–667. https://doi.org/10.1111/nph.14414
Badger, M.R., Hanson, D., Price, G.D., 2002. Evolution and diversity of CO2 concentrating mechanisms in cyanobacteria. Functional Plant Biology 29, 161. https://doi.org/10.1071/PP01213
Barh, A., Sharma, V.P., Annepu, S.K., Kamal, S., Sharma, S., Bhatt, P., 2019. Genetic improvement in Pleurotus (oyster mushroom): a review. 3 Biotech 9, 322. https://doi.org/10.1007/s13205-019-1854-x
Baumann, H., Talmage, S.C., Gobler, C.J., 2012. Reduced early life growth and survival in a fish in direct response to increased carbon dioxide. Nat Clim Chang 2, 38–41. https://doi.org/10.1038/nclimate1291
Becker, E.W., 2007. Micro-algae as a source of protein. Biotechnol Adv 25, 207–210. https://doi.org/10.1016/J.BIOTECHADV.2006.11.002
Beer, S., Eshel, A., 1985. Determining phycoerythrin and phycocyanin concentrations in aqueous crude extracts of red algae. Mar Freshw Res 36, 785. https://doi.org/10.1071/MF9850785
Beigbeder, J.-B., Lavoie, J.-M., 2022. Effect of photoperiods and CO2 concentrations on the cultivation of carbohydrate-rich P. kessleri microalgae for the sustainable production of bioethanol. Journal of CO2 utilization 58, 101934. https://doi.org/10.1016/j.jcou.2022.101934
Beigbeder, J.-B., Sanglier, M., de Medeiros Dantas, J.M., Lavoie, J.-M., 2021. CO2 capture and inorganic carbon assimilation of gaseous fermentation effluents using Parachlorella kessleri microalgae. Journal of CO2 utilization 50, 101581. https://doi.org/10.1016/j.jcou.2021.101581
Benner, P., Meier, L., Pfeffer, A., Krüger, K., Oropeza Vargas, J.E., Weuster-Botz, D., 2022. Lab-scale photobioreactor systems: principles, applications, and scalability. Bioprocess Biosyst Eng 45, 791–813. https://doi.org/10.1007/s00449-022-02711-1
Benson, A.A., Calvin, M., 2003. Carbon Dioxide Fixation By Green Plants. https://doi.org/10.1146/annurev.pp.01.060150.000325 1, 25–42. https://doi.org/10.1146/ANNUREV.PP.01.060150.000325
Bhatti, M.Z., Ali, A., Ahmad, A., Saeed, A., Malik, S.A., 2015a. Antioxidant and phytochemical analysis of Ranunculus arvensis L. extracts. BMC Res Notes 8, 279. https://doi.org/10.1186/s13104-015-1228-3
Bhatti, M.Z., Ali, A., Ahmad, A., Saeed, A., Malik, S.A., 2015b. Antioxidant and phytochemical analysis of Ranunculus arvensis L. extracts. BMC Res Notes 8, 279. https://doi.org/10.1186/s13104-015-1228-3
Bigogno, C., 2002. Lipid and fatty acid composition of the green oleaginous alga Parietochloris incisa, the richest plant source of arachidonic acid. Phytochemistry 60, 497–503. https://doi.org/10.1016/S0031-9422(02)00100-0
Biller, P., Ross, A.B., 2014. Pyrolysis GC–MS as a novel analysis technique to determine the biochemical composition of microalgae. Algal Res 6, 91–97. https://doi.org/10.1016/J.ALGAL.2014.09.009

Bleakley, S., Hayes, M., 2017. Algal Proteins: Extraction, Application, and Challenges Concerning Production. Foods 6, 33. https://doi.org/10.3390/foods6050033
Boussiba, S., 1991. Nitrogen fixing cyanobacteria potential uses. Plant Soil 137, 177–180. https://doi.org/10.1007/BF02187452
Brown, M.R., 1991. The amino-acid and sugar composition of 16 species of microalgae used in mariculture. J Exp Mar Biol Ecol 145, 79–99. https://doi.org/10.1016/0022-0981(91)90007-J
Bulut, O., Akın, D., Sönmez, Ç., Öktem, A., Yücel, M., Öktem, H.A., 2019. Phenolic compounds, carotenoids, and antioxidant capacities of a thermo-tolerant Scenedesmus sp. (Chlorophyta) extracted with different solvents. J Appl Phycol 31, 1675–1683. https://doi.org/10.1007/s10811-018-1726-5
Cao, C., Liu, H., Hou, Z., Mehmood, F., Liao, J., Feng, W., 2020. A Review of CO2 Storage in View of Safety and Cost-Effectiveness. Energies (Basel) 13, 600. https://doi.org/10.3390/en13030600
Capanoglu, E., Kamiloglu, S., Demirci Cekic, S., Sozgen Baskan, K., Avan, A.N., Uzunboy, S., Apak, R., 2021. Antioxidant Activity and Capacity Measurement. pp. 1–66. https://doi.org/10.1007/978-3-030-45299-5_22-1
Carvalho, A.P., Meireles, L.A., Malcata, F.X., 2006. Microalgal reactors: A review of enclosed system designs and performances. Biotechnol Prog. https://doi.org/10.1021/bp060065r
Castro-Ferreira, C., Gomes-Dias, J.S., Ferreira-Santos, P., Pereira, R.N., Vicente, A.A., Rocha, C.M.R., 2022. Phaeodactylum tricornutum extracts as structuring agents for food applications: Physicochemical and functional properties. Food Hydrocoll 124, 107276. https://doi.org/10.1016/j.foodhyd.2021.107276
Castro-Varela, P., Celis-Pla, P.S.M., Figueroa, F.L., Rubilar, M., 2022. Highly Efficient Water-Based Extraction of Biliprotein R-Phycoerythrin From Marine the Red-Macroalga Sarcopeltis skottsbergii by Ultrasound and High-Pressure Homogenization Methods. Front Mar Sci 9. https://doi.org/10.3389/fmars.2022.877177
Chandra, R., Iqbal, H.M.N., Vishal, G., Lee, H.-S., Nagra, S., 2019. Algal biorefinery: A sustainable approach to valorize algal-based biomass towards multiple product recovery. Bioresour Technol 278, 346–359. https://doi.org/10.1016/j.biortech.2019.01.104
Cheah, W.Y., Show, P.L., Chang, J.-S., Ling, T.C., Juan, J.C., 2015. Biosequestration of atmospheric CO2 and flue gas-containing CO2 by microalgae. Bioresour Technol 184, 190–201. https://doi.org/10.1016/j.biortech.2014.11.026
Chen, C.-Y., Jesisca, Hsieh, C., Lee, D.-J., Chang, C.-H., Chang, J.-S., 2016. Production, extraction and stabilization of lutein from microalga Chlorella sorokiniana MB-1. Bioresour Technol 200, 500–505. https://doi.org/10.1016/j.biortech.2015.10.071
Chen, H.B., Wu, J.Y., Wang, C.F., Fu, C.C., Shieh, C.J., Chen, C.I., Wang, C.Y., Liu, Y.C., 2010. Modeling on chlorophyll a and phycocyanin production by Spirulina platensis under various light-emitting diodes. Biochem Eng J 53, 52–56. https://doi.org/10.1016/J.BEJ.2010.09.004
Chen, L., Zhu, T., Fernandez, J.S.M., Chen, S., Li, D., 2017. Recycling nutrients from a sequential hydrothermal liquefaction process for microalgae culture. Algal Res 27, 311–317. https://doi.org/10.1016/j.algal.2017.09.023

Chen, M., Schliep, M., Willows, R.D., Cai, Z.-L., Neilan, B.A., Scheer, H., 2010. A Red-Shifted Chlorophyll. Science (1979) 329, 1318–1319. https://doi.org/10.1126/science.1191127
Cheng, S.-Y., Liu, Y.-Z., Qi, G.-S., 2019. Progress in the enhancement of gas–liquid mass transfer by porous nanoparticle nanofluids. J Mater Sci 54, 13029–13044. https://doi.org/10.1007/s10853-019-03809-w
Chew, K.W., Yap, J.Y., Show, P.L., Suan, N.H., Juan, J.C., Ling, T.C., Lee, D.-J., Chang, J.-S., 2017. Microalgae biorefinery: High value products perspectives. Bioresour Technol 229, 53–62. https://doi.org/10.1016/j.biortech.2017.01.006
Chi, Z., Elloy, F., Xie, Y., Hu, Y., Chen, S., 2014. Selection of Microalgae and Cyanobacteria Strains for Bicarbonate-Based Integrated Carbon Capture and Algae Production System. Appl Biochem Biotechnol 172, 447–457. https://doi.org/10.1007/s12010-013-0515-5
Chi, Z., Xie, Y., Elloy, F., Zheng, Y., Hu, Y., Chen, S., 2013. Bicarbonate-based Integrated Carbon Capture and Algae Production System with alkalihalophilic cyanobacterium. Bioresour Technol 133, 513–521. https://doi.org/10.1016/j.biortech.2013.01.150
Chisti, Y., 2016. Large-Scale Production of Algal Biomass: Raceway Ponds. pp. 21–40. https://doi.org/10.1007/978-3-319-12334-9_2
Chovancek, E., Zivcak, M., Botyanszka, L., Hauptvogel, P., Yang, X., Misheva, S., Hussain, S., Brestic, M., 2019. Transient Heat Waves May Affect the Photosynthetic Capacity of Susceptible Wheat Genotypes Due to Insufficient Photosystem I Photoprotection. Plants 8, 282. https://doi.org/10.3390/plants8080282
Cian, R.E., Fajardo, M.A., Alaiz, M., Vioque, J., González, R.J., Drago, S.R., 2014. Chemical composition, nutritional and antioxidant properties of the red edible seaweed *Porphyra columbina*. Int J Food Sci Nutr 65, 299–305. https://doi.org/10.3109/09637486.2013.854746
Cichoński, J., Chrzanowski, G., 2022a. Microalgae as a Source of Valuable Phenolic Compounds and Carotenoids. Molecules 27, 8852. https://doi.org/10.3390/molecules27248852
Cichoński, J., Chrzanowski, G., 2022b. Microalgae as a Source of Valuable Phenolic Compounds and Carotenoids. Molecules 27, 8852. https://doi.org/10.3390/molecules27248852
Ciempiel, W., Czemierska, M., Szymańska-Chargot, M., Zdunek, A., Wiącek, D., Jarosz-Wilkołazka, A., Krzemińska, I., 2022. Soluble Extracellular Polymeric Substances Produced by Parachlorella kessleri and Chlorella vulgaris: Biochemical Characterization and Assessment of Their Cadmium and Lead Sorption Abilities. Molecules 27, 7153. https://doi.org/10.3390/molecules27217153
Cole, G.M., Greene, J.M., Quinn, J.C., McDaniel, B., Kemp, L., Simmons, D., Hodges, T., Nobles, D., Weiss, T.L., McGowen, J., McDaniel, S., 2023. Integrated techno-economic and life cycle assessment of a novel algae-based coating for direct air carbon capture and sequestration. Journal of CO2 Utilization 69, 102421. https://doi.org/10.1016/j.jcou.2023.102421
Colman, B., Huertas, I.E., Bhatti, S., Dason, J.S., 2002. The diversity of inorganic carbon acquisition mechanisms in eukaryotic microalgae. Functional Plant Biology 29, 261. https://doi.org/10.1071/PP01184
Coward, T., Fuentes-Grünewald, C., Silkina, A., Oatley-Radcliffe, D.L., Llewellyn, G., Lovitt, R.W., 2016. Utilising light-emitting diodes of specific narrow

wavelengths for the optimization and co-production of multiple high-value compounds in Porphyridium purpureum. Bioresour Technol 221, 607–615. https://doi.org/10.1016/j.biortech.2016.09.093
Custódio, L., Justo, T., Silvestre, L., Barradas, A., Duarte, C.V., Pereira, H., Barreira, L., Rauter, A.P., Alberício, F., Varela, J., 2012. Microalgae of different phyla display antioxidant, metal chelating and acetylcholinesterase inhibitory activities. Food Chem 131, 134–140. https://doi.org/10.1016/J.FOODCHEM.2011.08.047
Davies, K.M., Jibran, R., Zhou, Y., Albert, N.W., Brummell, D.A., Jordan, B.R., Bowman, J.L., Schwinn, K.E., 2020. The Evolution of Flavonoid Biosynthesis: A Bryophyte Perspective. Front Plant Sci 11. https://doi.org/10.3389/fpls.2020.00007
de Souza Celente, G., de Cassia de Souza Schneider, R., Julich, J., Rizzetti, T.M., Lobo, E.A., Sui, Y., 2023. Life cycle assessment of microalgal cultivation medium: biomass, glycerol, and beta-carotene production by Dunaliella salina and Dunaliella tertiolecta. Int J Life Cycle Assess. https://doi.org/10.1007/s11367-023-02209-2
Ding, Y.-D., Zhao, S., Zhu, X., Liao, Q., Fu, Q., Huang, Y., 2016. Dynamic behaviour of the CO2 bubble in a bubble column bioreactor for microalgal cultivation. Clean Technol Environ Policy 18, 2039–2047. https://doi.org/10.1007/s10098-016-1189-9
Egbo, M.K., Okoani, A.O., Okoh, I.E., 2018. Photobioreactors for microalgae cultivation – An Overview.
Egeland, E.S., 2016. Carotenoids, in: The Physiology of Microalgae. Springer International Publishing, Cham, pp. 507–563. https://doi.org/10.1007/978-3-319-24945-2_20
Fal, S., Aasfar, A., Rabie, R., Smouni, A., Arroussi, H.EL., 2022. Salt induced oxidative stress alters physiological, biochemical and metabolomic responses of green microalga Chlamydomonas reinhardtii. Heliyon 8, e08811. https://doi.org/10.1016/j.heliyon.2022.e08811
Farooq, W., 2022. Maximizing Energy Content and CO2 Bio-fixation Efficiency of an Indigenous Isolated Microalga Parachlorella kessleri HY-6 Through Nutrient Optimization and Water Recycling During Cultivation. Front Bioeng Biotechnol 9. https://doi.org/10.3389/fbioe.2021.804608
Ferda Yylmaz, F., Demmrel, Z., Ulku Karabay-Yavasoglu, N., Ozdemmr, G., Conk-Dalay, M., 2017. Ann microbial and Ann oxidant Acc vii es of Porphyridium cruentum, Hacettepe University Journal of the Faculty of Pharmacy.
Fernández, I., Peña, J., Guzman, J.L., Berenguel, M., Acién, F.G., 2010. Modelling and Control Issues of pH in Tubular Photobioreactors. IFAC Proceedings Volumes 43, 186–191. https://doi.org/10.3182/20100707-3-BE-2012.0046
Ferreira, A., Ribeiro, B., Marques, P.A.S.S., Ferreira, A.F., Dias, A.P., Pinheiro, H.M., Reis, A., Gouveia, L., 2017. Scenedesmus obliquus mediated brewery wastewater remediation and CO 2 biofixation for green energy purposes. J Clean Prod 165, 1316–1327. https://doi.org/10.1016/j.jclepro.2017.07.232
Ferreira, A.S., Mendonça, I., Póvoa, I., Carvalho, H., Correia, A., Vilanova, M., Silva, T.H., Coimbra, M.A., Nunes, C., 2021. Impact of growth medium salinity on galactoxylan exopolysaccharides of Porphyridium purpureum. Algal Res 59, 102439. https://doi.org/10.1016/J.ALGAL.2021.102439

Foo, S.C., Yusoff, F.M., Ismail, M., Basri, M., Khong, N.M.H., Chan, K.W., Yau, S.K., 2015. Efficient solvent extraction of antioxidant-rich extract from a tropical diatom, Chaetoceros calcitrans (Paulsen) Takano 1968. Asian Pac J Trop Biomed 5, 834–840. https://doi.org/10.1016/j.apjtb.2015.06.003

Freile-Pelegrín, Y., Robledo, D., 2013. Bioactive Phenolic Compounds from Algae, in: Bioactive Compounds from Marine Foods. Wiley, pp. 113–129. https://doi.org/10.1002/9781118412893.ch6

Fuchs, T., Arnold, N.D., Garbe, D., Deimel, S., Lorenzen, J., Masri, M., Mehlmer, N., Weuster-Botz, D., Brück, T.B., 2021. A Newly Designed Automatically Controlled, Sterilizable Flat Panel Photobioreactor for Axenic Algae Culture. Front Bioeng Biotechnol 9. https://doi.org/10.3389/fbioe.2021.697354

Gao, B., Huang, L., Lei, X., Meng, G., Liu, J., Zhang, C., 2020. Evaluation and Transcriptome Analysis of the Novel Oleaginous Microalga Lobosphaera bisecta (Trebouxiophyceae, Chlorophyta) for Arachidonic Acid Production. Mar Drugs 18, 229. https://doi.org/10.3390/md18050229

Gao, B., Xu, M., Shan, D., Zhang, Chi, Yang, Y., Dong, Z., Zhang, H., Han, B., Huang, L., Zhang, Chengwu, 2023. The genomes of Vischeria oleaginous microalgae shed light on the molecular basis of hyper-accumulation of lipids. BMC Biol 21, 133. https://doi.org/10.1186/s12915-023-01618-x

Gao, B., Yang, J., Lei, X., Xia, S., Li, A., Zhang, C., 2016. Characterization of cell structural change, growth, lipid accumulation, and pigment profile of a novel oleaginous microalga, Vischeria stellata (Eustigmatophyceae), cultured with different initial nitrate supplies. J Appl Phycol 28, 821–830. https://doi.org/10.1007/s10811-015-0626-1

Garcia, R., Figueiredo, F., Brandão, M., Hegg, M., Castanheira, É., Malça, J., Nilsson, A., Freire, F., 2020. A meta-analysis of the life cycle greenhouse gas balances of microalgae biodiesel. Int J Life Cycle Assess 25, 1737–1748. https://doi.org/10.1007/s11367-020-01780-2

Gardner, R., Gardner, R., Peters, P., Peters, P., Peyton, B., Peyton, B., Cooksey, K., Cooksey, K., 2011. Medium pH and nitrate concentration effects on accumulation of triacylglycerol in two members of the chlorophyta. J Appl Phycol 23, 1005–1016. https://doi.org/10.1007/s10811-010-9633-4

Gardner, R.D., Cooksey, K.E., Mus, F., Macur, R., Moll, K., Eustance, E., Carlson, R.P., Gerlach, R., Fields, M.W., Peyton, B.M., 2012. Use of sodium bicarbonate to stimulate triacylglycerol accumulation in the chlorophyte Scenedesmus sp. and the diatom Phaeodactylum tricornutum. J Appl Phycol 24, 1311–1320. https://doi.org/10.1007/s10811-011-9782-0

Gardner-Dale, D.A., Bradley, I.M., Guest, J.S., 2017. Influence of solids residence time and carbon storage on nitrogen and phosphorus recovery by microalgae across diel cycles. Water Res 121, 231–239. https://doi.org/10.1016/j.watres.2017.05.033

Ge, S., Champagne, P., Plaxton, W.C., Leite, G.B., Marazzi, F., 2017. Microalgal cultivation with waste streams and metabolic constraints to triacylglycerides accumulation for biofuel production. Biofuels, Bioproducts and Biorefining 11, 325–343. https://doi.org/10.1002/bbb.1726

Gerardo, M.L., Van Den Hende, S., Vervaeren, H., Coward, T., Skill, S.C., 2015. Harvesting of microalgae within a biorefinery approach: A review of the developments and case studies from pilot-plants. Algal research (Amsterdam) 11, 248–262. https://doi.org/10.1016/j.algal.2015.06.019

Gernaey, K. V., Cervera-Padrell, A.E., Woodley, J.M., 2012. A perspective on PSE in pharmaceutical process development and innovation. Comput Chem Eng 42, 15–29. https://doi.org/10.1016/J.COMPCHEMENG.2012.02.022
Girmay, Z., Gorems, W., Birhanu, G., Zewdie, S., 2016. Growth and yield performance of Pleurotus ostreatus (Jacq. Fr.) Kumm (oyster mushroom) on different substrates. AMB Express 6, 87. https://doi.org/10.1186/s13568-016-0265-1
Goiris, K., Muylaert, K., Fraeye, I., Foubert, I., De Brabanter, J., De Cooman, L., 2012. Antioxidant potential of microalgae in relation to their phenolic and carotenoid content. J Appl Phycol 24, 1477–1486. https://doi.org/10.1007/s10811-012-9804-6
Goiris, K., Van Colen, W., Wilches, I., León-Tamariz, F., De Cooman, L., Muylaert, K., 2015. Impact of nutrient stress on antioxidant production in three species of microalgae. Algal Res 7, 51–57. https://doi.org/10.1016/J.ALGAL.2014.12.002
Gonçalves, A.L., Pires, J.C.M., Simões, M., 2016. The effects of light and temperature on microalgal growth and nutrient removal: an experimental and mathematical approach. RSC Adv 6, 22896–22907. https://doi.org/10.1039/C5RA26117A
González-López, C.V., Acién Fernández, F.G., Fernández-Sevilla, J.M., Sánchez Fernández, J.F., Molina Grima, E., 2012. Development of a process for efficient use of CO2 from flue gases in the production of photosynthetic microorganisms. Biotechnol Bioeng 109, 1637–1650. https://doi.org/10.1002/bit.24446
Gorgônio, C.M. da S., Aranda, D.A.G., Couri, S., 2013. Morphological and chemical aspects of <i>Chlorella pyrenoidosa, Dunaliella tertiolecta, Isochrysis galbana and Tetraselmis gracilis</i> microalgae. Nat Sci (Irvine) 05, 783–791. https://doi.org/10.4236/ns.2013.57094
Guihéneuf, F., Fouqueray, M., Mimouni, V., Ulmann, L., Jacquette, B., Tremblin, G., 2010. Effect of UV stress on the fatty acid and lipid class composition in two marine microalgae Pavlova lutheri (Pavlovophyceae) and Odontella aurita (Bacillariophyceae). J Appl Phycol 22, 629–638. https://doi.org/10.1007/s10811-010-9503-0
Guil-Guerrero, J.L., Navarro-Juárez, R., López-Martínez, J.C., Campra-Madrid, P., Rebolloso-Fuentes, M., 2004. Functional properties of the biomass of three microalgal species. J Food Eng 65, 511–517. https://doi.org/10.1016/j.jfoodeng.2004.02.014
Gülçin, İ., Topal, F., Çakmakçı, R., Bilsel, M., Gören, A.C., Erdogan, U., 2011. Pomological Features, Nutritional Quality, Polyphenol Content Analysis, and Antioxidant Properties of Domesticated and 3 Wild Ecotype Forms of Raspberries (*Rubus idaeus* L.). J Food Sci 76. https://doi.org/10.1111/j.1750-3841.2011.02142.x
Gündüz, M., Çiçek, Ş.K., Topuz, S., 2023. Extraction and optimization of phenolic compounds from butterbur plant (Petasites hybridus) by ultrasound-assisted extraction and determination of antioxidant and antimicrobial activity of butterbur extracts. J Appl Res Med Aromat Plants 35, 100491. https://doi.org/10.1016/J.JARMAP.2023.100491
Guo, F., Wang, H., Wang, J., Zhou, W., Gao, L., Chen, L., Dong, Q., Zhang, W., Liu, T., 2014. Special biochemical responses to nitrogen deprivation of

filamentous oleaginous microalgae Tribonema sp. Bioresour Technol 158, 19–24. https://doi.org/10.1016/J.BIORTECH.2014.01.144
Guo, W., Cheng, J., Song, Y., Kumar, S., Ali, K.A., Guo, C., Qiao, Z., 2019. Developing a CO 2 bicarbonation absorber for promoting microalgal growth rates with an improved photosynthesis pathway. RSC Adv 9, 2746–2755. https://doi.org/10.1039/C8RA09538H
Hall, R.A., de Sordi, L., MacCallum, D.M., Topal, H., Eaton, R., Bloor, J.W., Robinson, G.K., Levin, L.R., Buck, J., Wang, Y., Gow, N.A.R., Steegborn, C., Mühlschlegel, F.A., 2010. CO2 Acts as a Signalling Molecule in Populations of the Fungal Pathogen Candida albicans. PLoS Pathog 6, e1001193. https://doi.org/10.1371/JOURNAL.PPAT.1001193
Ham, P., Bun, S., Painmanakul, P., Wongwailikhit, K., 2021. Effective Analysis of Different Gas Diffusers on Bubble Hydrodynamics in Bubble Column and Airlift Reactors towards Mass Transfer Enhancement. Processes 9, 1765. https://doi.org/10.3390/pr9101765
Ho, L.-H., Zulkifli, N.A., Tan, T.-C., Ho, L.-H., Zulkifli, N.A., Tan, T.-C., 2020. Edible Mushroom: Nutritional Properties, Potential Nutraceutical Values, and Its Utilisation in Food Product Development. IntechOpen. https://doi.org/10.5772/intechopen.91827
Holdt, S.L., Christensen, L., Iversen, J.J.L., 2014. A novel closed system bubble column photobioreactor for detailed characterisation of micro- and macroalgal growth. J Appl Phycol 26, 825–835. https://doi.org/10.1007/s10811-013-0190-5
Hosseini Tafreshi, A., Shariati, M., 2009. *Dunaliella* biotechnology: methods and applications. J Appl Microbiol 107, 14–35. https://doi.org/10.1111/j.1365-2672.2009.04153.x
Hounslow, E., Evans, C.A., Pandhal, J., Sydney, T., Couto, N., Pham, T.K., Gilmour, D.J., Wright, P.C., 2021. Quantitative proteomic comparison of salt stress in Chlamydomonas reinhardtii and the snow alga Chlamydomonas nivalis reveals mechanisms for salt-triggered fatty acid accumulation via reallocation of carbon resources. Biotechnol Biofuels 14, 121. https://doi.org/10.1186/s13068-021-01970-6
Huang, D., Ou, B., Prior, R.L., 2005. The Chemistry behind Antioxidant Capacity Assays. J Agric Food Chem 53, 1841–1856. https://doi.org/10.1021/jf030723c
Hüner, N.P.A., Bode, R., Dahal, K., Busch, F.A., Possmayer, M., Szyszka, B., Rosso, D., Ensminger, I., Krol, M., Ivanov, A.G., Maxwell, D.P., 2013. Shedding some light on cold acclimation, cold adaptation, and phenotypic plasticity. Botany 91, 127–136. https://doi.org/10.1139/cjb-2012-0174
Ighalo, J.O., Dulta, K., Kurniawan, S.B., Omoarukhe, F.O., Ewuzie, U., Eshiemogie, S.O., Ojo, A.U., Abdullah, S.R.S., 2022a. Progress in Microalgae Application for CO2 Sequestration. Cleaner Chemical Engineering 3, 100044. https://doi.org/10.1016/J.CLCE.2022.100044
Ighalo, J.O., Dulta, K., Kurniawan, S.B., Omoarukhe, F.O., Ewuzie, U., Eshiemogie, S.O., Ojo, A.U., Abdullah, S.R.S., 2022b. Progress in Microalgae Application for CO2 Sequestration. Cleaner Chemical Engineering 3, 100044. https://doi.org/10.1016/J.CLCE.2022.100044
IPCC, 2022. Framing and Context, in: Global Warming of 1.5°C. Cambridge University Press, pp. 49–92. https://doi.org/10.1017/9781009157940.003
Iqbal Muhammad, A.R.I.S., 2005. Iqbal: Yield performance of oyster mushroom on different.

ISO, I.S.O., 2014. TS 14072: environmental management—life cycle assessment—requirements and guidelines for organizational life cycle assessment. International Organization for Standardization: Geneva, Switzerland.
Janssen, M., Tramper, J., Mur, L.R., Wijffels, R.H., 2003. Enclosed outdoor photobioreactors: Light regime, photosynthetic efficiency, scale-up, and future prospects. Biotechnol Bioeng 81, 193–210. https://doi.org/10.1002/bit.10468
Jerez-Martel, I., García-Poza, S., Rodríguez-Martel, G., Rico, M., Afonso-Olivares, C., Gómez-Pinchetti, J.L., 2017. Phenolic Profile and Antioxidant Activity of Crude Extracts from Microalgae and Cyanobacteria Strains. J Food Qual 2017, 1–8. https://doi.org/10.1155/2017/2924508
Jesumani, V., Du, H., Pei, P., Aslam, M., Huang, N., 2020. Comparative study on skin protection activity of polyphenol-rich extract and polysaccharide-rich extract from Sargassum vachellianum. PLoS One 15, e0227308. https://doi.org/10.1371/JOURNAL.PONE.0227308
Ji, X., Cheng, J., Gong, D., Zhao, X., Qi, Y., Su, Y., Ma, W., 2018a. The effect of NaCl stress on photosynthetic efficiency and lipid production in freshwater microalga—Scenedesmus obliquus XJ002. Science of The Total Environment 633, 593–599. https://doi.org/10.1016/J.SCITOTENV.2018.03.240
Ji, X., Cheng, J., Gong, D., Zhao, X., Qi, Y., Su, Y., Ma, W., 2018b. The effect of NaCl stress on photosynthetic efficiency and lipid production in freshwater microalga—Scenedesmus obliquus XJ002. Science of The Total Environment 633, 593–599. https://doi.org/10.1016/j.scitotenv.2018.03.240
Johnson, E.M., Kumar, K., Das, D., 2014a. Physicochemical parameters optimization, and purification of phycobiliproteins from the isolated Nostoc sp. Bioresour Technol 166, 541–547. https://doi.org/10.1016/j.biortech.2014.05.097
Johnson, E.M., Kumar, K., Das, D., 2014b. Physicochemical parameters optimization, and purification of phycobiliproteins from the isolated Nostoc sp. Bioresour Technol 166, 541–547. https://doi.org/10.1016/J.BIORTECH.2014.05.097
Juneja, A., Ceballos, R., Murthy, G., 2013a. Effects of Environmental Factors and Nutrient Availability on the Biochemical Composition of Algae for Biofuels Production: A Review. Energies (Basel) 6, 4607–4638. https://doi.org/10.3390/en6094607
Juneja, A., Ceballos, R.M., Murthy, G.S., 2013b. Effects of Environmental Factors and Nutrient Availability on the Biochemical Composition of Algae for Biofuels Production: A Review. Energies 2013, Vol. 6, Pages 4607-4638 6, 4607–4638. https://doi.org/10.3390/EN6094607
Jungnick, N., Ma, Y., Mukherjee, B., Cronan, J.C., Speed, D.J., Laborde, S.M., Longstreth, D.J., Moroney, J. V., 2014. The carbon concentrating mechanism in Chlamydomonas reinhardtii: Finding the missing pieces. Photosynth Res 121, 159–173. https://doi.org/10.1007/S11120-014-0004-X/METRICS
Kandasamy, S., Zhang, B., He, Z., Bhuvanendran, N., EL-Seesy, A.I., Wang, Q., Narayanan, M., Thangavel, P., Dar, M.A., 2022. Microalgae as a multipotential role in commercial applications: Current scenario and future perspectives. Fuel 308, 122053. https://doi.org/10.1016/J.FUEL.2021.122053
Khan, M.I., Shin, J.H., Kim, J.D., 2018. The promising future of microalgae: current status, challenges, and optimization of a sustainable and renewable industry for biofuels, feed, and other products. Microb Cell Fact 17, 36. https://doi.org/10.1186/s12934-018-0879-x

Khanna, P., 2020. Role of CO2 Monitoring in Mushroom Farming.
Khoo, K.S., Chew, K.W., Yew, G.Y., Leong, W.H., Chai, Y.H., Show, P.L., Chen, W.-H., 2020. Recent advances in downstream processing of microalgae lipid recovery for biofuel production. Bioresour Technol 304, 122996. https://doi.org/10.1016/j.biortech.2020.122996
KHOZINGOLDBERG, I., COHEN, Z., 2006. The effect of phosphate starvation on the lipid and fatty acid composition of the fresh water eustigmatophyte Monodus subterraneus. Phytochemistry 67, 696–701. https://doi.org/10.1016/j.phytochem.2006.01.010
Kim, H.W., Marcus, A.K., Shin, J.H., Rittmann, B.E., 2011. Advanced Control for Photoautotrophic Growth and CO2-Utilization Efficiency Using a Membrane Carbonation Photobioreactor (MCPBR). Environmental science & technology 45, 5032–5038. https://doi.org/10.1021/es104235v
Klein, M.G., Zwart, P., Bagby, S.C., Cai, F., Chisholm, S.W., Heinhorst, S., Cannon, G.C., Kerfeld, C.A., 2009. Identification and Structural Analysis of a Novel Carboxysome Shell Protein with Implications for Metabolite Transport. J Mol Biol 392, 319–333. https://doi.org/10.1016/j.jmb.2009.03.056
Klejdus, B., Lojková, L., Plaza, M., Šnóblová, M., Štěrbová, D., 2010. Hyphenated technique for the extraction and determination of isoflavones in algae: Ultrasound-assisted supercritical fluid extraction followed by fast chromatography with tandem mass spectrometry. J Chromatogr A 1217, 7956–7965. https://doi.org/10.1016/J.CHROMA.2010.07.020
Kordylewski, W., Sawicka, D., Falkowski, T., 2013. LABORATORY TESTS ON THE EFFICIENCY OF CARBON DIOXIDE CAPTURE FROM GASES IN NaOH SOLUTIONS. Journal of Ecological Engineering 14, 54–62. https://doi.org/10.5604/2081139X.1043185
Kováčik, J., Klejdus, B., Bačkor, M., 2010. Physiological Responses of *Scenedesmus quadricauda* (Chlorophyceae) to UV-A and UV-C Light. Photochem Photobiol 86, 612–616. https://doi.org/10.1111/j.1751-1097.2010.00708.x
Kovaleski, G., Kholany, M., Dias, L.M.S., Correia, S.F.H., Ferreira, R.A.S., Coutinho, J.A.P., Ventura, S.P.M., 2022. Extraction and purification of phycobiliproteins from algae and their applications. Front Chem 10. https://doi.org/10.3389/fchem.2022.1065355
Kües, U., Navarro-González, M., 2015. How do Agaricomycetes shape their fruiting bodies? 1. Morphological aspects of development. Fungal Biol Rev 29, 63–97. https://doi.org/10.1016/J.FBR.2015.05.001
Kumar, V., Jain, S., 2014. Plants and algae species: Promising renewable energy production source. Emir J Food Agric 26, 679. https://doi.org/10.9755/ejfa.v26i8.18364
Kushwaha, A., Yadav, A.N., Singh, B., Dwivedi, V., Kumar, S., Goswami, L., Hussain, C.M., 2022. Life cycle assessment and techno-economic analysis of algae-derived biodiesel: current challenges and future prospects. Waste-to-Energy Approaches Towards Zero Waste: Interdisciplinary Methods of Controlling Waste 343–372. https://doi.org/10.1016/B978-0-323-85387-3.00003-3
Lam, M.K., Lee, K.T., 2013. Effect of carbon source towards the growth of Chlorella vulgaris for CO2 bio-mitigation and biodiesel production. International Journal of Greenhouse Gas Control 14, 169–176. https://doi.org/10.1016/j.ijggc.2013.01.016

Lananan, F., Jusoh, A., Ali, N., Lam, S.S., Endut, A., 2013. Effect of Conway Medium and f/2 Medium on the growth of six genera of South China Sea marine microalgae. Bioresour Technol 141, 75–82. https://doi.org/10.1016/j.biortech.2013.03.006

Lee, J.Y., Yoo, C., Jun, S.Y., Ahn, C.Y., Oh, H.M., 2010. Comparison of several methods for effective lipid extraction from microalgae. Bioresour Technol 101, S75–S77. https://doi.org/10.1016/J.BIORTECH.2009.03.058

Li, J., Li, C., Lan, C.Q., Liao, D., 2018a. Effects of sodium bicarbonate on cell growth, lipid accumulation, and morphology of Chlorella vulgaris. Microb Cell Fact 17, 111. https://doi.org/10.1186/s12934-018-0953-4

Li, J., Li, C., Lan, C.Q., Liao, D., 2018b. Effects of sodium bicarbonate on cell growth, lipid accumulation, and morphology of Chlorella vulgaris. Microb Cell Fact. https://doi.org/10.1186/s12934-018-0953-4

Li, J., Li, C., Lan, C.Q., Liao, D., 2018c. Effects of sodium bicarbonate on cell growth, lipid accumulation, and morphology of Chlorella vulgaris. Microb Cell Fact 17, 111. https://doi.org/10.1186/s12934-018-0953-4

Li, K., Li, M., He, Y., Gu, X., Pang, K., Ma, Y., Lu, D., 2020. Effects of pH and nitrogen form on Nitzschia closterium growth by linking dynamic with enzyme activity. Chemosphere 249, 126154. https://doi.org/10.1016/j.chemosphere.2020.126154

Li, X., Přibyl, P., Bišová, K., Kawano, S., Cepák, V., Zachleder, V., Čížková, M., Brányiková, I., Vítová, M., 2013. The microalga Parachlorella kessleri--a novel highly efficient lipid producer. Biotechnol Bioeng 110, 97–107. https://doi.org/10.1002/bit.24595

Li, Y., Zhang, Z., Paciulli, M., Abbaspourrad, A., 2020. Extraction of phycocyanin—A natural blue colorant from dried spirulina biomass: Influence of processing parameters and extraction techniques. J Food Sci 85, 727–735. https://doi.org/10.1111/1750-3841.14842

Liang, M.-H., Wang, L., Wang, Q., Zhu, J., Jiang, J.-G., 2019. High-value bioproducts from microalgae: Strategies and progress. Crit Rev Food Sci Nutr 59, 2423–2441. https://doi.org/10.1080/10408398.2018.1455030

Liu, W., Bai, C., Liu, Q., Yao, J., 2020. Study on the effect of temperature on the gas–liquid mass transfer rate of volatile liquid. The European Physical Journal Plus 135, 437. https://doi.org/10.1140/epjp/s13360-020-00442-4

López, C.V.G., del Carmen Cerón García, M., Fernández, F.G.A., Bustos, C.S., Chisti, Y., Sevilla, J.M.F., 2010. Protein measurements of microalgal and cyanobacterial biomass. Bioresour Technol 101, 7587–7591. https://doi.org/10.1016/J.BIORTECH.2010.04.077

Lu, X., Nan, F., Feng, J., Lv, J., Liu, Q., Liu, X., Xie, S., 2020. Effects of Different Environmental Factors on the Growth and Bioactive Substance Accumulation of Porphyridium purpureum. Int J Environ Res Public Health 17, 2221. https://doi.org/10.3390/ijerph17072221

Luangpipat, T., Chisti, Y., 2017. Biomass and oil production by Chlorella vulgaris and four other microalgae — Effects of salinity and other factors. J Biotechnol 257, 47–57. https://doi.org/10.1016/j.jbiotec.2016.11.029

Luis, P., 2016. Use of monoethanolamine (MEA) for CO2 capture in a global scenario: Consequences and alternatives. Desalination 380, 93–99. https://doi.org/10.1016/J.DESAL.2015.08.004

MARKOU, G., VANDAMME, D., MUYLAERT, K., 2014. Microalgal and cyanobacterial cultivation: the supply of nutrients. Water research (Oxford) 65, 186–202. https://doi.org/10.1016/j.watres.2014.07.025
Maryshamya, A., Rajasekar, T., Rengasamy, R., 2019. Carbon sequestration potential of Scenedesmus quadricauda (Turpin) and evaluation on Zebra fish (Danio rerio). Aquac Rep 13. https://doi.org/10.1016/j.aqrep.2018.100178
Mata, T.M., Martins, A.A., Caetano, N.S., 2010. Microalgae for biodiesel production and other applications: A review. Renewable and Sustainable Energy Reviews 14, 217–232. https://doi.org/10.1016/J.RSER.2009.07.020
Matsudo, M.C., Bezerra, R.P., Converti, A., Sato, S., Carvalho, J.C.M., 2011. CO2 from alcoholic fermentation for continuous cultivation of Arthrospira (Spirulina) platensis in tubular photobioreactor using urea as nitrogen source. Biotechnol Prog 27, 650–656. https://doi.org/10.1002/btpr.581
Mayers, J.J., Flynn, K.J., Shields, R.J., 2013. Rapid determination of bulk microalgal biochemical composition by Fourier-Transform Infrared spectroscopy. Bioresour Technol 148, 215–220. https://doi.org/10.1016/j.biortech.2013.08.133
Mc Gee, D., Archer, L., Fleming, G.T.A., Gillespie, E., Touzet, N., 2020a. The effect of nutrient and phytohormone supplementation on the growth, pigment yields and biochemical composition of newly isolated microalgae. Process Biochemistry 92, 61–68. https://doi.org/10.1016/J.PROCBIO.2020.03.001
Mc Gee, D., Archer, L., Fleming, G.T.A., Gillespie, E., Touzet, N., 2020b. The effect of nutrient and phytohormone supplementation on the growth, pigment yields and biochemical composition of newly isolated microalgae. Process Biochemistry 92, 61–68. https://doi.org/10.1016/j.procbio.2020.03.001
Meylan, F.D., Moreau, V., Erkman, S., 2015. CO2 utilization in the perspective of industrial ecology, an overview. Journal of CO2 Utilization 12, 101–108. https://doi.org/10.1016/J.JCOU.2015.05.003
Mirón, A.S., García, M.C.C., Gómez, A.C., Camacho, F.G., Grima, E.M., Chisti, Y., 2003. Shear stress tolerance and biochemical characterization of Phaeodactylum tricornutum in quasi steady-state continuous culture in outdoor photobioreactors. Biochem Eng J. https://doi.org/10.1016/s1369-703x(03)00072-x
Moheimani, N.R., 2013. Inorganic carbon and pH effect on growth and lipid productivity of Tetraselmis suecica and Chlorella sp (Chlorophyta) grown outdoors in bag photobioreactors. J Appl Phycol 25, 387–398. https://doi.org/10.1007/s10811-012-9873-6
Moheimani, N.R., Parlevliet, D., McHenry, M.P., Bahri, P.A., de Boer, K., 2015. Past, Present and Future of Microalgae Cultivation Developments. pp. 1–18. https://doi.org/10.1007/978-3-319-16640-7_1
Monteiro, M., Santos, R.A., Iglesias, P., Couto, A., Serra, C.R., Gouvinhas, I., Barros, A., Oliva-Teles, A., Enes, P., Díaz-Rosales, P., 2019. Effect of extraction method and solvent system on the phenolic content and antioxidant activity of selected macro- and microalgae extracts. J Appl Phycol 32, 349–362. https://doi.org/10.1007/s10811-019-01927-1
Moorberg, C.J., Crouse, D.A., 2021. Soil Carbon and Respiration.
Morales, M., Cabello, J., Revah, S., 2015. Gas Balances and Growth in Algal Cultures, in: Algal Biorefineries. Springer International Publishing, Cham, pp. 263–314. https://doi.org/10.1007/978-3-319-20200-6_8

Moroney, J. V., Ynalvez, R.A., 2007. Proposed Carbon Dioxide Concentrating Mechanism in *Chlamydomonas reinhardtii*. Eukaryot Cell 6, 1251–1259. https://doi.org/10.1128/EC.00064-07

Moulin, P., Andría, J.R., Axelsson, L., Mercado, J.M., 2011. Different mechanisms of inorganic carbon acquisition in red macroalgae (Rhodophyta) revealed by the use of TRIS buffer. Aquat Bot 95, 31–38. https://doi.org/10.1016/J.AQUABOT.2011.03.007

Mtaki, K., Kyewalyanga, M.S., Mtolera, M.S.P., 2020. Assessment of Antioxidant Contents and Free Radical-Scavenging Capacity of Chlorella vulgaris Cultivated in Low Cost Media. Applied Sciences 10, 8611. https://doi.org/10.3390/app10238611

Muswati, C., Simango, K., Tapfumaneyi, L., Mutetwa, M., Ngezimana, W., 2021. The Effects of Different Substrate Combinations on Growth and Yield of Oyster Mushroom (Pleurotus ostreatus). International Journal of Agronomy 2021, 1–10. https://doi.org/10.1155/2021/9962285

Narala, R.R., Garg, S., Sharma, K.K., Thomas-Hall, S.R., Deme, M., Li, Y., Schenk, P.M., 2016. Comparison of Microalgae Cultivation in Photobioreactor, Open Raceway Pond, and a Two-Stage Hybrid System. Front Energy Res 4. https://doi.org/10.3389/fenrg.2016.00029

Ozdal, T., Capanoglu, E., Altay, F., 2013. A review on protein–phenolic interactions and associated changes. Food Research International 51, 954–970. https://doi.org/10.1016/j.foodres.2013.02.009

Pal, D., Khozin-Goldberg, I., Didi-Cohen, S., Solovchenko, A., Batushansky, A., Kaye, Y., Sikron, N., Samani, T., Fait, A., Boussiba, S., 2013. Growth, lipid production and metabolic adjustments in the euryhaline eustigmatophyte Nannochloropsis oceanica CCALA 804 in response to osmotic downshift. Appl Microbiol Biotechnol 97, 8291–8306. https://doi.org/10.1007/s00253-013-5092-6

Pancha, I., Chokshi, K., Ghosh, T., Paliwal, C., Maurya, R., Mishra, S., 2015. Bicarbonate supplementation enhanced biofuel production potential as well as nutritional stress mitigation in the microalgae Scenedesmus sp. CCNM 1077. Bioresour Technol 193, 315–323. https://doi.org/10.1016/j.biortech.2015.06.107

Pavlík, M., Fleischer, P.P., Fleischer, P.P., Pavlík, M., Šuleková, M., 2020. Evaluation of the Carbon Dioxide Production by Fungi Under Different Growing Conditions. Curr Microbiol. https://doi.org/10.1007/s00284-020-02033-z

Peng, X., Liu, S., Zhang, W., Zhao, Y., Chen, L., Wang, H., Liu, T., 2013. Triacylglycerol accumulation of Phaeodactylum tricornutum with different supply of inorganic carbon. J Appl Phycol 26, 131–139. https://doi.org/10.1007/s10811-013-0075-7

Pérez, M., Dominguez-López, I., Lamuela-Raventós, R.M., 2023. The Chemistry Behind the Folin–Ciocalteu Method for the Estimation of (Poly)phenol Content in Food: Total Phenolic Intake in a Mediterranean Dietary Pattern. J Agric Food Chem 71, 17543–17553. https://doi.org/10.1021/acs.jafc.3c04022

Piiparinen, J., Barth, D., Eriksen, N.T., Teir, S., Spilling, K., Wiebe, M.G., 2018. Microalgal CO2 capture at extreme pH values. Algal Res 32, 321–328. https://doi.org/10.1016/j.algal.2018.04.021

Prasad, R., Gupta, S.K., Shabnam, N., Oliveira, C.Y.B., Nema, A.K., Ansari, F.A., Bux, F., 2021a. Role of Microalgae in Global CO2 Sequestration:

Physiological Mechanism, Recent Development, Challenges, and Future Prospective. Sustainability 13, 13061. https://doi.org/10.3390/su132313061
Prasad, R., Gupta, S.K., Shabnam, N., Oliveira, C.Y.B., Nema, A.K., Ansari, F.A., Bux, F., 2021b. Role of Microalgae in Global CO2 Sequestration: Physiological Mechanism, Recent Development, Challenges, and Future Prospective. Sustainability 13, 13061. https://doi.org/10.3390/su132313061
Pronina, N.A., Semenenko, V.E., 1990. Membrane-Bound Carbonic Anhydrase Takes Part in CO2 Concentration in Algae Cells, in: Current Research in Photosynthesis. Springer Netherlands, Dordrecht, pp. 3283–3286. https://doi.org/10.1007/978-94-009-0511-5_739
Qin, S., Wang, K., Gao, F., Ge, B., Cui, H., Li, W., 2023. Biotechnologies for bulk production of microalgal biomass: from mass cultivation to dried biomass acquisition. Biotechnology for Biofuels and Bioproducts 16, 131. https://doi.org/10.1186/s13068-023-02382-4
Qiu, R., Gao, S., Lopez, P.A., Ogden, K.L., 2017. Effects of pH on cell growth, lipid production and CO2 addition of microalgae Chlorella sorokiniana. Algal Res 28, 192–199. https://doi.org/10.1016/j.algal.2017.11.004
Quelhas, P.M., Trovão, M., Silva, J.T., Machado, A., Santos, T., Pereira, H., Varela, J., Simões, M., Silva, J.L., 2019. Industrial production of Phaeodactylum tricornutum for CO2 mitigation: biomass productivity and photosynthetic efficiency using photobioreactors of different volumes. J Appl Phycol 31, 2187–2196. https://doi.org/10.1007/s10811-019-1750-0
Rahman, Md.M., Islam, Md.B., Biswas, M., Khurshid Alam, A.H.M., 2015. In vitro antioxidant and free radical scavenging activity of different parts of Tabebuia pallida growing in Bangladesh. BMC Res Notes 8, 621. https://doi.org/10.1186/s13104-015-1618-6
Ras, M., Steyer, J.-P., Bernard, O., 2013. Temperature effect on microalgae: a crucial factor for outdoor production. Rev Environ Sci Biotechnol 12, 153–164. https://doi.org/10.1007/s11157-013-9310-6
Ravindran, B., Gupta, S., Cho, W.-M., Kim, J., Lee, S., Jeong, K.-H., Lee, D., Choi, H.-C., 2016. Microalgae Potential and Multiple Roles—Current Progress and Future Prospects—An Overview. Sustainability 8, 1215. https://doi.org/10.3390/su8121215
Reichmann, F., Herath, J., Mensing, L., Kockmann, N., 2021. Gas-liquid mass transfer intensification for bubble generation and breakup in micronozzles. J Flow Chem 11, 429–444. https://doi.org/10.1007/s41981-021-00180-3
Remias, D., Nicoletti, C., Krennhuber, K., Möderndorfer, B., Nedbalová, L., Procházková, L., 2020. Growth, fatty, and amino acid profiles of the soil alga Vischeria sp. E71.10 (Eustigmatophyceae) under different cultivation conditions. Folia Microbiol (Praha) 65, 1017–1023. https://doi.org/10.1007/s12223-020-00810-8
Rezayian, M., Niknam, V., Faramarzi, M.A., 2019. Antioxidative responses of Nostoc ellipsosporum and Nostoc piscinale to salt stress. J Appl Phycol 31, 157–169. https://doi.org/10.1007/s10811-018-1506-2
Rogers, G., 2015. Understanding and managing the impacts of climate change on Australian mushroom production.
Rosa, G.M. da, Moraes, L., de Souza, M. da R.A.Z., Costa, J.A.V., 2016. Spirulina cultivation with a CO2 absorbent: Influence on growth parameters and macromolecule production. Bioresour Technol 200, 528–534. https://doi.org/10.1016/j.biortech.2015.10.025

Royse, D.J., Baars, J., Tan, Q., 2017. Current Overview of Mushroom Production in the World, in: Edible and Medicinal Mushrooms. Wiley, pp. 5–13. https://doi.org/10.1002/9781119149446.ch2
Ryan, A.S., Keske, M.A., Hoffman, J.P., Nelson, E.B., 2009. Clinical overview of algal-docosahexaenoic Acid: Effects on triglyceride levels and other Cardiovascular risk factors. Am J Ther 16, 183–192. https://doi.org/10.1097/MJT.0b013e31817fe2be
Saini, R.K., Prasad, P., Shang, X., Keum, Y.-S., 2021. Advances in Lipid Extraction Methods—A Review. Int J Mol Sci 22, 13643. https://doi.org/10.3390/ijms222413643
Sakamoto, Y., 2018. Influences of environmental factors on fruiting body induction, development and maturation in mushroom-forming fungi. Fungal Biol Rev 32, 236–248. https://doi.org/10.1016/J.FBR.2018.02.003
Salami, R., Kordi, M., Bolouri, P., Delangiz, N., Behnam, &, Lajayer, A., 2021. Algae-Based Biorefinery as a Sustainable Renewable Resource. Circular Economy and Sustainability 2021 1:4 1, 1349–1365. https://doi.org/10.1007/S43615-021-00088-Z
Salvucci, M.E., Crafts-Brandner, S.J., 2004. Relationship between the Heat Tolerance of Photosynthesis and the Thermal Stability of Rubisco Activase in Plants from Contrasting Thermal Environments. Plant Physiol 134, 1460–1470. https://doi.org/10.1104/pp.103.038323
Sánchez-Saavedra, M. del P., Castro-Ochoa, F.Y., Nava-Ruiz, V.M., Ruiz-Güereca, D.A., Villagómez-Aranda, A.L., Siqueiros-Vargas, F., Molina-Cárdenas, C.A., 2018. Effects of nitrogen source and irradiance on Porphyridium cruentum. J Appl Phycol 30, 783–792. https://doi.org/10.1007/s10811-017-1284-2
Sanna, A., Vega, F., Navarrete, B., Maroto-Valer, M.M., 2014. Accelerated MEA Degradation Study in Hybrid CO2 Capture Systems. Energy Procedia 63, 745–749. https://doi.org/10.1016/J.EGYPRO.2014.11.082
Sariburun, E., Şahin, S., Demir, C., Türkben, C., Uylaşer, V., 2010. Phenolic Content and Antioxidant Activity of Raspberry and Blackberry Cultivars. J Food Sci 75. https://doi.org/10.1111/j.1750-3841.2010.01571.x
Sarker, N.K., Kaparaju, P., 2023. A Critical Review on the Status and Progress of Microalgae Cultivation in Outdoor Photobioreactors Conducted over 35 Years (1986–2021). Energies (Basel) 16, 3105. https://doi.org/10.3390/en16073105
Sayre, R., 2010. Microalgae: The Potential for Carbon Capture. Bioscience 60, 722–727. https://doi.org/10.1525/bio.2010.60.9.9
Sekar, S., Chandramohan, M., 2008. Phycobiliproteins as a commodity: trends in applied research, patents and commercialization. J Appl Phycol 20, 113–136. https://doi.org/10.1007/s10811-007-9188-1
Shalaby, E.A., 2015. Algae as a natural source of antioxidant active compounds., in: Plants as a Source of Natural Antioxidants. CABI, UK, pp. 129–147. https://doi.org/10.1079/9781780642666.0129
Sharma, P.K., Saharia, M., Srivstava, R., Kumar, S., Sahoo, L., 2018. Tailoring Microalgae for Efficient Biofuel Production. Front Mar Sci 5. https://doi.org/10.3389/fmars.2018.00382
Sinetova, M.A., Sidorov, R.A., Medvedeva, A.A., Starikov, A.Y., Markelova, A.G., Allakhverdiev, S.I., Los, D.A., 2021. Effect of salt stress on physiological parameters of microalgae Vischeria punctata strain IPPAS H-242, a superproducer of eicosapentaenoic acid. J Biotechnol 331, 63–73. https://doi.org/10.1016/j.jbiotec.2021.03.001

Singh, J., Dhar, D.W., 2019. Overview of Carbon Capture Technology: Microalgal Biorefinery Concept and State-of-the-Art. Front Mar Sci 6. https://doi.org/10.3389/fmars.2019.00029
Singh, M., Kamal, S., 2017. Genetic Aspects and Strategies for Obtaining Hybrids, in: Edible and Medicinal Mushrooms. Wiley, pp. 35–87. https://doi.org/10.1002/9781119149446.ch4
Singh, R.N., Sharma, S., 2012. Development of suitable photobioreactor for algae production – A review. Renewable and Sustainable Energy Reviews 16, 2347–2353. https://doi.org/10.1016/J.RSER.2012.01.026
Singh, R.P., Yadav, P., Kumar, A., Hashem, A., Al-Arjani, A.-B.F., Abd_Allah, E.F., Rodríguez Dorantes, A., Gupta, R.K., 2022. Physiological and Biochemical Responses of Bicarbonate Supplementation on Biomass and Lipid Content of Green Algae Scenedesmus sp. BHU1 Isolated From Wastewater for Renewable Biofuel Feedstock. Front Microbiol 13, 839800. https://doi.org/10.3389/fmicb.2022.839800
Singh, S.K., Sundaram, S., Kishor, K., 2014. Carbon-Concentrating Mechanism. pp. 5–38. https://doi.org/10.1007/978-3-319-09123-5_2
Singh, S.K., Sundaram, S., Sinha, S., Rahman, Md.A., Kapur, S., 2016. Recent advances in CO $_2$ uptake and fixation mechanism of cyanobacteria and microalgae. Crit Rev Environ Sci Technol 46, 1297–1323. https://doi.org/10.1080/10643389.2016.1217911
Singh, S.P., Singh, P., 2015. Effect of temperature and light on the growth of algae species: A review. Renewable & sustainable energy reviews 50, 431–444. https://doi.org/10.1016/j.rser.2015.05.024
Singleton, V.L., Rossi, J.A., 1965. Colorimetry of Total Phenolics with Phosphomolybdic-Phosphotungstic Acid Reagents. Am J Enol Vitic 16, 144–158. https://doi.org/10.5344/ajev.1965.16.3.144
Širić, I., Abou Fayssal, S., Adelodun, B., Mioč, B., Andabaka, Ž., Bachheti, A., Goala, M., Kumar, P., AL-Huqail, A.A., Taher, M.A., Eid, E.M., 2023. Sustainable Use of CO2 and Wastewater from Mushroom Farm for Chlorella vulgaris Cultivation: Experimental and Kinetic Studies on Algal Growth and Pollutant Removal. Horticulturae 9, 308. https://doi.org/10.3390/horticulturae9030308
Solovchenko, A., Lukyanov, A., Solovchenko, O., Didi-Cohen, S., Boussiba, S., Khozin-Goldberg, I., 2014. Interactive effects of salinity, high light, and nitrogen starvation on fatty acid and carotenoid profiles in *Nannochloropsis oceanica* CCALA 804. European Journal of Lipid Science and Technology 116, 635–644. https://doi.org/10.1002/ejlt.201300456
Solovchenko, A.E., Khozin-Goldberg, I., Didi-Cohen, S., Cohen, Z., Merzlyak, M.N., 2008. Effects of light intensity and nitrogen starvation on growth, total fatty acids and arachidonic acid in the green microalga Parietochloris incisa. J Appl Phycol 20, 245–251. https://doi.org/10.1007/s10811-007-9233-0
Song, M., Pei, H., Hu, W., Han, F., Ji, Y., Ma, G., Han, L., 2014. Growth and lipid accumulation properties of microalgal Phaeodactylum tricornutum under different gas liquid ratios. Bioresour Technol 165, 31–37. https://doi.org/10.1016/j.biortech.2014.03.070
Srinivasan, R., Mageswari, A., Subramanian, P., Suganthi, C., Chaitanyakumar, A., Aswini, V., Gothandam, K.M., 2018. Bicarbonate supplementation enhances growth and biochemical composition of Dunaliella salina V-101 by reducing

oxidative stress induced during macronutrient deficit conditions. Sci Rep 8, 6972. https://doi.org/10.1038/s41598-018-25417-5
Stolaroff, J.K., Keith, D.W., Lowry, G. V., 2008a. Carbon Dioxide Capture from Atmospheric Air Using Sodium Hydroxide Spray. Environ Sci Technol 42, 2728–2735. https://doi.org/10.1021/es702607w
Stolaroff, J.K., Keith, D.W., Lowry, G. V., 2008b. Carbon Dioxide Capture from Atmospheric Air Using Sodium Hydroxide Spray. Environ Sci Technol 42, 2728–2735. https://doi.org/10.1021/es702607w
Stoykova, P., Stoyneva-Gärtner, M., Uzunov, B., Gärtner, G., Atanassov, I., Draganova, P., Borisova, C., 2019. Morphological characterization and phylogenetic analysis of aeroterrestrial *Vischeria/Eustigmatos* strains with industrial potential. Biotechnology & Biotechnological Equipment 33, 231–242. https://doi.org/10.1080/13102818.2018.1561212
Su, G., Jiao, K., Chang, J., Li, Z., Guo, X., Sun, Y., Zeng, X., Lu, Y., Lin, L., 2016. Enhancing total fatty acids and arachidonic acid production by the red microalgae Porphyridium purpureum. Bioresour Bioprocess 3, 1–9. https://doi.org/10.1186/s40643-016-0110-z
Sudhir, P., Murthy, S.D.S., 2004. Effects of salt stress on basic processes of photosynthesis. Photosynthetica 42, 481–486. https://doi.org/10.1007/S11099-005-0001-6
Sukačová, K., Lošák, P., Brummer, V., Máša, V., Vícha, D., Zavřel, T., 2021. Perspective Design of Algae Photobioreactor for Greenhouses—A Comparative Study. Energies (Basel) 14, 1338. https://doi.org/10.3390/en14051338
Sulochana, S.B., Arumugam, M., 2020. Targeted Metabolomic and Biochemical Changes During Nitrogen Stress Mediated Lipid Accumulation in Scenedesmus quadricauda CASA CC202. Front Bioeng Biotechnol 8. https://doi.org/10.3389/fbioe.2020.585632
Sun, Y., Wollman, A.J.M., Huang, F., Leake, M.C., Liu, L.-N., 2019. Single-Organelle Quantification Reveals Stoichiometric and Structural Variability of Carboxysomes Dependent on the Environment. Plant Cell 31, 1648–1664. https://doi.org/10.1105/tpc.18.00787
Suthar, S., Verma, R., 2018. Production of Chlorella vulgaris under varying nutrient and abiotic conditions: A potential microalga for bioenergy feedstock. Process Safety and Environmental Protection 113, 141–148. https://doi.org/10.1016/J.PSEP.2017.09.018
Tabita, F.R., Hanson, T.E., Li, H., Satagopan, S., Singh, J., Chan, S., 2007. Function, Structure, and Evolution of the RubisCO-Like Proteins and Their RubisCO Homologs. Microbiology and Molecular Biology Reviews 71, 576–599. https://doi.org/10.1128/MMBR.00015-07
Tan, H.T., Khong, N.M.H., Khaw, Y.S., Ahmad, S.A., Yusoff, F.M., 2020. Optimization of the Freezing-Thawing Method for Extracting Phycobiliproteins from Arthrospira sp. Molecules 25, 3894. https://doi.org/10.3390/molecules25173894
Tang, D., Han, W., Li, P., Miao, X., Zhong, J., 2011a. CO2 biofixation and fatty acid composition of Scenedesmus obliquus and Chlorella pyrenoidosa in response to different CO2 levels. Bioresour Technol 102, 3071–3076. https://doi.org/10.1016/j.biortech.2010.10.047
Tang, D., Han, W., Li, P., Miao, X., Zhong, J., 2011b. CO2 biofixation and fatty acid composition of Scenedesmus obliquus and Chlorella pyrenoidosa in

response to different CO2 levels. Bioresour Technol 102, 3071–3076. https://doi.org/10.1016/j.biortech.2010.10.047
Tesson, S.V.M., 2023. Physiological responses to pH in the freshwater microalga *Limnomonas gaiensis*. J Basic Microbiol 63, 944–956. https://doi.org/10.1002/jobm.202300107
Thorat, P.R., Nagare, N.S., Datir, M., 2023. A Review On "Spirulina (Arthrospira) Blue Green Alga," International Journal of Creative Research Thoughts.
Tibbetts, S.M., Milley, J.E., Lall, S.P., 2015. Chemical composition and nutritional properties of freshwater and marine microalgal biomass cultured in photobioreactors. J Appl Phycol 27, 1109–1119. https://doi.org/10.1007/s10811-014-0428-x
Tirumani, S., Kokkanti, M., Chaudhari, V., Shukla, M., Rao, B.J., 2014. Regulation of CCM genes in Chlamydomonas reinhardtii during conditions of light-dark cycles in synchronous cultures. Plant Mol Biol 85, 277–286. https://doi.org/10.1007/S11103-014-0183-Z/METRICS
Tripathi, S., Choudhary, S., Meena, A., Poluri, K.M., 2023. Carbon capture, storage, and usage with microalgae: a review. Environ Chem Lett 21, 2085–2128. https://doi.org/10.1007/s10311-023-01609-y
Umetani, I., Janka, E., Sposób, M., Hulatt, C.J., Kleiven, S., Bakke, R., 2021. Bicarbonate for microalgae cultivation: a case study in a chlorophyte, Tetradesmus wisconsinensis isolated from a Norwegian lake. J Appl Phycol 33, 1341–1352. https://doi.org/10.1007/s10811-021-02420-4
Vidyashankar, S., Deviprasad, K., Chauhan, V.S., Ravishankar, G.A., Sarada, R., 2013. Selection and evaluation of CO2 tolerant indigenous microalga Scenedesmus dimorphus for unsaturated fatty acid rich lipid production under different culture conditions. Bioresour Technol 144, 28–37. https://doi.org/10.1016/j.biortech.2013.06.054
Vignaud, J., Loiseau, C., Hérault, J., Mayer, C., Côme, M., Martin, I., Ulmann, L., 2023. Microalgae Produce Antioxidant Molecules with Potential Preventive Effects on Mitochondrial Functions and Skeletal Muscular Oxidative Stress. Antioxidants 12, 1050. https://doi.org/10.3390/antiox12051050
Walker, G.M., White, N.A., 2017. Introduction to Fungal Physiology, in: Fungi. Wiley, pp. 1–35. https://doi.org/10.1002/9781119374312.ch1
Walter L. Smith, M.H.C., 1975. Culture of Marine Invertebrate Animals. Springer US. https://doi.org/10.1007/978-1-4615-8714-9
Wan Mahari, W.A., Wan Razali, W.A., Manan, H., Hersi, M.A., Ishak, S.D., Cheah, W., Chan, D.J.C., Sonne, C., Show, P.L., Lam, S.S., 2022. Recent advances on microalgae cultivation for simultaneous biomass production and removal of wastewater pollutants to achieve circular economy. Bioresour Technol 364, 128085. https://doi.org/10.1016/j.biortech.2022.128085
Wang, F., Gao, B., Huang, L., Su, M., Dai, C., Zhang, C., 2018. Evaluation of oleaginous eustigmatophycean microalgae as potential biorefinery feedstock for the production of palmitoleic acid and biodiesel. Bioresour Technol 270, 30–37. https://doi.org/10.1016/j.biortech.2018.09.016
Wang, L., Addy, M., Lu, Q., Cobb, K., Chen, P., Chen, X., Liu, Y., Wang, H., Ruan, R., 2019. Cultivation of Chlorella vulgaris in sludge extracts: Nutrient removal and algal utilization. Bioresour Technol 280, 505–510. https://doi.org/10.1016/j.biortech.2019.02.017
Wang, Y., Stessman, D.J., Spalding, M.H., 2015. The <scp>CO</scp> 2 concentrating mechanism and photosynthetic carbon assimilation in limiting

<scp>CO</scp> 2 : how Chlamydomonas works against the gradient. The Plant Journal 82, 429–448. https://doi.org/10.1111/tpj.12829
Wang, Yuxin, Yang, S., Liu, J., Wang, J., Xiao, M., Liang, Q., Ren, X., Wang, Ying, Mou, H., Sun, H., 2023. Realization process of microalgal biorefinery: The optional approach toward carbon net-zero emission. Science of The Total Environment 901, 165546. https://doi.org/10.1016/J.SCITOTENV.2023.165546
White, D.A., Pagarette, A., Rooks, P., Ali, S.T., 2013. The effect of sodium bicarbonate supplementation on growth and biochemical composition of marine microalgae cultures. J Appl Phycol 25, 153–165. https://doi.org/10.1007/s10811-012-9849-6
Williams, P.J. le B., Laurens, L.M.L., 2010a. Microalgae as biodiesel & biomass feedstocks: Review & analysis of the biochemistry, energetics & economics. Energy Environ Sci 3, 554. https://doi.org/10.1039/b924978h
Williams, P.J. le B., Laurens, L.M.L., 2010b. Microalgae as biodiesel & biomass feedstocks: Review & analysis of the biochemistry, energetics & economics. Energy Environ Sci 3, 554. https://doi.org/10.1039/b924978h
Wright, D.A., Sherman, W.M., Dernbach, A.R., 1991. Carbohydrate feedings before, during, or in combination improve cycling endurance performance. J Appl Physiol (1985) 71, 1082–8. https://doi.org/10.1152/jappl.1991.71.3.1082
Wright, S., Jeffrey, S., Mantoura, R., Llewellyn, C., Bjornland, T., Repeta, D., Welschmeyer, N., 1991. Improved HPLC method for the analysis of chlorophylls and carotenoids from marine phytoplankton. Mar Ecol Prog Ser 77, 183–196. https://doi.org/10.3354/meps077183
Wu, M., Wu, G., Lu, F., Wang, H., Lei, A., Wang, J., 2022. Microalgal photoautotrophic growth induces pH decrease in the aquatic environment by acidic metabolites secretion. Biotechnology for Biofuels and Bioproducts 15, 115. https://doi.org/10.1186/s13068-022-02212-z
Xu, J., Li, T., Li, C.-L., Zhu, S.-N., Wang, Z.-M., Zeng, E.Y., 2020. Lipid accumulation and eicosapentaenoic acid distribution in response to nitrogen limitation in microalga Eustigmatos vischeri JHsu-01 (Eustigmatophyceae). Algal Res 48, 101910. https://doi.org/10.1016/j.algal.2020.101910
Yadav, A., Choudhary, P., Atri, N., Teir, S., Mutnuri, S., 2016. Pilot project at Hazira, India, for capture of carbon dioxide and its biofixation using microalgae. Environmental Science and Pollution Research 23, 22284–22291. https://doi.org/10.1007/s11356-016-6479-6
Yadav, G., Dash, S.K., Sen, R., 2019a. A biorefinery for valorization of industrial waste-water and flue gas by microalgae for waste mitigation, carbon-dioxide sequestration and algal biomass production. Science of The Total Environment 688, 129–135. https://doi.org/10.1016/j.scitotenv.2019.06.024
Yadav, G., Dash, S.K., Sen, R., 2019b. A biorefinery for valorization of industrial waste-water and flue gas by microalgae for waste mitigation, carbon-dioxide sequestration and algal biomass production. Science of The Total Environment 688, 129–135. https://doi.org/10.1016/j.scitotenv.2019.06.024
Yeh, K.L., Chang, J.S., Chen, W.M., 2010. Effect of light supply and carbon source on cell growth and cellular composition of a newly isolated microalga Chlorella vulgaris ESP-31. Eng Life Sci 10, 201–208. https://doi.org/10.1002/ELSC.200900116

Yi, S., Zhang, A.-H., Huang, J., Yao, T., Feng, B., Zhou, X., Hu, Y., Pan, M., 2024. Maximizing Polysaccharides and Phycoerythrin in Porphyridium purpureum via the Addition of Exogenous Compounds: A Response-Surface-Methodology Approach. Mar Drugs 22, 138. https://doi.org/10.3390/md22030138

Yimin Chen a, Changan Xu a, 2021. How to narrow the CO2 gap from growth-optimal to flue gas levels by using microalgae for carbon capture and sustainable biomass production. J Clean Prod 280, 124448. https://doi.org/10.1016/J.JCLEPRO.2020.124448

Yoo, M., Han, S.J., Wee, J.H., 2013. Carbon dioxide capture capacity of sodium hydroxide aqueous solution. J Environ Manage 114, 512–519. https://doi.org/10.1016/J.JENVMAN.2012.10.061

Yustinadiar, N., Manurung, R., Suantika, G., 2020. Enhanced biomass productivity of microalgae Nannochloropsis sp. in an airlift photobioreactor using low-frequency flashing light with blue LED. Bioresour Bioprocess 7, 43. https://doi.org/10.1186/s40643-020-00331-9

Zeng, X., Danquah, M.K., Zhang, S., Zhang, X., Wu, M., Chen, X.D., Ng, I.-S., Jing, K., Lu, Y., 2012. Autotrophic cultivation of Spirulina platensis for CO2 fixation and phycocyanin production. Chemical Engineering Journal 183, 192–197. https://doi.org/10.1016/j.cej.2011.12.062

Zhang, D., An, S., Yao, R., Fu, W., Han, Y., Du, M., Chen, Z., Lei, A., Wang, J., 2022. Life cycle assessment of auto-tropically cultivated economic microalgae for final products such as food, total fatty acids, and bio-oil. Front Mar Sci 9. https://doi.org/10.3389/fmars.2022.990635

Zhang, W., Wang, F., Gao, B., Huang, L., Zhang, C., 2018. An integrated biorefinery process: Stepwise extraction of fucoxanthin, eicosapentaenoic acid and chrysolaminarin from the same Phaeodactylum tricornutum biomass. Algal research (Amsterdam) 32, 193–200. https://doi.org/10.1016/j.algal.2018.04.002

Zhao, B., Sun, Y., Yuan, Y., Gao, J., Wang, S., Zhuo, Y., Chen, C., 2011. Study on corrosion in CO2 chemical absorption process using amine solution. Energy Procedia 4, 93–100. https://doi.org/10.1016/j.egypro.2011.01.028

Zhou, W., Wang, J., Chen, P., Ji, C., Kang, Q., Lu, B., Li, K., Liu, J., Ruan, R., 2017. Bio-mitigation of carbon dioxide using microalgal systems: Advances and perspectives. Renewable and Sustainable Energy Reviews 76, 1163–1175. https://doi.org/10.1016/J.RSER.2017.03.065

Zhu, C., Zhang, R., Cheng, L., Chi, Z., 2018. A recycling culture of Neochloris oleoabundans in a bicarbonate-based integrated carbon capture and algae production system with harvesting by auto-flocculation. Biotechnol Biofuels 11, 204. https://doi.org/10.1186/s13068-018-1197-6

Zhu, L., Li, Z., Ketola, T., 2011. Biomass accumulations and nutrient uptake of plants cultivated on artificial floating beds in China's rural area. Ecol Eng 37, 1460–1466. https://doi.org/10.1016/j.ecoleng.2011.03.010

Zion, 2021. Mushroom Market Size, Share, Trends, Growth Report and Forecast [WWW Document]. Zion Market Research. URL https://www.zionmarketresearch.com/report/mushroom-market

Appendices

Appendix A

The following dataset from this section describes the representative data from the quantitative measurements on the biochemical composition and pigments estimated in the microalgal biomass from an FTIR spectra and HPLC based on their statistical analysis. The presented dataset in Appendix A is described in chapter 3 of the thesis.

Table A. 1 Biomass composition of estimated lipid, protein, and carbohydrate content from the biomass of *Parachlorella kessleri* cultivated in different bicarbonate concentrations. Data values expressed as mean ± standard deviation, n=3.

	Lipid					**Protein**					**Carbohydrate**			
Sample	Control (A)	2g L^{-1} (B)	4g L^{-1} (C)	6g L^{-1} (D)		Sample	Control (A)	2g L^{-1} (B)	4g L^{-1} (C)		Sample	Control (A)	2g L^{-1} (B)	4g L^{-1} (C)
1	3.91	12.04	12.52	16.23		15.31	16.31	18.22	18.52		38.61	44.65	46.84	44.33
2	4.11	11.52	10.33	16.82		15.22	16.53	19.41	16.83		38.42	44.52	48.05	43.17
3	4.32	11.51	9.31	15.72		15.51	16.82	20.52	17.72		37.90	44.81	50.82	45.73

Table A. 2 Results of the one-way ANOVA test comparing the means of lipid content from *P. kessleri* cultivated at different inorganic carbon concentration.

ANOVA: Single Factor						
SUMMARY						
Groups	*Count*	*Sum*	*Average*	*Variance*		
Control (A)	3	11.9	3.966667	0.00333333		
2g L^{-1} (B)	3	34.6	11.53333	0.20333333		
4g L^{-1} (C)	3	32.7	10.9	2.56		
6g L^{-1} (D)	3	48.7	16.23333	0.30333333		
ANOVA						
Source of Variation	*SS*	*df*	*MS*	*F*	*P-value*	*F crit*
Between Groups	230.0492	3	76.68306	99.912776	1.11E-06	4.066181
Within Groups	6.14	8	0.7675			
Total	236.1892	11				

Table A. 3 Results of the one-way ANOVA test comparing the means of protein content from *P. kessleri* cultivated at different inorganic carbon concentration.

SUMMARY						
Groups	*Count*	*Sum*	*Average*	*Variance*		
Control (A)	3	45.8	15.26667	0.06333333		
2g L^{-1} (B)	3	49.6	16.53333	0.06333333		
4g L^{-1} (C)	3	58.1	19.36667	1.32333333		
6g L^{-1} (D)	3	53	17.66667	0.72333333		
ANOVA						
Source of Variation	*SS*	*df*	*MS*	*F*	*P-value*	*F crit*
Between Groups	27.2825	3	9.094167	16.7377301	0.000828	4.066181
Within Groups	4.346667	8	0.543333			
Total	31.62917	11				

Table A. 4 Results of the one-way ANOVA test comparing the means of carbohydrate content from *P. kessleri* cultivated at different inorganic carbon concentration.

SUMMARY						
Groups	*Count*	*Sum*	*Average*	*Variance*		
Control (A)	3	114.7	38.23333	0.083333		
2g L^{-1} (B)	3	133.9	44.63333	0.023333		
4g L^{-1} (C)	3	146.4	48.8	4		
6g L^{-1} (D)	3	137.1	45.7	6.76		
ANOVA						
Source of Variation	*SS*	*df*	*MS*	*F*	*P-value*	*F crit*
Between Groups	177.3558	3	59.11861	21.76145	0.000334	4.066181
Within Groups	21.73333	8	2.716667			
Total	199.0892	11				

Lipid

Tukey HSD results			
treatments pair	Tukey HSD Q statistic	Tukey HSD p-value	Tukey HSD inferfence
A vs B	14.9598	0.0010053	** p<0.01
A vs C	13.7077	0.0010053	** p<0.01
A vs D	24.2520	0.0010053	** p<0.01
B vs C	1.2521	0.7947903	insignificant
B vs D	9.2922	0.0010053	** p<0.01
C vs D	10.5444	0.0010053	** p<0.01

Protein

Tukey HSD results			
treatments pair	Tukey HSD Q statistic	Tukey HSD p-value	Tukey HSD inferfence
A vs B	2.9764	0.2303983	insignificant
A vs C	9.6341	0.0010053	** p<0.01
A vs D	5.6395	0.0169354	* p<0.05
B vs C	6.6577	0.0066415	** p<0.01
B vs D	2.6631	0.3066277	insignificant
C vs D	3.9946	0.0852718	insignificant

Carbohydrate

Tukey HSD results			
treatments pair	Tukey HSD Q statistic	Tukey HSD p-value	Tukey HSD inferfence
A vs B	6.7255	0.0062526	** p<0.01
A vs C	11.1040	0.0010053	** p<0.01
A vs D	7.8464	0.0024183	** p<0.01
B vs C	4.3786	0.0581041	insignificant
B vs D	1.1209	0.8422603	insignificant
C vs D	3.2576	0.1762603	insignificant

Figure A. 1 Effect of inorganic carbon concentrations on lipid, protein, and carbohydrate composition in *Parachlorella kessleri*. Treatment pairs defines the comparison between (A) control 1 g L^{-1}, (B) 2 g L^{-1}, (C) 4 g L^{-1}, (D) 6 g L^{-1}.

Table A. 5 Biomass composition of estimated lipid and carbohydrate content from the biomass of *Phaeodactylum tricornutum* cultivated in different bicarbonate concentrations. Data values expressed as mean ± standard deviation, n=3.

	Lipid					**Carbohydrate**			
Sample	Control (A)	2g L^{-1} (B)	4g L^{-1} (C)	6g L^{-1} (D)		Control (A)	2g L^{-1} (B)	4g L^{-1} (C)	6g L^{-1} (D)
1	22.60	21.22	20.12	19.60		66.12	58.61	53.22	48.92
2	22.17	19.72	19.45	18.41		61.91	58.80	53.63	49.22
3	21.53	20.51	18.71	17.14		57.73	58.94	52.72	49.40

Table A. 6 Results of the one-way ANOVA test comparing the means of lipid content from *Phaeodactylum tricornutum* cultivated at different inorganic carbon concentration.

Anova: Single Factor

SUMMARY

Groups	*Count*	*Sum*	*Average*	*Variance*
Control (A)	3	66.2	22.06667	0.30333333
2g L^{-1} (B)	3	61.4	20.46667	0.56333333
4g L^{-1} (C)	3	58.2	19.4	0.49
6g L^{-1} (D)	3	55.1	18.36667	1.56333333

ANOVA

Source of Variation	*SS*	*df*	*MS*	*F*	*P-value*	*F crit*
Between Groups	22.4825	3	7.494167	10.2659817	0.004064	4.066181
Within Groups	5.84	8	0.73			
Total	28.3225	11				

Table A. 7 Results of the one-way ANOVA test comparing the means of carbohydrate content from *Phaeodactylum tricornutum* cultivated at different inorganic carbon concentration.

Anova: Single Factor

SUMMARY

Groups	*Count*	*Sum*	*Average*	*Variance*
Control (A)	3	185.7	61.9	17.64
2g L^{-1} (B)	3	176.3	58.76667	0.023333
4g L^{-1} (C)	3	159.5	53.16667	0.203333
6g L^{-1} (D)	3	147.6	49.2	0.04

ANOVA

Source of Variation	*SS*	*df*	*MS*	*F*	*P-value*	*F crit*
Between Groups	289.4958	3	96.49861	21.55591	0.000345	4.066181
Within Groups	35.81333	8	4.476667			
Total	325.3092	11				

Lipid

Tukey HSD results

treatments pair	Tukey HSD Q statistic	Tukey HSD p-value	Tukey HSD inferfence
A vs B	3.2435	0.1786783	insignificant
A vs C	5.4059	0.0211686	* p<0.05
A vs D	7.5007	0.0032136	** p<0.01
B vs C	2.1624	0.4662043	insignificant
B vs D	4.2571	0.0655948	insignificant
C vs D	2.0948	0.4901414	insignificant

Carbohydrate

Tukey HSD results

treatments pair	Tukey HSD Q statistic	Tukey HSD p-value	Tukey HSD inferfence
A vs B	2.5650	0.3341917	insignificant
A vs C	7.1493	0.0043255	** p<0.01
A vs D	10.3965	0.0010053	** p<0.01
B vs C	4.5843	0.0473371	* p<0.05
B vs D	7.8315	0.0024473	** p<0.01
C vs D	3.2472	0.1780499	insignificant

Figure A. 2 The biochemical variation of *Phaeodactylum tricornutum* cultivated at different inorganic carbon concentration. Treatment pairs defines the comparison between (A) control 1 g L^{-1}, (B) 2 g L^{-1}, (C) 4 g L^{-1}, (D) 6 g L^{-1}.

The chlorophyll-*a* content in different microalgal strains were calculated using a High-performance liquid chromatography. The results for each strain are displayed in Table A-8 with the chlorophyll-*a* content from *P. kessleri* and *P. tricornutum* biomass

Table A. 8 Chlorophyll-*a* content in the biomass of *P. kessleri* and *Phaeodactylum tricornutum* cultivated in different inorganic carbon concentrations. Data values expressed as mean ± standard deviation, n=3.

	P. kessleri					***P. tricornutum***			
	Chlorophyll-*a*					Chlorophyll-*a*			
Sample	Control (A)	2g L^{-1} (B)	4g L^{-1} (C)	6g L^{-1} (D)		Control (A)	2g L^{-1} (B)	4g L^{-1} (C)	6g L^{-1} (D)
1	3.86	4.29	6.87	6.96		2.87	1.99	1.84	0.79
2	3.45	4.76	6.57	6.85		2.82	1.78	1.85	0.82
3	3.65	4.32	6.82	6.88		2.76	1.84	1.92	0.81

Table A. 9 Results of the one-way ANOVA test comparing the means of on chlorophyll-*a* content from *P. kessleri* cultivated at different inorganic carbon concentration.

Anova: Single Factor						
SUMMARY						
Groups	*Count*	*Sum*	*Average*	*Variance*		
Control (A)	3	10.96	3.653333	0.042033		
2g L^{-1} (B)	3	13.37	4.456667	0.069233		
4g L^{-1} (C)	3	20.3	6.766667	0.032033		
6g L^{-1} (D)	3	20.69	6.896667	0.003233		
ANOVA						
Source of Variation	*SS*	*df*	*MS*	*F*	*P-value*	*F crit*
Between Groups	24.123	3	8.041	219.4995	5.08E-08	4.066181
Within Groups	0.293067	8	0.036633			
Total	24.41607	11				

Table A. 10 Results of the one-way ANOVA test comparing the means of on chlorophyll-*a* content from *P. tricornutum* cultivated at different inorganic carbon concentration.

Anova: Single Factor						
SUMMARY						
Groups	*Count*	*Sum*	*Average*	*Variance*		
Control (A)	3	8.45	2.816667	0.003033		
2g L^{-1} (B)	3	5.61	1.87	0.0117		
4g L^{-1} (C)	3	5.61	1.87	0.0019		
6g L^{-1} (D)	3	2.42	0.806667	0.000233		
ANOVA						
Source of Variation	*SS*	*df*	*MS*	*F*	*P-value*	*F crit*
Between Groups	6.070358	3	2.023453	479.8702	2.29E-09	4.066181
Within Groups	0.033733	8	0.004217			
Total	6.104092	11				

P. kessleri

Tukey HSD results

treatments pair	Tukey HSD Q statistic	Tukey HSD p-value	Tukey HSD inferfence
A vs B	7.2697	0.0039042	** p<0.01
A vs C	28.1740	0.0010053	** p<0.01
A vs D	29.3504	0.0010053	** p<0.01
B vs C	20.9042	0.0010053	** p<0.01
B vs D	22.0807	0.0010053	** p<0.01
C vs D	1.1764	0.8221783	insignificant

P. tricornutum

Tukey HSD results

treatments pair	Tukey HSD Q statistic	Tukey HSD p-value	Tukey HSD inferfence
A vs B	25.2507	0.0010053	** p<0.01
A vs C	25.2507	0.0010053	** p<0.01
A vs D	53.6132	0.0010053	** p<0.01
B vs C	0.0000	0.8999947	insignificant
B vs D	28.3626	0.0010053	** p<0.01
C vs D	28.3626	0.0010053	** p<0.01

Figure A. 3 Chlorophyll-*a* content cultivated at each inorganic carbon concentration for *P. kessleri* and *P. tricornutum* respectively.

Appendix B

Data representation on the biochemical compositions from chapter 4.

Table B. 1 Chlorophyll-*a* content in the biomass of *Vischeria* sp. cultivated under synthetic media (SB) and mushroom-bicarbonate media (MB) at pH 5, 7, and 9. Data values expressed as mean ± standard deviation, n=3.

	Synthetic media (SB)				Mushroom-bicarbonate media (MB)		
Sample	SB-pH 5 (mg g^{-1})	SB-pH 7 (mg g^{-1})	SB-pH 9 (mg g^{-1})		MB-pH 5 (mg g^{-1})	MB-pH 7 (mg g^{-1})	MB-pH 9 (mg g^{-1})
1	27.14	31.94	39.96		19.15	42.15	27.38
2	28.06	30.89	35.21		16.15	43.14	27.32
3	27.86	33.37	36.78		13.15	37.23	23.85

Table B. 2 Results of the one-way ANOVA test comparing the means of chlorophyll-*a* content at pH 5 in *Vischeria* sp. cultivated under synthetic media (SB) and mushroom-bicarbonate media (MB).

SUMMARY						
Groups	*Count*	*Sum*	*Average*	*Variance*		
SB-pH 5	3	83.06	27.6866667	0.23413333		
MB-pH 5	3	48.45	16.15	9		
ANOVA						
Source of Variation	*SS*	*df*	*MS*	*F*	*P-value*	*F crit*
Between Groups	199.642017	1	199.642017	43.2400117	0.00276835	7.70864742
Within Groups	18.4682667	4	4.61706667			
Total	218.110283	5				

Table B. 3 Results of the one-way ANOVA test comparing the means of chlorophyll-*a* content at pH 7 in *Vischeria* sp. cultivated under synthetic media (SB) and mushroom-bicarbonate media (MB).

Anova: Single Factor						
SUMMARY						
Groups	*Count*	*Sum*	*Average*	*Variance*		
SB-pH 7	3	96.2	32.0666667	1.54963333		
MB-pH 7	3	122.52	40.84	10.0191		
ANOVA						
Source of Variation	*SS*	*df*	*MS*	*F*	*P-value*	*F crit*
Between Groups	115.457067	1	115.457067	19.9601916	0.01109445	7.70864742
Within Groups	23.1374667	4	5.78436667			
Total	138.594533	5				

Table B. 4 Results of the one-way ANOVA test comparing the means of chlorophyll-*a* content at pH 9 in *Vischeria* sp. cultivated under synthetic media (SB) and mushroom-bicarbonate media (MB).

Anova: Single Factor						
SUMMARY						
Groups	*Count*	*Sum*	*Average*	*Variance*		
SB-pH9	3	111.95	37.3166667	5.85663333		
MB-pH 9	3	78.55	26.1833333	4.08423333		
ANOVA						
Source of Variation	*SS*	*df*	*MS*	*F*	*P-value*	*F crit*
Between Groups	185.926667	1	185.926667	37.4065306	0.0036188	7.70864742
Within Groups	19.8817333	4	4.97043333			
Total	205.8084	5				

Table B. 5 chlorophyll-*a* content at pH 5, 7, and 9 cultivated in both synthetic media (SB) and mushroom-bicarbonate media (MB) for *P. purpureum*. Data values expressed as mean ± standard deviation, n=3.

	Synthetic media (SB)				Mushroom-bicarbonate media (MB)		
Sample	SB-pH 5 (mg g^{-1})	SB-pH 7 (mg g^{-1})	SB-pH 9 (mg g^{-1})		MB-pH 5 (mg g^{-1})	MB-pH 7 (mg g^{-1})	MB-pH 9 (mg g^{-1})
1	14.02	20.53	19.59		7.58	24.79	3.59
2	13.47	25.89	14.44		8.99	17.59	3.86
3	12.93	28.99	15.43		7.23	25.63	4.23

Table B. 6 Results of the one-way ANOVA test comparing the means of chlorophyll-*a* content at pH 5 in *Vischeria* sp. cultivated under synthetic media (SB) and mushroom-bicarbonate media (MB).

Anova: Single Factor						
SUMMARY						
Groups	*Count*	*Sum*	*Average*	*Variance*		
SB-pH 5	3	7.67	2.55666667	0.00443333		
MB-pH 5	3	3.87	1.29	0.0028		
ANOVA						
Source of Variation	*SS*	*df*	*MS*	*F*	*P-value*	*F crit*
Between Groups	2.40666667	1	2.40666667	665.437788	1.3415E-05	7.70864742
Within Groups	0.01446667	4	0.00361667			
Total	2.42113333	5				

Table B. 7 Results of the one-way ANOVA test comparing the means of chlorophyll-*a* content at pH 7 in *Vischeria* sp. cultivated under synthetic media (SB) and mushroom-bicarbonate media (MB).

Anova: Single Factor						
SUMMARY						
Groups	*Count*	*Sum*	*Average*	*Variance*		
SB-pH 7	3	14.63	4.87666667	0.70863333		
MB-pH 7	3	9.65	3.21666667	0.06663333		
ANOVA						
Source of Variation	*SS*	*df*	*MS*	*F*	*P-value*	*F crit*
Between Groups	4.1334	1	4.1334	10.6631697	0.03092144	7.70864742
Within Groups	1.55053333	4	0.38763333			
Total	5.68393333	5				

Table B. 8 Biomass composition of estimated protein content for *Vischeria* sp. cultivated both in synthetic media (SB) and mushroom-bicarbonate media (MB) at pH 5, 7, and 9. Data values expressed as mean ± standard deviation, n=3.

Sample	SB-pH 5 (mg g^{-1})	SB-pH 7 (mg g^{-1})	SB-pH 9 (mg g^{-1})		MB-pH 5 (mg g^{-1})	MB-pH 7 (mg g^{-1})	MB-pH 9 (mg g^{-1})
1	36.71	38.90	43.24		19.21	35.06	39.92
2	39.24	42.43	43.42		24.46	36.32	38.74
3	38.32	40.16	42.61		21.83	33.64	38.41

Table B. 9 Results of the one-way ANOVA test comparing the means of protein content from synthetic media (SB) and mushroom-bicarbonate media (MB) cultivated at pH 5 for *Vischeria* sp.

Anova: Single Factor						
SUMMARY						
Groups	*Count*	*Sum*	*Average*	*Variance*		
SB-pH 5	3	114.2	38.06667	1.603333		
MB-pH 5	3	65.4	21.8	6.76		
ANOVA						
Source of Variation	*SS*	*df*	*MS*	*F*	*P-value*	*F crit*
Between Groups	396.9067	1	396.9067	94.9159	0.000622	7.708647
Within Groups	16.72667	4	4.181667			
Total	413.6333	5				

Table B. 10 Results of the one-way ANOVA test comparing the means of protein content from synthetic media (SB) and mushroom-bicarbonate (MB) media cultivated at pH 7 for *Vischeria* sp.

Anova: Single Factor						
SUMMARY						
Groups	*Count*	*Sum*	*Average*	*Variance*		
MB-pH 7	3	121.4	40.46667	3.163333		
MB-pH 7	3	104.9	34.96667	1.823333		
ANOVA						
Source of Variation	*SS*	*df*	*MS*	*F*	*P-value*	*F crit*
Between Groups	45.375	1	45.375	18.19853	0.012992	7.708647
Within Groups	9.973333	4	2.493333			
Total	55.34833	5				

Appendix C

Data representation on the inorganic carbon utilisation and biochemical composition on experimental results from chapter 5.

Table C. 1 Represents inorganic carbon utilisation capacity by *Vischeria* sp. and *Porphyridium purpureum*. Data values expressed as mean ± standard deviation, n=3.

	Vischeria sp.		*Porphyridium purpureum*	
Sample	Synthetic media (mg $L^{-1}d^{-1}$)	Mushroom-bicarbonate media (mg $L^{-1}d^{-1}$)	Synthetic media (mg $L^{-1}d^{-1}$)	Mushroom-bicarbonate media (mg $L^{-1}d^{-1}$)
1	134.47	43.33	25.72	53.61
2	134.58	44.23	25.81	53.72
3	134.26	43.23	25.11	53.51

Table C. 2 Results of the one-way ANOVA test comparing the means of inorganic carbon utilisation by *Vischeria* sp. cultivated in synthetic media and mushroom-bicarbonate media.

Anova: Single Factor						
SUMMARY						
Groups	*Count*	*Sum*	*Average*	*Variance*		
Synthetic media	3	403.31	134.436667	0.02643333		
Mushroom media	3	130.79	43.5966667	0.30333333		
ANOVA						
Source of Variation	*SS*	*df*	*MS*	*F*	*P-value*	*F crit*
Between Groups	12377.8584	1	12377.8584	75070.4037	1.0646E-09	7.70864742
Within Groups	0.65953333	4	0.16488333			
Total	12378.5179	5				

Table C. 3 Results of the one-way ANOVA test comparing the means of inorganic carbon utilisation by *Porphyridium purpureum* cultivated in synthetic media and mushroom-bicarbonate media.

Anova: Single Factor						
SUMMARY						
Groups	*Count*	*Sum*	*Average*	*Variance*		
Synthetic media	3	76.64	25.5466667	0.14503333		
Mushroom media	3	160.84	53.6133333	0.01103333		
ANOVA						
Source of Variation	*SS*	*df*	*MS*	*F*	*P-value*	*F crit*
Between Groups	1181.60667	1	1181.60667	15142.3323	2.6156E-08	7.70864742
Within Groups	0.31213333	4	0.07803333			
Total	1181.9188	5				

Table C. 4 Biomass composition of lipid, protein, and carbohydrate content from the biomass of *Vischeria* sp. cultivated in synthetic and mushroom-bicarbonate media using FTIR. Data values expressed as mean ± standard deviation, n=3.

	Synthetic media (% DW)				Mushroom-bicarbonate media (% DW)		
Sample	Protein	Lipid	Carbohydrate		Protein	Lipid	Carbohydrate
1	30.91	22.12	47.44		17.51	13.51	47.32
2	32.13	20.25	46.87		19.22	12.54	50.41
3	31.54	21.65	47.21		18.25	12.75	48.85

Table C. 5 Results of the one-way ANOVA test comparing the means of lipid content accumulated by *Vischeria* sp. cultivated in both synthetic and mushroom-bicarbonate media using FTIR quantification analysis.

Anova: Single Factor						
SUMMARY						
Groups	*Count*	*Sum*	*Average*	*Variance*		
Synthetic media	3	63	21	1		
Mushroom media	3	38.25	12.75	0.5625		
ANOVA						
Source of Variation	*SS*	*df*	*MS*	*F*	*P-value*	*F crit*
Between Groups	102.0938	1	102.0938	130.68	0.000334	7.708647
Within Groups	3.125	4	0.78125			
Total	105.2188	5				

Table C. 6 Results of the one-way ANOVA test comparing the means of protein content accumulated by *Vischeria* sp. cultivated in both synthetic and mushroom-bicarbonate media using FTIR quantification analysis.

Anova: Single Factor						
SUMMARY						
Groups	*Count*	*Sum*	*Average*	*Variance*		
Synthetic media	3	94.5	31.5	0.36		
Mushroom media	3	54.75	18.25	0.5625		
ANOVA						
Source of Variation	*SS*	*df*	*MS*	*F*	*P-value*	*F crit*
Between Groups	263.3438	1	263.3438	570.935	1.82E-05	7.708647
Within Groups	1.845	4	0.46125			
Total	265.1888	5				

Appendix D

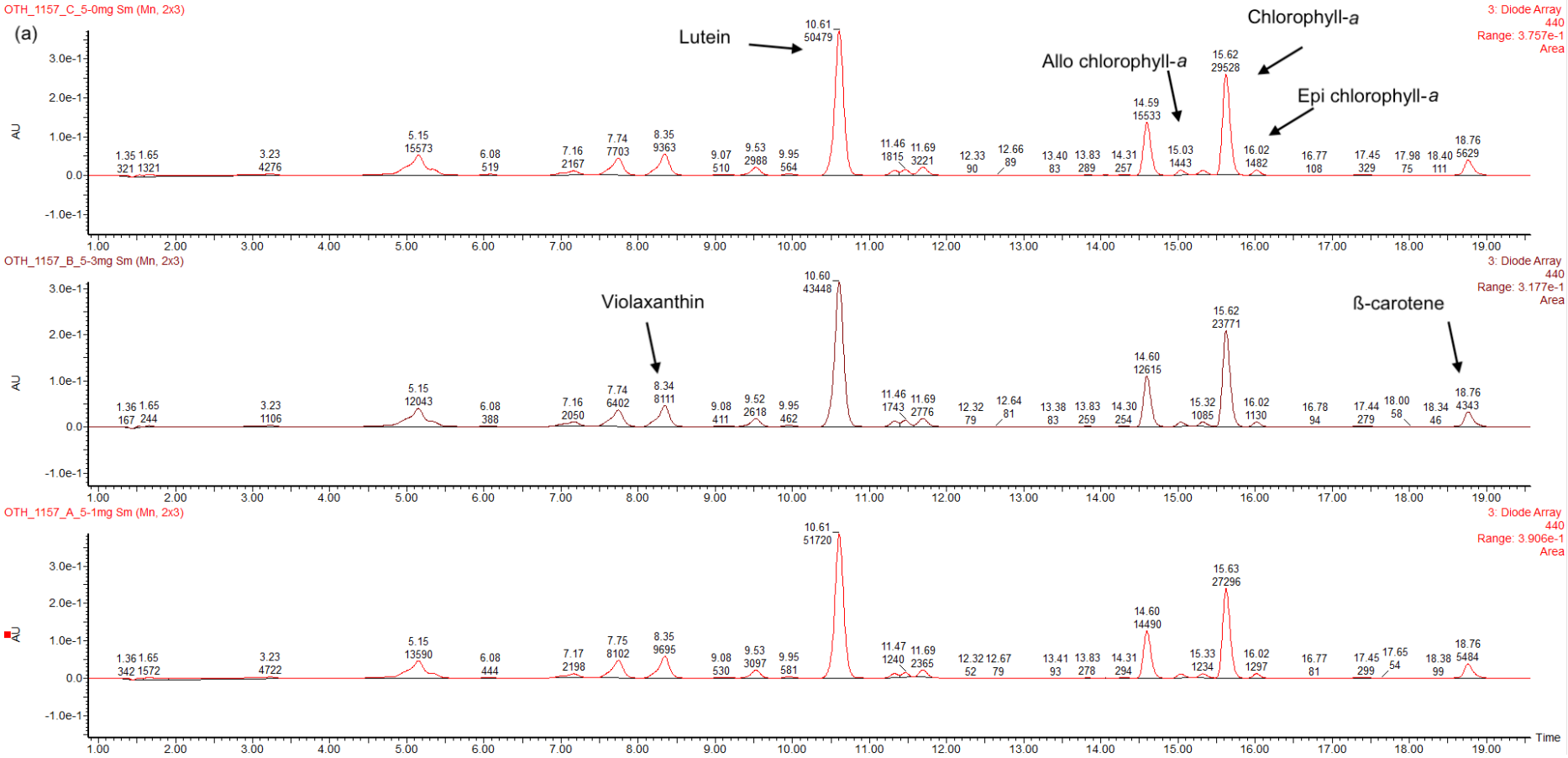
OTH_1157_C_5-0mg Sm (Mn, 2x3)
(a)
3: Diode Array
440
Range: 3.757e-1
Area
Lutein
Chlorophyll-a
Allo chlorophyll-a
Epi chlorophyll-a
10.61 50479
15.62 29528
14.59 15533
5.15 15573
7.74 7703
8.35 9363
1.35 321
1.65 1321
3.23 4276
6.08 519
7.16 2167
9.07 510
9.53 2988
9.95 564
11.46 1815
11.69 3221
12.33 90
12.66 89
13.40 83
13.83 289
14.31 257
15.03 1443
16.02 1482
16.77 108
17.45 329
17.98 75
18.40 111
18.76 5629
OTH_1157_B_5-3mg Sm (Mn, 2x3)
3: Diode Array
440
Range: 3.177e-1
Area
Violaxanthin
ß-carotene
10.60 43448
15.62 23771
14.60 12615
5.15 12043
7.74 6402
8.34 8111
1.36 167
1.65 244
3.23 1106
6.08 388
7.16 2050
9.08 411
9.52 2618
9.95 462
11.46 1743
11.69 2776
12.32 79
12.64 81
13.38 83
13.83 259
14.30 254
15.32 1085
16.02 1130
16.78 94
17.44 279
18.00 58
18.34 46
18.76 4343
OTH_1157_A_5-1mg Sm (Mn, 2x3)
3: Diode Array
440
Range: 3.906e-1
Area
10.61 51720
15.63 27296
14.60 14490
5.15 13590
7.75 8102
8.35 9695
1.36 342
1.65 1572
3.23 4722
6.08 444
7.17 2198
9.08 530
9.53 3097
9.95 581
11.47 1240
11.69 2365
12.32 52
12.67 79
13.41 93
13.83 278
14.31 294
15.33 1234
16.02 1297
16.77 81
17.45 299
17.65 54
18.38 99
18.76 5484
AU
Time

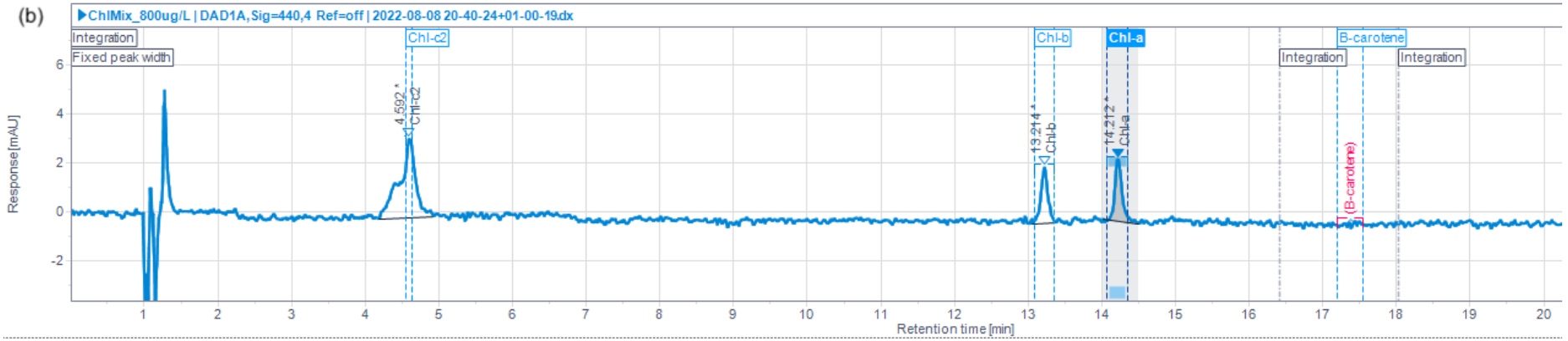

Figure D. 1 A Reverse-phase high-performance liquid chromatography (C18-RP HPLC) spectra for quantified photosynthetic pigments from *P. kessleri* and at a wavelength of 440 nm and (b) standard trace for chlorophyll and ß-carotene spectra analysed using a Hewlett Packard instrument with a Nova-Pak C18 4 µm and 3.9x150 mm column.

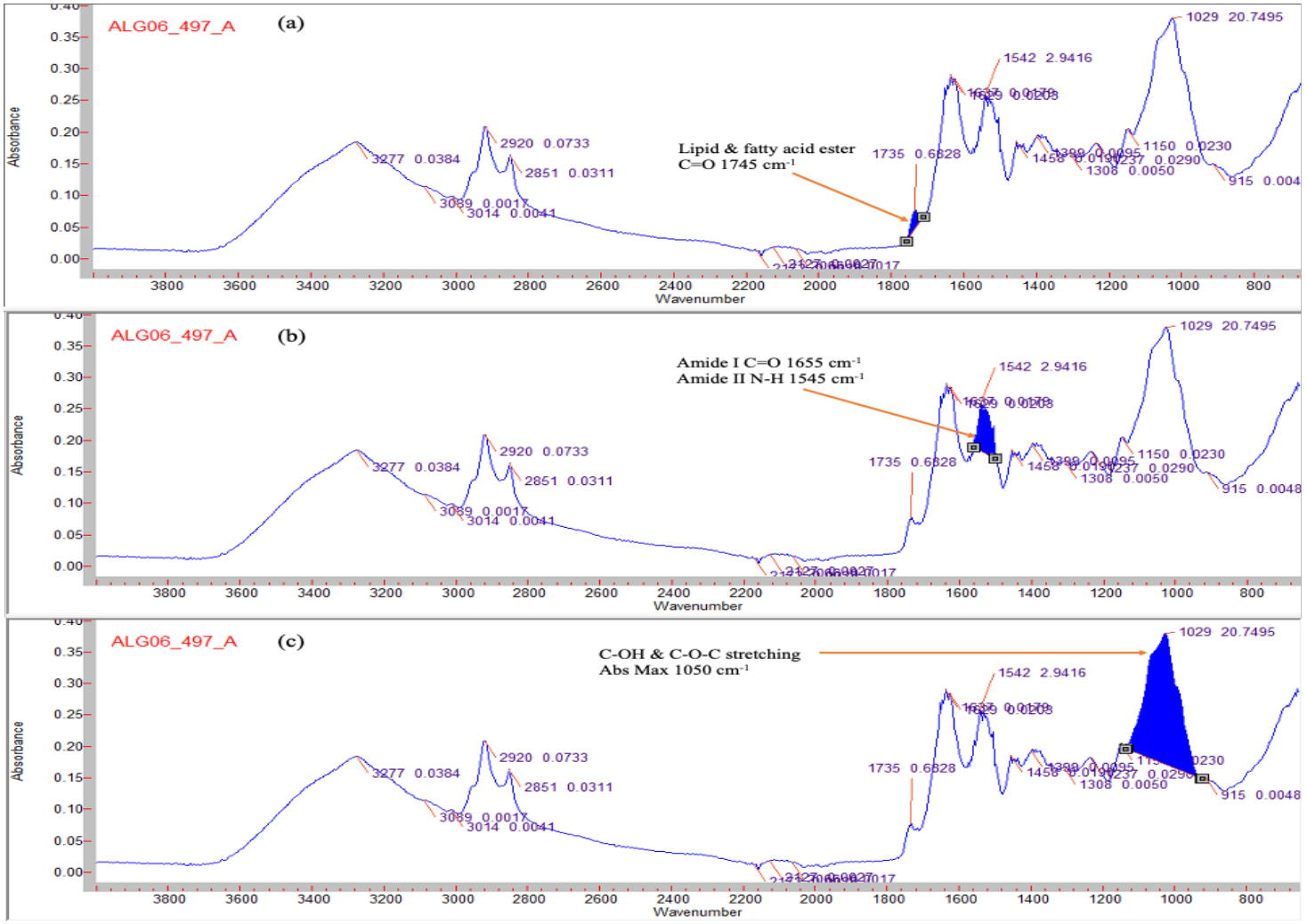

Figure D. 2 Describes the determination of the biochemical content in an algal biomass for (a) lipid, (b) protein, and (c) carbohydrate analysed using Fourier Transform Infrared Spectroscopy (Cary 630) instrument. The infrared spectra were scanned in the range 4000–450 cm^{-1}, and the characteristic absorbance peaks based on specific chemical groups within the biomass were selected for Lipid (C =O ester stretching at 1760–1715 cm^{-1}), protein (C =O amide II band at 1545 cm^{-1}), and carbohydrate (C-O-C stretching at 1070–020 cm^{-1}).

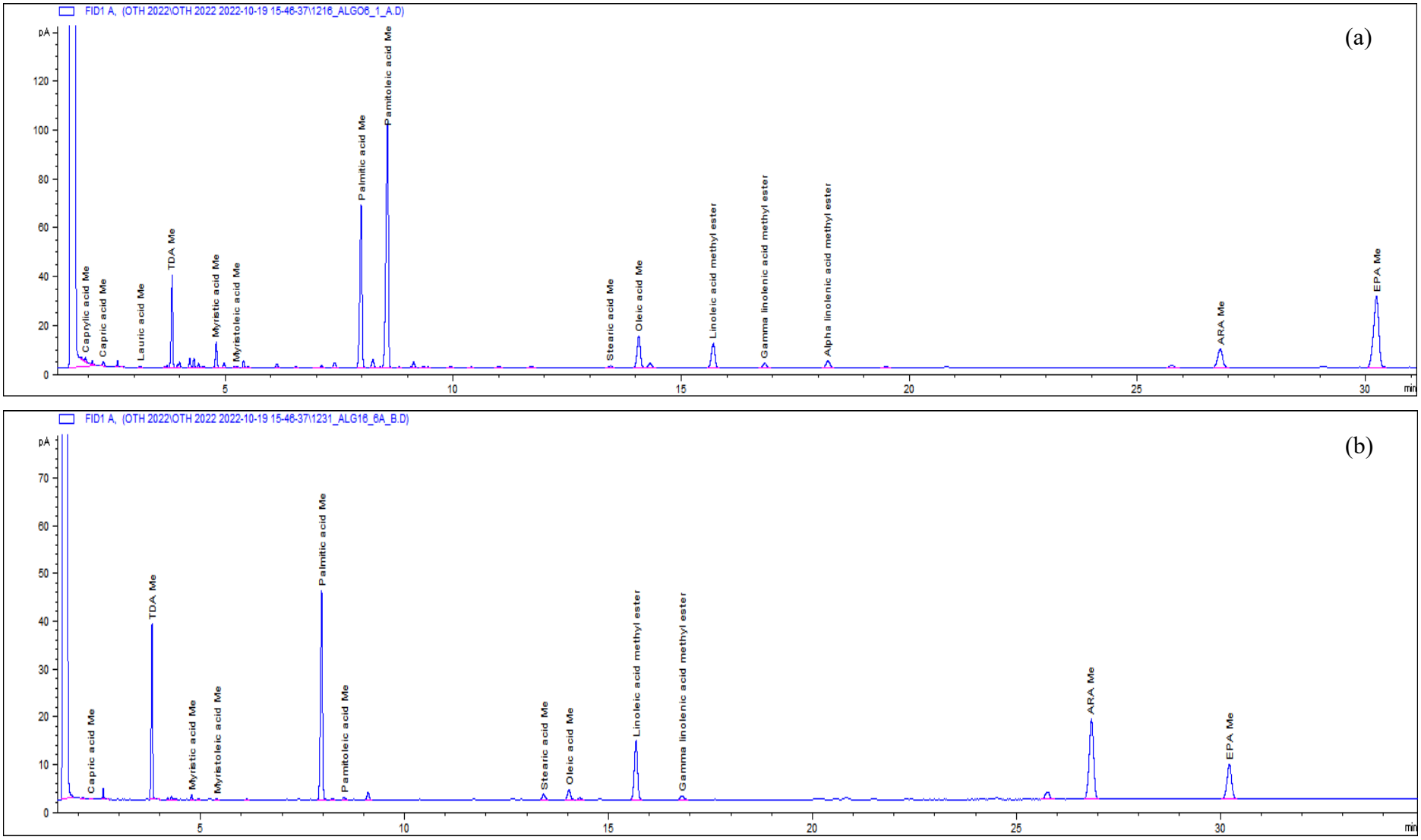
FID1 A, (OTH 2022\OTH 2022 2022-10-19 15-46-37\1216_ALG06_1_A.D)
pA
Caprylic acid Me
Capric acid Me
Lauric acid Me
TDA Me
Myristic acid Me
Myristoleic acid Me
Palmitic acid Me
Pamitoleic acid Me
Stearic acid Me
Oleic acid Me
Linoleic acid methyl ester
Gamma linolenic acid methyl ester
Alpha linolenic acid methyl ester
ARA Me
EPA Me
min
(a)
FID1 A, (OTH 2022\OTH 2022 2022-10-19 15-46-37\1231_ALG16_6A_B.D)
pA
Capric acid Me
TDA Me
Myristic acid Me
Myristoleic acid Me
Palmitic acid Me
Pamitoleic acid Me
Stearic acid Me
Oleic acid Me
Linoleic acid methyl ester
Gamma linolenic acid methyl ester
ARA Me
EPA Me
min
(b)

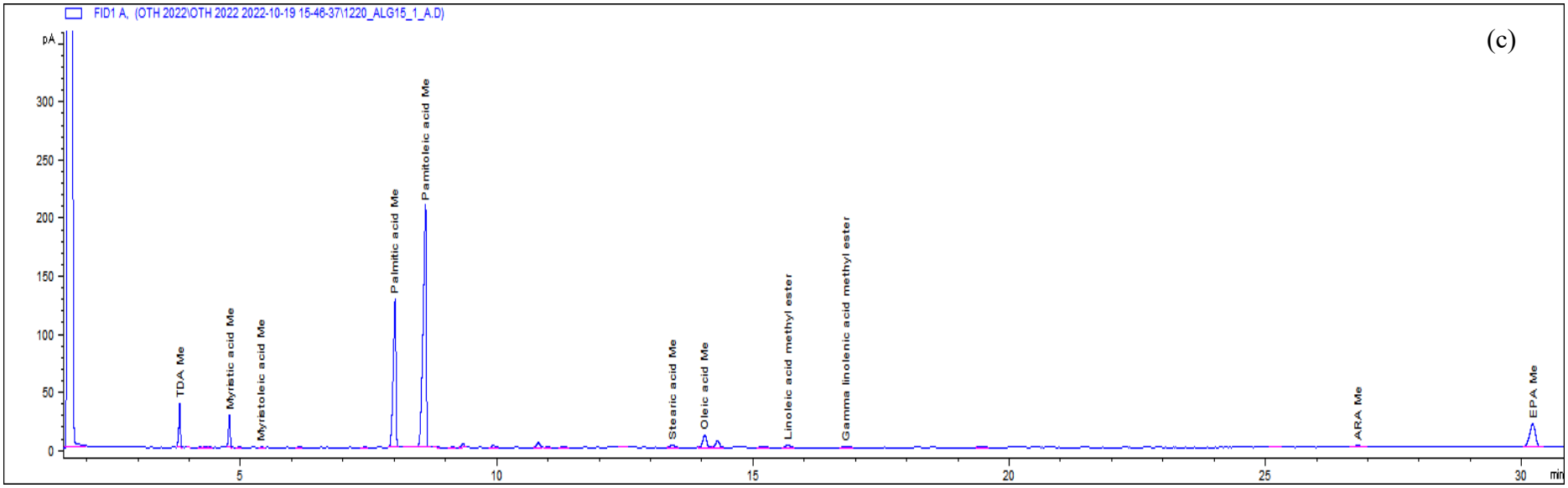
FID1 A, (OTH 2022\OTH 2022 2022-10-19 15-46-37\1220_ALG15_1_A.D)
(c)
pA
300
250
200
150
100
50
0
TDA Me
Myristic acid Me
Myristoleic acid Me
Palmitic acid Me
Palmitoleic acid Me
Stearic acid Me
Oleic acid Me
Linoleic acid methyl ester
Gamma linolenic acid methyl ester
ARA Me
EPA Me
5
10
15
20
25
30
min

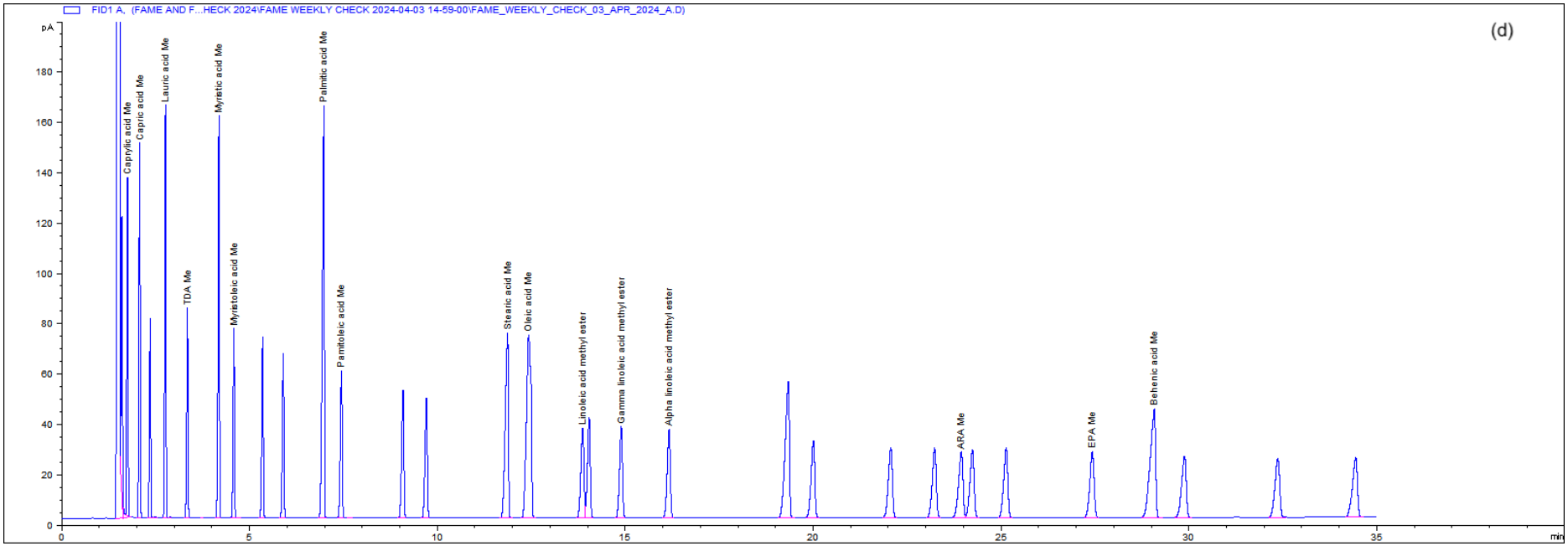

Figure D. 3 Represents the fatty acid profile for (a) *Vischeria* sp., (b) *Porphyridium purpureum,* (c) *Phaeodactylum tricornutum* cultivated at different inorganic carbon concentration, and (d) showing the standard traces of the fatty acid methyl esters (FAME) composition based on their retention time comparison with internal FAME standards with reference to named compounds from a Gas Chromatography-flame ionisation detector (GC-FID) equipped with a variable spit-flow injector and a 52 CB GC column (Agilent 6890A).